The Institute of Paper Science and Technology

Atlanta, Georgia

Doctor's Dissertation

An Investigation of the Effects of Polymer Partitioning on Fines Retention

Charles E. Miller

October, 1989

AN INVESTIGATION OF THE EFFECTS OF POLYMER PARTITIONING ON FINES RETENTION

A thesis submitted by

Charles E. Miller

B.S. 1985, Miami University
Oxford, Ohio

M. S. 1987, Lawrence University - The Insititute of Paper Chemistry
Appleton, Wisconsin

in partial fulfillment of the requirements
for the degree of Doctor of Philosophy
from The Institute of Paper Science and Technology
Atlanta, Georgia
(formerly The Institute of Paper Chemistry)

October 24, 1989

TABLE OF CONTENTS

TABLE OF CONTENTS (cont.)

TABLE OF CONTENTS (cont.)

FIGURES AND TABLES

TABLE OF CONTENTS (cont.)

ABSTRACT

Cationic polymers, used in the paper industry to effect changes in retention, drainage, and formation, are known to adsorb onto the surfaces of the fines, fillers, and fibers, thus changing the electrokinetic properties of these particles. Recent literature indicates that zeta potential distributions, instead of averages, may be required to adequately describe the charge within a furnish sample. Limited studies to date have failed, however, to correlate zeta potential distributions with retention.

The cause of distributions in zeta potential or electrophoretic mobility could arise from uneven adsorption of the polymer within a papermaking furnish. Thus, the basis for this thesis was to partition the dosage of a polymeric retention aid throughout a model headbox furnish consisting of polystyrene latex particles and oxidized cotton linters. Based upon the observed electrophoretic mobility, the location of polymer, and the dosage, a statistical model of retention was developed.

Electrophoretic mobility distributions graphically demonstrated which particles were preferentially retained in the dynamic drainage jar. As more polymer was directly adsorbed onto the fibers, increasingly negative particles were retained. As more polymer was added to the fines or latex, increasingly positive fines were retained. These observations showed that polymer treated latex particles were retained by attaching themselves to the fibers. When the polymer was preferentially added to the fibers, the more negative particles were drawn toward the polymer loops and tails near the fiber surface. Consequently, the location of polymer was a critical factor in determining whether particles attached onto larger fibers.

From the above observations, two forms of bridging were identified. The first type resulted when a polymer-treated particle attached to a fiber. The second and most efficient form resulted from heteroflocculation between polymer-treated fibers and the latex. As the amount of polymer added to the cotton linters was increased, the retention increased to a maximum which occurred between 50 and 60% addition onto the fibers. Therefore, preferential adsorption of the retention aid onto the long fiber fraction of a papermaking furnish is desirable.

INTRODUCTION

Possibly the first publication investigating zeta potential distributions in papermaking systems was published by Rudolf Schmut[1] in 1964. Schmut measured 50 particles per sample to obtain whitewater zeta potential distributions. Penniman[2] introduced an automatic microelectrophoresis instrument which was capable of providing zeta potential distributions. Smith,[3] in 1978, presented distributions for newsprint furnishes which were derived, like Schmut's work, from the measurement of hundreds of single particles on a Zeta-meter. Smith tried to explain variations in retention on a tissue machine with the zeta potential distribution. He felt, however, that the zeta potential distribution was more important in the press section since turbulent hydrodynamic disturbances associated with drainage on the wire are diminished allowing the electrokinetic effects to dominate.[3]

It is possible that zeta potential distributions are a function of the location of polymeric retention aid within a papermaking furnish. This thesis investigates the relationship between the location of polymer within the furnish and filler retention. The data presented show that under the conditions studied, the electrophoretic mobility distribution (from which zeta potential is calculated) of the filler does not play an important role in the retention of polystyrene latex particles in a model system consisting of latex spheres and oxidized cotton linters.

BACKGROUND

Microelectrophoresis has been used in the paper industry to measure the electrophoretic mobility of wood fines. The problem with this type of measurement is that large particles cannot be measured. Consequently, there has been a standing argument in the literature as to whether fines and larger fibers have the same average zeta potential. Research has also shown that distributions of zeta potential can be noted in newsprint furnishes. Two such furnishes have been shown to have the same average zeta potential and quite different zeta potential distributions. This is an apparent contradiction to the belief that the surface potential of fines and fibers is the same. These findings also imply that single point zeta potential measurements inadequately describe the surface potential of a wood furnish.

There is still more uncertainty in that the effect of zeta potential or electrophoretic mobility distributions on retention or drainage is not known. To fully investigate these relationships, it is necessary to discuss the theory behind electrophoresis and zeta potential.

LITERATURE REVIEW

THE ELECTRIC DOUBLE LAYER

When solids are suspended in a liquid, they acquire a negative charge, the magnitude of which depends on the surface chemistry of the particle. This negative surface charge will attract oppositely charged counterions from the bulk solution, forming an immobile layer about the particle. When the particle moves through the bulk solution, this immobilized layer of counterions also moves with the particle, causing the actual plane of shear to be at a distance approximated by the diameter of the counterions. The term "immobile" is perhaps a misnomer, because the ions which make up this layer are not bound within it. The ions are continuously interchanging with other counterions. The fact that counterions are always present gives rise to the term. The charged surface, the counterion layer, and the mobile layer of excess counterions together form the electric double layer.

The electric double layer is represented by the Gouy-Chapman model in Fig. 1. Independently, they developed this model from theory by assuming the ions to be point charges distributed according to the Boltzmann distribution. The charged surface was taken to be a uniform flat plate with a surface potential, Ψ_0. The potential at the Helmholtz plane, Ψ_δ, is the effective charge on a particle; however, this potential can only be estimated by the potential at the plane of shear at the outer edge of the Stern layer, δ, and thus is termed the Stern potential. Using the Debye approximation, the potential at a distance x from the surface, Ψ, can be described by,[4]

$$\Psi = \Psi_0 e^{-\kappa x}. \qquad [1]$$

The thickness of the double layer is approximated by the reciprocal of the Debye-Hückel parameter, κ, defined as

$$\kappa = [e^2 N_A \Sigma(c_i z_i^2)/\varepsilon\varepsilon_o kT]^{0.5} \qquad [2]$$

where,

e = electronic charge
z_i = electrolyte valency of ion "i"
N_A = Avogadro's number
c_i = concentration of ion "i", moles/L
ε = dielectric constant of medium
ε_o = permittivity of free space
k = Boltzmann's constant
T = absolute temperature.

Hence, the potential is decreased by $^1/_e$ at a distance κ^{-1} from the surface.[4] More detailed discussions of the electric double layer can be found in publications by Kruyt,[5] Dukhin and Derjaguin,[6] Shaw,[7] and Hunter.[8]

ZETA POTENTIAL

An estimation of the Stern potential is known as the zeta potential, ζ. It is defined as the potential at the slip plane between the immobile Stern layer and the diffuse layer of ions. Since it is measured at a shear plane of unknown location, the zeta potential is always less than or equal to the Helmholtz potential, Ψ_δ.

In this thesis, zeta potential is actually derived from the electrophoretic mobility which is measured by electrophoresis. The other electrokinetic phenomena, electroosmosis, streaming potential, streaming current, and sedimentation potential are discussed elsewhere in the literature.[5,6,7,8] In electrophoresis, particles suspended in a liquid are induced to

move by an applied electric field. The velocity of the particle per unit electric field is known as the electrophoretic mobility.

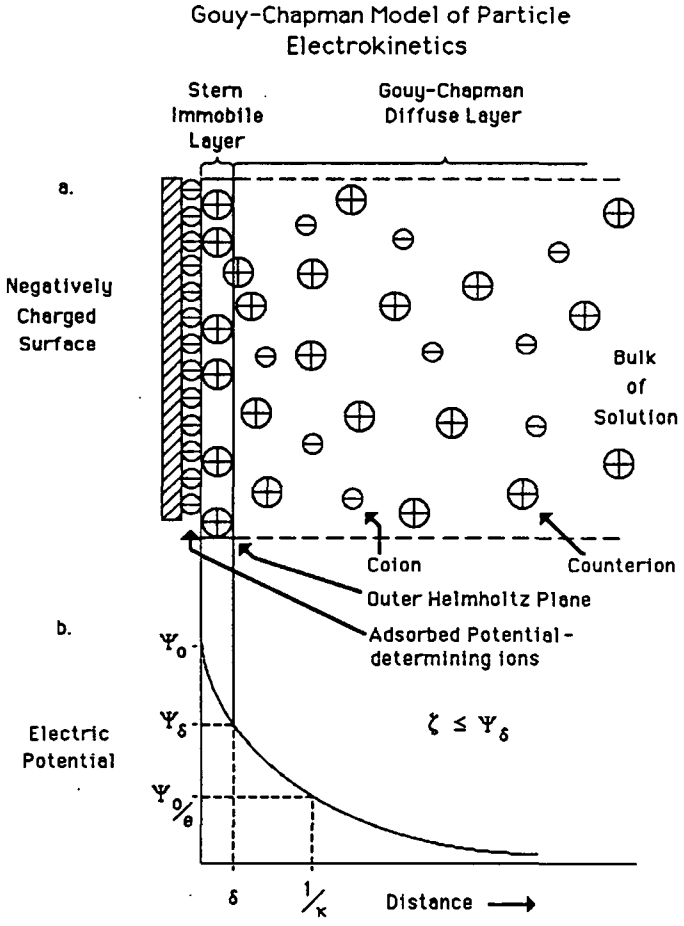

Figure 1. a. The electric double layer.
b. The potential distribution in the double layer.

The zeta potential of a curved surface can be calculated from the electrophoretic mobility. The relative size of the double layer is described by a ratio of the radius of curvature of the particle to the double layer thickness. This dimensionless ratio, κa, determines which equation can be used to calculate the zeta potential. The generalized form of the mobility-zeta potential relationship is given by the Henry equation (in SI units):

$$EM = \frac{(4\pi\varepsilon_o)\,\varepsilon\zeta}{6\pi\eta} f(\kappa a) = \frac{2\varepsilon\varepsilon_o\zeta}{3\eta} f(\kappa a) \qquad [3]$$

where,

EM = electrophoretic mobility, (μm/s) / (volt/cm)
ε_o = permittivity in vacuum, farad/m
ε = dielectric constant
ζ = zeta potential, mV
η = viscosity, Ns/m^2
κ = Debye-Hückel parameter, 1/m
a = radius of curvature, m
$f(\kappa a)$ = function depending on particle shape.

When κa is small, the suspended particle can be approximated by a point charge; when κa is large, the double layer is essentially flat.

When κa is small, the Hückel equation:

$$EM = \frac{(4\pi\varepsilon_o)\,\varepsilon\zeta}{6\pi\eta} = \frac{2\varepsilon\varepsilon_o\zeta}{3\eta} \qquad [4]$$

is valid. Equation 4 usually does not apply to particle electrophoresis in aqueous media. It can apply, however, to electrophoresis in non-aqueous media of low conductance.[7] When κa is large (κa>100), the Smoluchowski equation:

$$EM = \frac{(4\pi\varepsilon_o)\,\varepsilon\zeta}{4\pi\eta} = \frac{\varepsilon\varepsilon_o\zeta}{\eta} \qquad [5]$$

is applicable assuming that ε and η are constant. This equation implies that the mobility is independent of particle size and shape provided that the zeta potential is constant.

The effectiveness of a retention aid is due in part to the electric double layer which develops when cellulosic fibers and fines and inorganic fillers are suspended in water. In the pH range of 4-9, the fiber and filler particles acquire a negative charge primarily because of the ionization of surface functional groups. In a papermaking system, the zeta potential gives a direct indication of the change in potential or particle charge caused by the adsorption of polymeric retention aids, alum, drainage aids, or any other surface active agent. As the amount of adsorbed polymer increases, the change in zeta potential becomes greater.

ZETA POTENTIAL DISTRIBUTIONS

Despite the particle size implications of the Smoluchowski equation for $\kappa a>100$, the effect of particle size on zeta potential is still argued. This argument extends to whether fibers have the same zeta potential as fines. According to Strazdins,[9] fines generated in refining are covered with hemicelluloses and other polysaccharides released during refining that adsorb onto the fiber or fine surface; therefore, fines and fibers have the same surface chemistry, surface charge, and zeta potential.

Smith[3] has published data which seems to be contradictory to Strazdins' hypothesis. Smith stated that in newsprint systems "pulps in a mixed furnish can act independently from an electrokinetic point of view, and while the average zeta potential can remain constant, the zeta potential distribution can be changed significantly."[3] Therefore, while average values of zeta potential indicated an "overall" charge in the system, they could not fully describe the electrokinetic state of the suspension. Smith also noted that modification of zeta potential before the headbox could effect increased retention, wet web strength, drainage, and operating efficiency in newsprint furnishes.

Examples of zeta potential distributions for softwood bleached kraft, thermomechanical, and groundwood pulps are shown in Fig. 2. Those pulps which were not full chemical pulps were characterized by bimodal distributions. Smith hypothesized that the lower and higher zeta potential peaks represent those particles that have mainly cellulose and lignin surfaces, respectively. Full chemical pulps were more uniform in their surface characteristics and showed an almost Gaussian distribution.

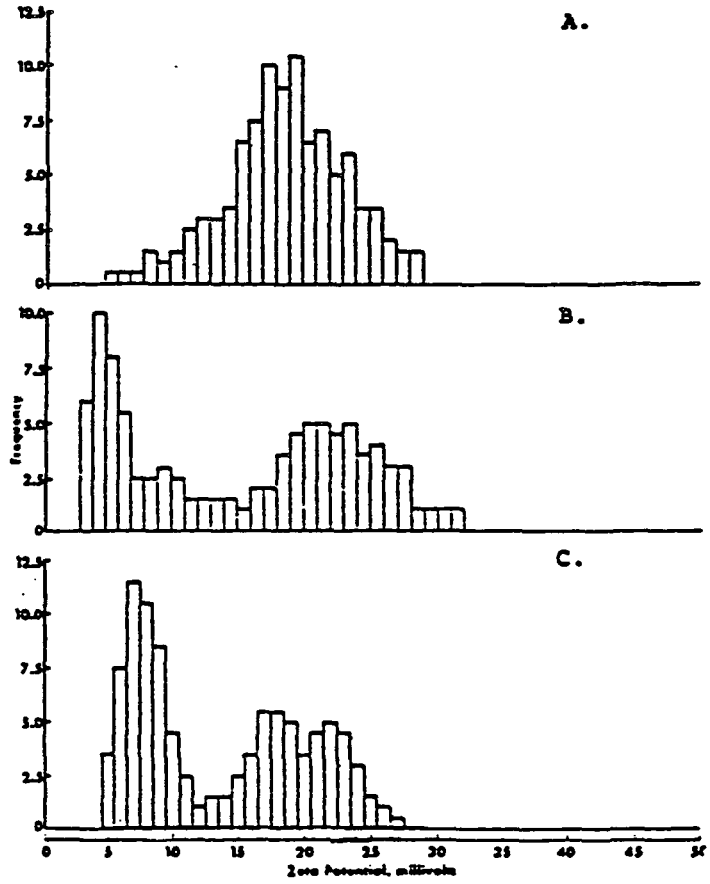

Figure 2. Zeta potential distributions for softwood bleached kraft (A), groundwood (B), and thermomechanical (C) pulps.[3]

In 1977, Penniman[2] introduced an automated method of determining zeta potential distributions. Sanders and Schaefer[10] reported results from another automated system which provided zeta potential distributions. The distributions, however, were not used in the analysis, but Sanders did hypothesize a relationship between electrokinetics and retention. These views are included below in the section entitled "theories of retention." Consequently, the relationship between zeta potential distributions and retention has yet to be evaluated.

The effects of average zeta potential on retention, however, have been investigated. By plotting Britt jar retention versus average zeta potential, Arno and co-workers[11] found that a zeta potential between -10 and +10 mV was desirable in their system for maximum filler retention. Nichols[12] has stated that, in general, coagulation is maximized at zero zeta potential. But maximum flocculation may not occur at zero zeta potential; consequently, maximum retention may or may not occur in a system whose charge is near zero.

MEASUREMENT OF ZETA POTENTIAL

Manual Methods

Zeta-meter

The measurement of zeta potential by electrophoresis can be done several ways--all of which measure the velocity of a particle whose motion is caused by an applied electric field. The Zeta-meter by Zeta-meter, Inc. applies an electric field across a clear plexiglass cell. This cell is illuminated with a light source on the side of the cell. Colloidal particles are tracked on a grid with a light microscope. Electrophoretic mobility can then be calculated by noting the time required for a particle to travel a given distance on the grid. One problem with this test is operator error in tracking and timing the particles. Another problem

is focusing the instrument to read particles moving at the stationary layer. As with all electrophoretic measurements, if the instrument is not focused on the stationary layer, the data are in error.

Light Scattering Methods

The basis for light scattering theory for small particles was developed by Rayleigh. The theory states that the relative intensity of scattered light per unit volume is a function of geometrical, optical, and thermodynamic factors. The Rayleigh ratio, R_θ, expresses the geometry of the system in terms of the incident and scattered light and the scattering angle. The optical and thermodynamic factors are present in the final equation[13]

$$\frac{Kc_2}{R_\theta} = \frac{1}{M} + 2Bc_2 \qquad [6]$$

where,

M = molecular weight
B = second virial coefficient
c_2 = solute concentration

$$R_\theta = \frac{i_s}{I_o} \frac{r^2}{1 + \cos^2 \theta}$$

and

$$K = \frac{2\pi^2 (\tilde{n}\, d\tilde{n}/dc_2)^2}{\lambda_o^4 N_A}$$

where,

i_s = scattering per unit volume
I_o = intensity of light incident
r = radial distance to the point of observation
θ = scattering angle
$\tilde{n}$ = refractive index of the solute
λ_o = wavelength of incident light
N_A = Avogadro's number.

Rayleigh theory, however, assumes that interference is not present; therefore, to apply this theory to particles whose dimensions are greater than $\lambda/20$, light scattering must be measured at several angles and the data extrapolated to $\theta = 0$.[13] The Rayleigh-Gans-Debye theory corrects the Rayleigh theory to allow for interference effects, but with a few new assumptions. If one assumes that a scatterer can be subdivided into an array of scattering sites which individually obey Rayleigh theory, one can then assume that the observed interference is the cumulative effect of the individual scattering particles and that solute-solute interactions are negligible. This approach is only valid if $(4\pi R/\lambda)(\tilde{n}_2/\tilde{n}_1 - 1) \ll 1$, where R is the radius of the overall molecule and $\tilde{n}_2$ and $\tilde{n}_1$ are the refractive indices of the solute and solvent, respectively. The Rayleigh-Gans-Debye theory provides a correction to the right hand side of Eq. 6 with a form factor, $P(\theta)$, such that

$$\frac{Kc_2}{R_\theta} = \left(\frac{1}{M} + 2Bc_2\right)\frac{1}{P(\theta)} \qquad [7]$$

where,

$$P(\theta) = \frac{i_{s,\,actual}}{i_{s,\,Rayleigh}}$$

and again where

i_s = scattering per unit volume.

From these theories, the weight averaged molecular weight and the particle size of a polymer or particle can be determined by extrapolations of Zimm plots representing the scattering data.[13]

Light scattering can also be used to determine particle velocities when lasers are used as the light source.[14] Velocities are measured by

quantifying the Doppler frequency shift of scattered light which results when a transmitter is moving at a relative velocity to the receiver. The shift in Doppler frequency, $\Delta\nu$, is given by[15]

$$\Delta\nu = 2\tilde{n}\, v \sin(\theta/2)/\lambda_o \qquad [8]$$

where,

v = relative transmitter velocity.

Another useful quantity is the scattering vector which is given by

$$k' = 4\pi\tilde{n} \sin(\theta/2)/\lambda_o. \qquad [9]$$

For a more complete discussion of the technique of laser Doppler anemometry refer to Drain.[15]

Laser Zee System 3000

Pen Kem, Inc. markets the Laser Zee System 3000 which uses a multistage photomultiplier and a frequency tracker to determine the average particle velocity in the sample. The mobility frequency distribution is calculated with a real-time spectrum analyzer. This instrument provided the first mobility histogram obtained from automated equipment.[2]

Malvern Zetasizer IIC

Particle velocities are measured on the Malvern Zetasizer IIC with laser Doppler anemometry. Laser Doppler anemometry is named after the Austrian physicist who first discovered the frequency (Doppler) shift in 1842.[15] This frequency (Doppler) shift occurs because of motion among the source, receiver, propagating medium, or intervening reflector or scatterer. In the

measurement of electrophoretic mobility, there is no motion between the source and receiver. Instead, the frequency shift is caused by the movement of a particle which scatters light between the source and receiver. The light pulses generated by a moving particle are registered by a photomultiplier tube. The data are then processed to provide particle size, electrophoretic mobility, or zeta potential values. The data in this thesis are from this instrument and are reported as electrophoretic mobility.

Coulter DELSA 440

This instrument also uses laser Doppler anemometry to measure the Doppler shifts of scattered laser light and thus particle velocities. The DELSA, however, uses four angles of laser light which allows the instrument to differentiate between distribution broadening caused by charge heterogeneity and by Brownian motion of particles less than 1 μm in diameter.[16]

FLOCCULATION OF COLLOIDAL SUSPENSIONS

DLVO Theory

Derjaguin and Landau and, independently, Verwey and Overbeek theorized how lyophobic colloids were stabilized.[4] There are basically two forces acting on two approaching particles: double layer interactions (coulombic repulsion) and van der Waal's forces (attraction). Recent contributions by Israelachvili[17] have shown that two other forces are also present, an oscillatory force and a hydration force. The consequences of these forces with respect to DLVO theory, however, is not yet established. Formation of a dimer occurs when the attractive forces overcome the double layer interactions. Repulsive forces can be reduced by ion or polymer adsorption onto the particle, thereby changing the surface charge, or by electrolyte addition which compresses the double layer. The end result in each case is that the electrophoretic mobility of

the particles is reduced. Elimination of the double layer would yield particles with zero electrophoretic mobility and no repulsive forces. Under these conditions, a colloidal suspension would destabilize, flocculate, and precipitate.

The above discussion generally applies to particles of the same size, shape, and composition. In a papermaking system, flocculation occurs among negatively charged particles such as fibers, fines, clay, and TiO_2. Cationic retention aids are used to flocculate these particles. Heterocoagulation also has been shown to take place between particles of similar charge if the difference in surface potential between the two is sufficiently large.[18,19] This demonstrates that a zero zeta potential or mobility is not necessary for flocculation and, perhaps, not even desirable.

Flocculation Mechanisms

Compression of the double layer with electrolytes has been shown to increase retention in papermaking systems since the zeta potential of each particle is reduced. However, strong flocculation is obtained with polymeric flocculation aids.

There are two major theories of polymer-aided flocculation: bridging and electrostatic patch. The bridging mechanism occurs when high molecular weight, low or zero charge density polymers are employed.[20] These polymers adsorb onto a particle in a series of loops and tails. When a second particle approaches, it is "bridged" by the polymer tails and/or loops now present on the first particle. These bridges must be long enough to cross the double layer associated with each particle so that electrostatic repulsion is overcome.

The electrostatic patch mechanism is associated with high charge density polymers.[21,22] These polymers have a strong affinity for the negatively charged particles in a papermaking furnish. Hence, the polymer tends to form a "patch" of positive charge when adsorbed onto a particle. This patch can attract other negatively charged particles or negative regions thus effecting flocculation.

RETENTION

Flocculation is a desired effect for the papermaker due to the method by which paper is produced. A paper web is made by spraying a low solids (typically 0.5% solids), aqueous suspension of wood fiber, fiber fines, and fillers (collectively termed the "furnish") from a flow spreader (termed a headbox) onto one or in between two moving synthetic screens or "wires." As water drains through the wire, the sheet of paper is formed by a combination of filtration and attachment of smaller particles onto larger fibers or fines. The water collected underneath the wire, including the solids which also pass through the screen, is termed whitewater; the whitewater is recycled to reclaim these solids that were not retained on the screen or wire. Flocculation can be used to increase the effects of both filtration and particle attachment to increase the amount of solids retained on the wire.

The retention can now be defined as the percentage of the total mass (of solids) which was retained on the wire to form the web of paper. Therefore, a high retention value is desired for full raw material utilization. Mathematically, retention can be defined as:

$$\%R = 100\% \times \frac{\text{Headbox mass - whitewater mass}}{\text{Headbox mass}} \quad [10]$$

However, it is also useful to monitor the retention of fines in the papermaking system, since the retention of these particles is the ultimate goal. Fines retention in papermaking is of great importance as the fines content affects the optical,[23,24] strength,[25] and surface properties of the paper. The retention of fines can be calculated, when the percentage of fines in the headbox furnish and whitewater are known, by

$$\% \text{ Fines Retention, FR} = 100\% \times (1 - \text{WWF/HBXF}) \qquad [11]$$

where,

WWF = fines solids in whitewater = (sample weight) x (whitewater solids) x (percent fines in whitewater)

HBXF = fines solids in headbox = (sample weight) x (headbox solids) x (percent fines in headbox).

The assumption that the solids in the whitewater are 100% fines eliminates the need to determine the percentage of fines in the whitewater. This assumption can be made without significantly adding error.[26] More detailed calculations and discussions of fines retention can be found in Unbehend.[27] The same argument follows for the retention of filler.

The percentage of filler in the headbox was known and held at 20%, and the percentage in the whitewater was taken as 100% since the fiber fines associated with the cotton linters were removed by washing prior to use. The retention calculated in this thesis was the filler retention.

Theories of Retention

In 1936, Haslam and Steele[28] postulated three retention mechanisms. The first two, filtration by the fiber mat and entrapment in the pores and lumens, are mechanical in nature. Coflocculation, the third, is

electrochemical. Basically, these three theories are still endorsed in the literature today. The only difference is that now polymeric retention aids are used to enhance the retention in a given headbox furnish. When retention aids are present, three retention mechanisms can be envisioned:[29]

1. Retention aids promote filler attachment to the fiber before mat formation;
2. Retention aids cause the fines and fillers to agglomerate in flocs too large to pass through the screen or wire; and
3. Retention aids promote deposition of filler within the mat.

Williams and Swanson[30] stated that pre-mat formation retention, attachment of filler particles to fibers by colloidal adhesion, is the most likely source of pigment retention in papermaking systems. Very high retentions were found by Britt[31] when he flocculated papermaking systems with electrolytes in a "dynamic drainage jar". He found that flocs formed with electrostatic attraction were "soft" and easily broken and reformed; tenacious "hard" flocs were formed when polymeric retention aids were employed. Britt[32] also determined that retention was dependent upon the type of flocculation mechanism, patch or bridging, and upon the degree of shear in the system. Since Britt's system did not involve mat formation, all retention was presumed due to adsorption of small fines and filler particles onto larger fibers.

According to Stratton,[33] retention develops in a series of three distinct steps:

1. Adsorption of polymer onto fiber, fine, and filler surfaces;
2. Attachment of the filler to the fines and fiber; and
3. Attachment of the fines to the fibers.

The first step depends on the dispersion of the polymer and the rate of

adsorption. Franco and Stratton[34] have shown that, under conditions of high turbulence, the flocculation of TiO_2 with a low charge density, high molecular weight polymer (designated Q5) is completed in less than 1 s. Due to this short time frame, the mixing conditions at the point of addition are crucial to obtaining a uniform distribution of polymer in the sample. Hence, polymer location may play an important role in retention. The second two steps are dependent upon diffusion and collision theory principles. All three of Stratton's steps may occur simultaneously.

Davison,[35] however, believes that the adsorption of fine particles onto larger fibers is not a predominant mechanism of retention. Davison concedes that particles less than 1 μm in diameter may adsorb and permanently stick to the fibers.[36] Filtration of flocs by a fiber mat is supported by Davison as the major mechanism of fines retention in a papermaking system. Therefore, any experiments dealing with retention must include the formation of a fiber mat. This was the same conclusion reached by Abson and co-workers,[37] Arno and co-workers,[11] and Gess.[38] Flocs ranging in diameter from 10 μm to 500 μm are hypothesized to form so that retention is also increased due to particles too large to fit through the 76 μm wire used in the jar. Hence, by varying the hole size of the screen, retention can be increased or decreased at will.[34]

The hypothesis that small flocs are deposited in the fiber mat was part of the theory proposed by Haslam and Steele.[28] Han[39] also endorsed this view stating that flocs formed before the mat was formed would break and then be deposited when the mat was formed. These studies did not include polymeric retention aids. Since the use of retention aids became commonplace, there has been no evidence that this retention mechanism is a viable one.[29]

Other opinions are also prevalent in the literature. Sanders and Schaefer[10] believe that the mechanism of retention is only slightly related to electrokinetics. They suggest that soft flocs which develop near the isoelectric point and are controlled electrokinetically are the flocs responsible for strength and formation, but not retention and drainage.

The mechanism of retention is most likely a combination of mechanical and colloidal mechanisms as postulated by Britt.[32] Therefore, a combination of particle attachment and filtration may account for fines retention; but, the contribution of each mechanism to the total retention is not known. For two excellent reviews of electrokinetics and its application to papermaking, refer to Lindström[40] and Hubbe.[29] This thesis investigates how particle attachment and flocculation is affected by the distribution of polymeric retention aids in a suspension of oxidized cotton linters and polystyrene latex particles. The location of polymer is then related to the retention of the latex in studies with a dynamic drainage jar.

PRESENTATION OF THE PROBLEM AND THESIS OBJECTIVES

The previous discussion focuses on the surface charge of a suspended particle, measurement of this charge, and phenomena related to retention. The results of Smith indicate that simple averages of zeta potential are not sufficient to characterize a particle suspension. Instead, zeta potential distributions may be required. This may explain why the effects of zeta potential on retention are not fully understood.

Therefore, the objective of this thesis is to investigate the effect of polymer partitioning on filler retention. Several related objectives were derived from the thesis objective:

(1) to determine and document variations in headbox and white-water mobilities using a model system;
(2) to determine whether the headbox and whitewater mobility variations were due to a selective retention of fines with a certain mobility;
(3) to investigate the relationship between electrophoretic mobility distributions and polymer location; and
(4) to statistically analyze the retention data using the variables mentioned above.

GENERAL APPROACH

In order to accomplish the objectives of this thesis, headbox electrophoretic mobility distributions in a model system were manually altered by adjusting or partitioning the polymeric retention aid among three furnish fractions: the oxidized cotton linter long fibers, the polymer treated latex "filler," and the untreated latex "filler." A similar partitioning was done by Das and Lomas.[41] They overdosed a fines fraction to produce what they called "super flocculants." These "super flocculants" were then used to flocculate a fines suspension. The resulting flocs were found to be very stable under shear.

The model system used was chosen for several reasons. The cotton linters are composed of cellulosic fibers which resemble wood fibers. When the linters are refined, the surface becomes fibrillated also similar to wood fibers. Cotton linters, in contrast to fibers, are basically free of hemicelluloses and lignin which can readsorb on the the linter surface and interfere with polymer adsorption.[42,43] Also in contrast to the fibers, the cotton linters have a low surface charge. Additional charges, carboxyl functional groups, can be obtained by oxidation of the fibers. Consequently, cotton linters which have been refined and oxidized are clean model fibers for wood fibers.

The polystyrene latex polymerized for this thesis was also chosen as a model particle for several reasons. Latex particles have been used in the past as model colloidal particles.[21,44,45,46] They are chosen because of their spherical shape and consistent surface chemistry. The size of the particle was another consideration especially for this work. Filler particles, such as TiO_2, have a particle diameter ranging from 0.15 to 0.35 μm.[47,48] This range of particle

diameters was the target for the latex polymerization in this study. Polystyrene latex particles also have a density which is only slightly greater than that of water. Consequently, they form very stable colloidal suspensions and do not readily settle with gravity. This was an important consideration with regard to measurements on the Zetasizer IIC. Particles which tend to settle will not remain within the cross section of the laser beams. This causes distortions in the scattered light impulses which introduce errors in the mobility determination. Errors are also introduced because the velocity of a "heavy" particle is not purely electrophoretic in nature. Because of the reasons listed above, polystyrene latex was chosen as a model papermaking filler particle.

So, in this thesis, treated latex particles were combined with untreated latex particles to provide the "headbox filler" from which the mobility distribution could be determined. After combining the latex "headbox filler" fraction with the oxidized cotton linters, filler retention of each sample furnish was determined with a modified dynamic drainage tester. The fibers were also treated with varying amounts of polymer such that the polymer dosage was distributed throughout the entire model furnish.

Whitewater mobility distributions were also obtained so that the electrophoretic mobility distribution of the retained particles could be calculated by subtracting the whitewater distribution from the headbox distribution. The dependence of retention on polymer location, headbox and whitewater mobility distributions, and total polymer dosage was then statistically evaluated.

EXPERIMENTAL

MATERIALS

Water

All water used in this thesis was deionized and distilled.

Oxidized Cotton Linters

These fibers have been previously characterized.[49,50] Preparation of the fibers was done by Arnson.[49] To prepare the linters, Arnson: (1) refined the linters to 250 mL CSF, (2) removed the fines with two passes over The Institute of Paper Chemistry's web former, (3) extracted with ethanol:benzene, (4) oxidized with potassium dichromate and acidified sodium chlorite, and (5) washed and air dried the resulting long fiber fraction. These long fiber cotton linters were then stored in polyethylene bags until needed.

The carboxyl content of these fibers was reported by Proxmire to be 3.03 meq/100 oven-dried grams (od g) of fiber.[50] Methylene blue determinations were run to check the stability of the fibers with time. The methods used and results of this test are given in Appendix I. These results gave an acid content of 3.08 meq/100 od g of fiber. The electrophoretic mobility of the cotton linter fines was determined to be 1.00 (μm/s) / (volt/cm).[51] Single point BET surface area was also run on the fibers to determine the surface area per oven-dried gram of fiber.[52,53] The physical properties of the linters are given in Table 1. The hydrodynamic surface area was determined according to Ingmanson and Whitney.[54]

Table 1. Physical characteristics of oxidized cotton linters.[50]

Fiber Length	
-Arithmetic length average	1.2 mm
-Weighted length average	1.5 mm
BET Surface Area	1.0 m^2/g
Hydrodynamic Specific Surface Area	1.04 m^2/g
Carboxyl Content	3.08 meq/100 od g

Before use, the cotton linters were soaked in distilled water overnight and then mixed in the British disintegrator for 20 min. The linters were then washed in a Britt Jar with a 76 μm hole size screen at 1000 rpm to remove any small fines generated in the disintegrator. Washing was accepted as complete when fines were no longer visible in the filtrate. The linters were then stored in a refrigerator at approximately 1.5% consistency until needed.

Polystyrene Latex

The polystyrene latex used in this study was polymerized using a modification of the procedure published by Goodwin.[55] The exact procedure is given in Appendix II. At pH 6.0, the electrophoretic mobility of the latex was determined to be -6.60 (μm/s) / (volt/cm) (-81.5 mV zeta potential) with a 0.01 M NaCl electrolyte background. The surface charge density was determined conductometrically to be 0.75 meq/100 od g or 5.82 $\mu C/cm^2$. The surface of the latex contains sulfate groups which act as the charge determining groups. These functional groups arise from the persulfate initiator used in the polymerization. The absence of any carboxyl groups was also verified by the conductometric titration. The titration curve did not contain two areas of distinct slope prior to the point of neutralization (see Fig. A4, Appendix III). Two breaks in the

conductometric titration curve have been shown to indicate weak and strong surface groups.[56] The particle size was also determined with the Zetasizer IIC and with the scanning electron microscope to be 0.47 μm. Figures regarding the size and characterization of the latex can be found in Appendix III. The latex is monodispersed as seen in Fig. 3.

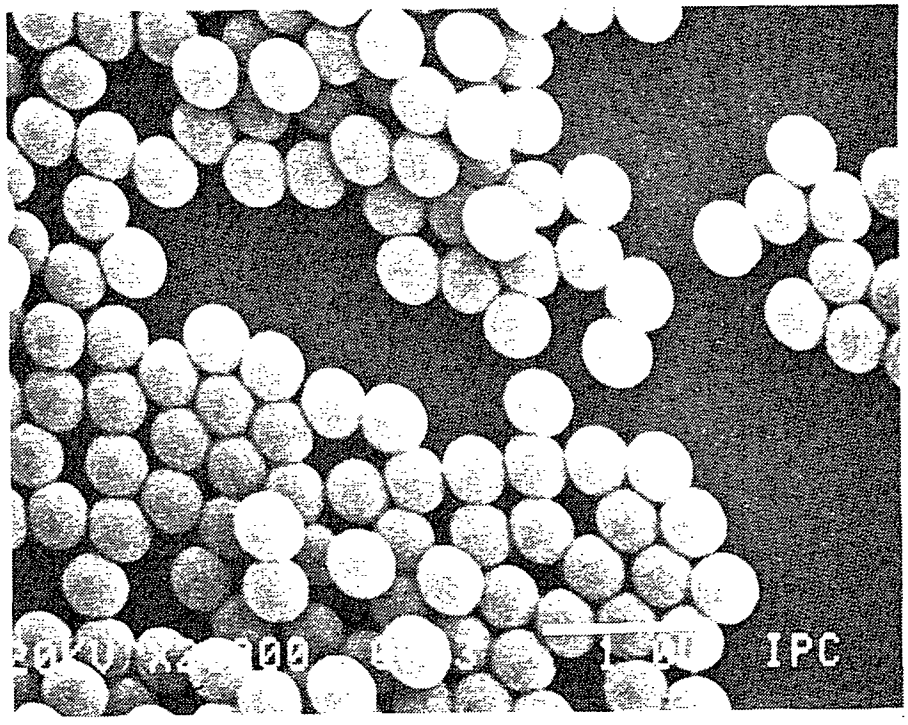

Figure 3. Scanning electron micrograph of latex polymerized for this thesis.

Polymeric Retention Aid

The polymeric retention aid used in this study was a cationic polyacrylamide copolymer. This copolymer, molecular weight 2.7×10^6,[57] is 5 mole percent methacryloxyethyl trimethyl-ammonium methosulfate and 95 mole percent acrylamide monomer.[50] The designation, Q5, is used to identify this low charge density polymer. The polymer was made up in stock solutions of 0.1%. The viscosity of this 0.1% stock solution was shown to be stable for a period not exceeding 13 days; therefore, new stock solutions were made every week as needed. Dilutions for each dosage were made daily. The polyacrylamide

was added in dosages of 0.5, 1.0, and 1.5 mg/od g furnish (1, 2, and 3 lb/ton furnish, respectively).

APPARATUS

Polymer Injection System

The apparatus, Fig. 4, used for polymer addition in this thesis was described previously.[49,50,51] This system was designed to inject a polymer retention aid into a fiber slurry as it fell from an upper tank to a lower modified Britt jar. The duration of the injection was timed so that polymer was dispensed only while the pulp passed the point of injection. Static mixer bars before and after the point of injection provided sufficient mixing so that polymer distribution throughout the sample was uniform. The multiport wand injector and the mixing zone is represented in Fig. 5. Several modifications to this apparatus were made. First, the ultrafiltration device at the bottom of the Britt jar was removed. Second, a screenless, removable bottom was installed on the lower Britt jar so that polymer treated samples could be made without screening.

Malvern Zetasizer IIC

The Zetasizer, Fig. 6, as mentioned earlier uses laser Doppler anemometry to measure particle velocities. These velocities are then converted into electrophoretic mobility data. To accomplish this, the Zetasizer uses a 5 mW helium-neon red laser at a wavelength of 633 nm.[58] The beam is split and reflected such that one of the two beams is modulated so that it is out of phase with the unchanged portion of the original beam. The two are then directed with mirrors so that they cross in the cell.

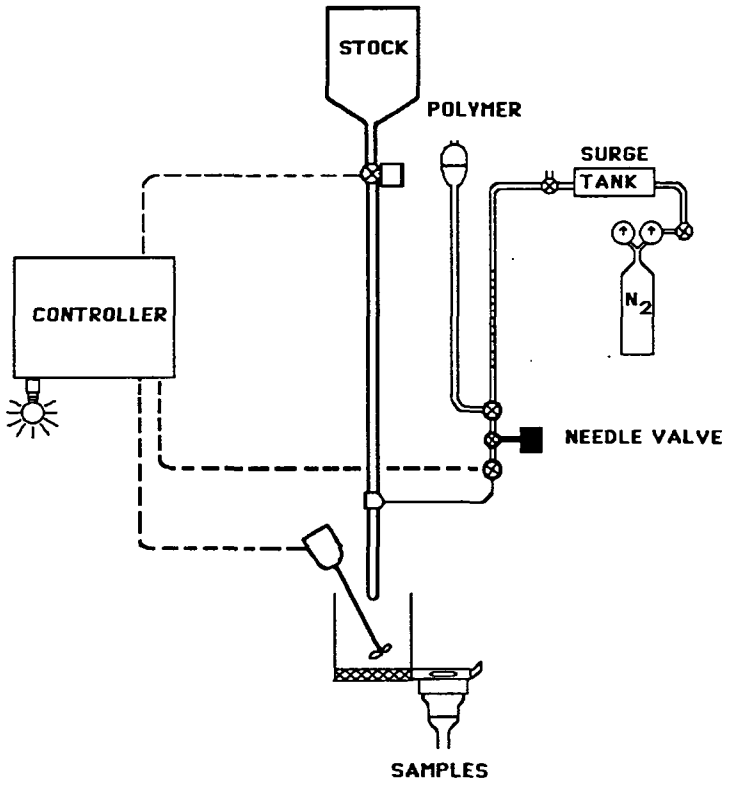

Figure 4. Experimental apparatus for polymer adsorption onto latex particles and cotton linters.

The crossing of two laser beams forms a fringe area consisting of high and low intensity light or lines of constructive and destructive interference, Fig. 7, which moves in a direction parallel to the applied field. When a particle passes through this probe volume, the particle scatters light at a frequency proportional to its velocity. The scattered light is captured by a photomultiplier tube and the generated frequency evaluated in a 64 channel correlator to provide the electrophoretic mobility or zeta potential distributions.[58] The particle direction is determined by making one of the laser beams slightly out of phase with the other. An example distribution of standard latex 2-27-92, particle size 0.29 μm, provided by Interfacial Dynamics Corporation is given in Fig. 8. The

distribution of the latex prepared for this thesis is given in Fig. 9. These distributions were calculated by the Zetasizer from approximately 2000 particle counts, that is, 2000 velocity determinations.

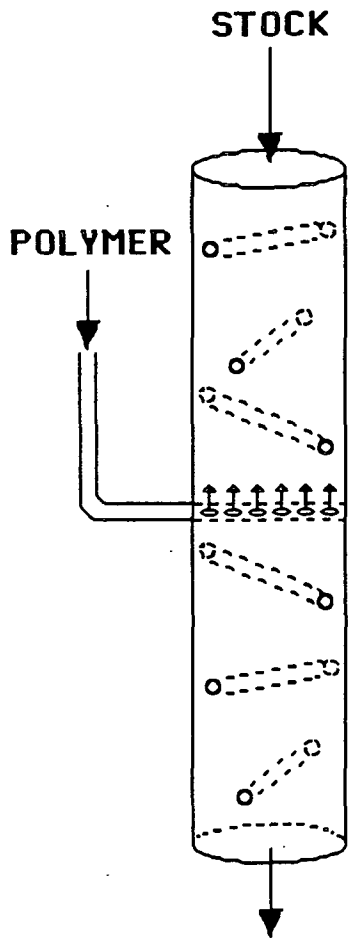

Figure 5. Mixing zone including static mixer bars and multiport wand injector.

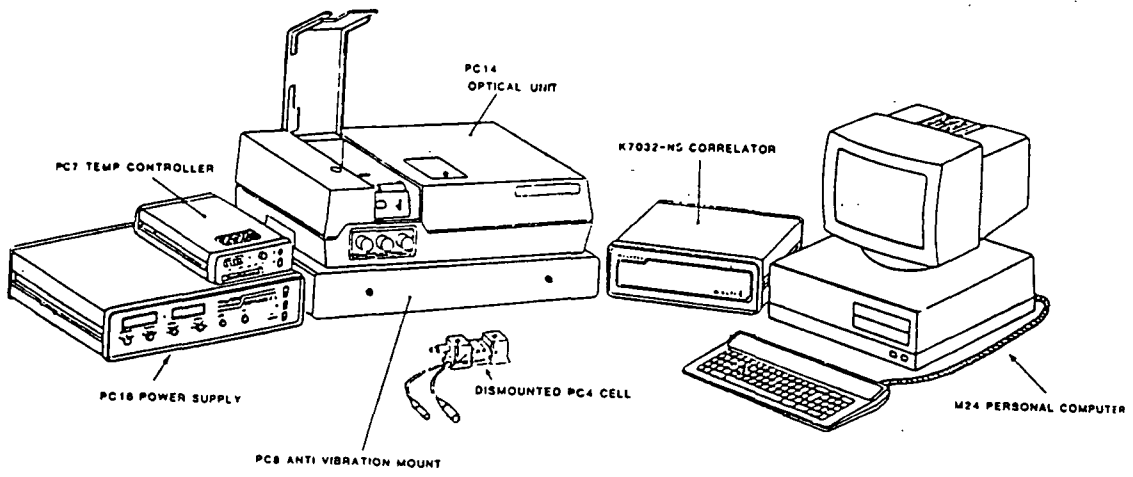

Figure 6. The Malvern Zetasizer IIC.[58]

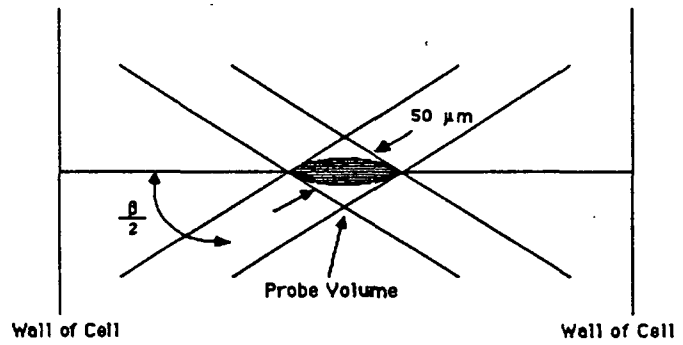

Figure 7. Laser fringes in the probe volume of two crossing laser beams.

Britt Dynamic Drainage Jar

The Britt Dynamic Drainage Jar (DDJ) used in this study was modified in two ways. First, an air line was added to create an air pad underneath the screen to prevent any premature drainage through the wire.[37] There were also four one-half inch baffles installed in the DDJ at 90° intervals to increase mixing in the jar. A stirrer speed of 750 rpm was used throughout the experiments.

```
MALVERN     ZETASIZER   II  c
sample  : standard

 Live data from correlator  Cell type  1
Refractive Index 1.33 Viscosity  0.8905  Dielectric const.  80.0 Temperature 25.0

      f(Hz)    MOBILITY (Mic/sec / Volt/cm)                          % VALUE
-----------------------------------------------------------------------------
21    313.7   -1.44   |+                                              (  0.0)
22    322.7   -1.64   |+                                              (  0.0)
23    331.6   -1.84   |+                                              (  0.0)
24    340.6   -2.04   |+                                              (  0.0)
25    349.6   -2.25   |+                                              (  0.0)
26    358.6   -2.45   |+                                              (  0.0)
27    367.6   -2.65   |+                                              (  0.0)
28    376.6   -2.85   |—+                                             (  0.8)
29    385.5   -3.06   |——+                                            (  1.7)
30    394.5   -3.26   |———+                                           (  3.2)
31    403.5   -3.46   |————+                                          (  5.7)
32    412.5   -3.67   |—————+                                         (  8.2)
33    421.5   -3.87   |——————+                                        ( 10.7)
34    430.5   -4.07   |———————+                                       ( 13.3)
35    439.5   -4.27   |———————+                                       ( 13.8)
36    448.4   -4.48   |——————+                                        ( 11.3)
37    457.4   -4.68   |—————+                                         (  8.1)
38    466.4   -4.88   |————+                                          (  5.1)
39    475.4   -5.08   |———+                                           (  2.6)
40    484.4   -5.29   |—+                                             (  1.2)
41    493.4   -5.49   |-+                                             (  0.3)
42    502.3   -5.69   |+                                              (  0.0)
43    511.3   -5.90   |+                                              (  0.0)
44    520.3   -6.10   |+                                              (  0.0)
45    529.3   -6.30   |+                                              (  0.0)
46    538.3   -6.50   |+                                              (  0.0)
47    547.3   -6.71   |+                                              (  0.0)
48    556.3   -6.91   |+                                              (  0.0)

02:41:15 Mean value  -4.16      Xwidth   10.9 Integration Limits  30 to  39
 Cell Voltage   99.3   Field strength (V/cm)   19.9
```

Figure 7. Standard latex, 2-27-92, mobility distribution.

```
MALVERN     ZETASIZER   II  c
sample  : LATEX, pH 6.0, 0.01 M NaCl

 File data from b:mark.3 block : 1 Cell type  1
Refractive Index 1.33 Viscosity  0.8905  Dielectric const.  80.0 Temperature 25.0

      f(Hz)    MOBILITY (Mic/sec / Volt/cm)                          % VALUE
-----------------------------------------------------------------------------
27    367.6   -2.63   |+                                              (  0.0)
28    376.6   -2.83   |+                                              (  0.0)
29    385.5   -3.03   |+                                              (  0.0)
30    394.5   -3.23   |+                                              (  0.0)
31    403.5   -3.43   |+                                              (  0.0)
32    412.5   -3.63   |+                                              (  0.0)
33    421.5   -3.83   |+                                              (  0.0)
34    430.5   -4.03   |+                                              (  0.0)
35    439.5   -4.23   |+                                              (  0.0)
36    448.4   -4.43   |+                                              (  0.0)
37    457.4   -4.63   |+                                              (  0.0)
38    466.4   -4.83   |+                                              (  0.0)
39    475.4   -5.03   |+                                              (  0.0)
40    484.4   -5.23   |+                                              (  0.0)
41    493.4   -5.43   |-+                                             (  0.4)
42    502.3   -5.64   |——+                                            (  1.9)
43    511.3   -5.84   |———+                                           (  4.2)
44    520.3   -6.04   |————+                                          (  7.1)
45    529.3   -6.24   |——————+                                        (  9.7)
46    538.3   -6.44   |———————+                                       ( 11.1)
47    547.3   -6.64   |———————+                                       ( 11.6)
48    556.3   -6.84   |———————+                                       ( 11.2)
49    565.2   -7.04   |—————+                                         (  9.2)
50    574.2   -7.24   |————+                                          (  5.8)
51    583.2   -7.44   |———+                                           (  2.9)
52    592.2   -7.64   |—+                                             (  1.0)
53    601.2   -7.84   |+                                              (  0.0)
54    610.2   -8.04   |+                                              (  0.0)
55    619.1   -8.24   |+                                              (  0.0)
56    628.1   -8.44   |+                                              (  0.0)
57    637.1   -8.65   |+                                              (  0.0)
58    646.1   -8.85   |+                                              (  0.0)
59    655.1   -9.05   |+                                              (  0.0)
60    664.1   -9.25   |+                                              (  0.0)
61    673.0   -9.45   |+                                              (  0.0)
62    682.0   -9.65   |+                                              (  0.0)
63    691.0   -9.85   |+                                              (  0.0)

Mean value  -6.59      Xwidth    6.8 Integration Limits  42 to  51
Cell Voltage  100.3   Field strength (V/cm)   20.1
```

Figure 8. Electrophoretic mobility distribution of the latex used in this study.

PROCEDURES

Determination of System Parameters

Adsorption time of polyacrylamide onto oxidized cotton linters

The adsorption of polyacrylamide onto cotton linters was studied to determine the length of time required for 90% of the polymer to adsorb onto the latex. The procedures used for this experiment are given in Appendix IV. The latex was calculated to have a surface area of 12.5 m^2/g. This is 12.5 times that of the linters. Therefore, if sufficient time is given for adsorption onto the linters, the time required for the adsorption of the polymer onto the latex will be much less. Based on the data given in Fig. 10, mixing periods of two minutes for fibers and one minute for latex were selected for 90% adsorption. The line drawn is not a regression line but an indication of the trend generally observed in adsorption data.

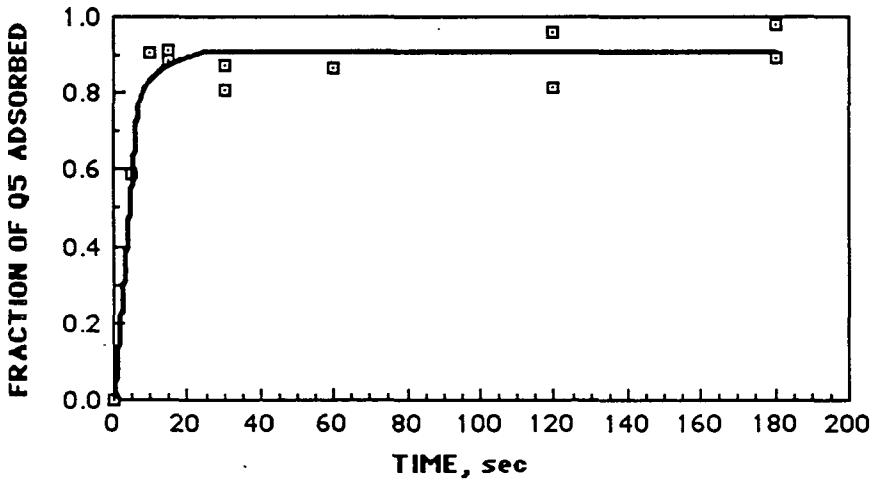

Figure 10. Results of experiment to determine time required for 90% adsorption onto oxidized cotton linters at a dosage of 1.5 mg/g based on 1.5 od g furnish in headbox.

Timing for the polymer injection system

Several parameters were evaluated to fix the operating conditions of the injection system. The first was the volume of sample to be treated. Once a sample size of 200 mL was chosen, the timing system parameters, injector delay and duration, could be determined to ensure proper treatment of the sample. Based on the geometry of the polymer injection system and the 200 mL sample size, the delay before injection was determined to be 0.5 s. This is the time required for the initial sample to fall from the top jar to the multiport wand injector. The period of time during which the sample is passing by the wand, the injector duration, was determined to be 1.5 s.

Measurements on the Zetasizer IIC

Accuracy of the Zetasizer IIC

Recent literature has suggested that single beam instruments such as the Zetasizer do not provide an accurate representation of the mobility distribution. Oja and Bott[59] recently reported that the percent width or standard deviation of the mobility distribution is a function of two components: Brownian motion and actual mobility variations. They state that Brownian diffusion broadening becomes dominant as particle size decreases because diffusion broadening is proportional to the square of the scattering vector. Recalling Eq. 9, the scattering vector is a function of the scattering angle. Therefore, Oja and Bott[59] believe that multiple angle measurements are needed to determine the effect of Brownian motion. The electrophoretic heterogeneity broadening is a linear function of the scattering vector and can be masked by the Brownian "interference."

Malvern Instruments, Ltd. does recognize Brownian motion as a possible source of distribution broadening.[58] When a sample is measured, an autocorrelation function is developed from the intensity of light scattered by the particles being measured. The autocorrelation function is approximated by a damped cosine wave whose periodicity reflects the velocity distribution. This damping is a result of EM distributions and Brownian motion. Malvern, however, feels that the effect of Brownian motion is small.[60] Consequently, there is no compensation for any effects of the Brownian motion in the system software. Comparative testing between single and multiangle instruments gave the same results indicating that the technology of multiangle instruments enhanced only particle size measurements not mobility measurements.[60]

The multiple angle approach has been used by Sanders and Schaefer[10] with a papermaking system. However, in their work, conclusions were not drawn regarding the effect of Brownian motion and how this affected the mobility distributions. In the present work, the effects of Brownian motion were assumed to be negligible. These effects become more dominant as particle sizes diminish below 1 μm. Since the size of the latex particles used in this study were 0.47 μm, the effects of Brownian motion was assumed to be small. Also when the latex was flocculated the particle sizes would be 0.94 μm and 1.41 μm for a doublet and triplet, respectively.

Reproducibility of Zetasizer measurements

The 50-2 series was chosen as a central point in the design to check the reproducibility of the entire polymer injection procedure. The goal was to see whether the average electrophoretic mobility could be reproduced for each sample in the series. One month after this series was run for the first time, it was re-run. The electrophoretic mobility results are given in Fig. 11. It can be seen

that the reproducibility was quite good for all samples in the series as the line in Fig. 11 is a 1:1 line, not a best fit line. After finding the trend in Fig. 11, it was decided that no further duplicates were required and that the polymer injection system and mixing procedures were satisfactory. The mobility distributions were also reproduced. This is discussed on pages 60-62.

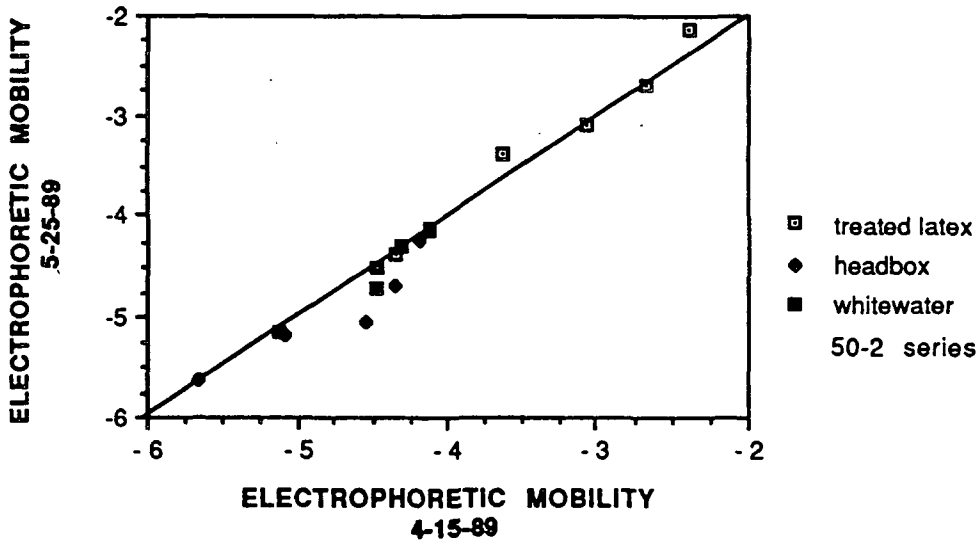

Figure 11. Reproducibility of 50-2 series on two different days. Line drawn is 1:1.

Reproducibility of focusing on the stationary layer

Before samples can be measured, the laser beams must be focused on the stationary layer of the quartz cell. To focus the instrument, a particle suspension, in this thesis standard latex 2-27-92, was injected into the capillary. The walls of the cell were then located with the aid of a small magnifying eyepiece. The coordinates of the wall were entered into the computer, which returned the stationary layer coordinates.

The accuracy of the focusing procedure was also tested with the standard latex 2-27-92. The mobility of this standard was checked at the two stationary layers to see whether the values agree. This was done by making a cell profile, that is, by moving the laser beam cross section across the cell from wall to wall. The profile should be flat and symmetrical as demonstrated in Fig. 12. This standard latex has been demonstrated to have an average electrophoretic mobility of -4.19 (μm/s) / (volt/cm) based on 26 such standardizations. These standardization tests also give an indication of the variability of the Zetasizer since the standard deviation about the mean was 0.048 (μm/s) / (volt/cm). All measurements on the Zetasizer were made at the stationary layer closest to the photomultiplier tube.

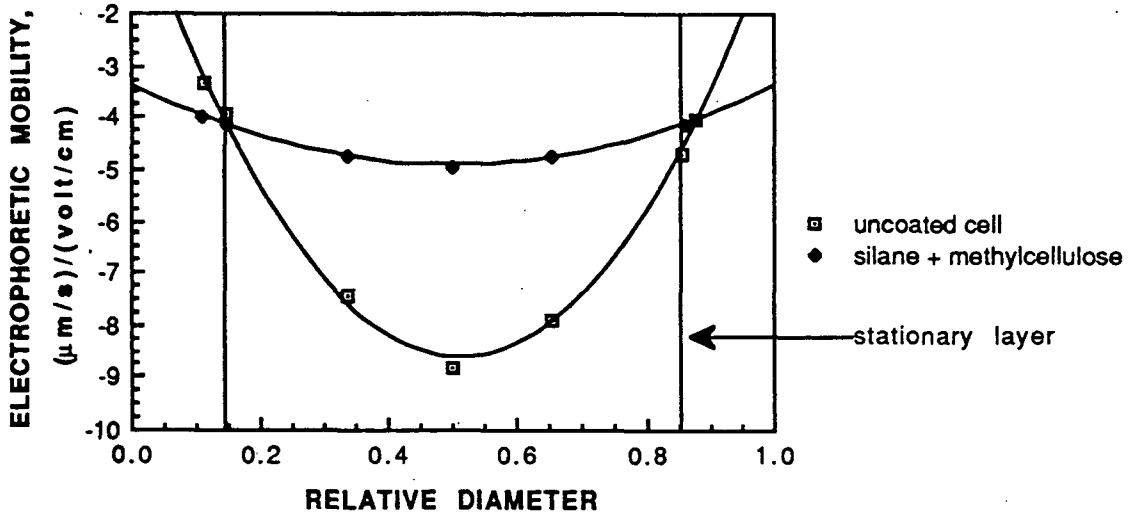

Figure 12. Example cell profile also showing effectiveness of cell coating.

Figure 12 also indicates that the cell was treated with a silane and methylcellulose coating to obtain the flat profile desired. The stability of the mobility profile across the cell was an area of great concern. With the Zetasizer, the mobility of the latex particle or any other particle is calculated from a

determination of the particle's velocity in the cell using laser Doppler anemometry. The glass cell, when filled with an electrolyte such as 0.01 M NaCl as used in this study, has a charge which arises from the ionization of surface groups.[7] When the electric field is generated between the two electrodes, electroosmotic as well as electrophoretic flows are generated. The laminar flow profile is shown in Fig. 13.

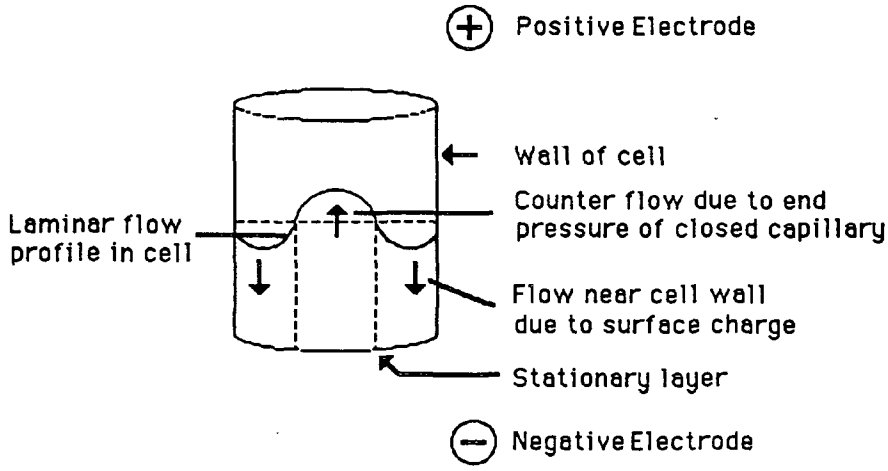

Figure 13. Flow profile in an electrophoresis cell with closed ends.

Measurement of the mobility must take place at the stationary layer where the electroosmotic flow is zero. However, since this stationary layer is infinitely thin, electroosmosis is always a source of error.[61] This error can be reduced if the slope of the profile line can be reduced at the stationary layer. The velocity profile can be flattened by coating the surface of the glass cell with a neutral polymer. Methylcellulose has been used as a coating because it contains few charged groups and the long polymer chains extend beyond the double layer (Debye length) giving rise to a near zero zeta potential near the cell wall.[62]

Coating of capillaries to minimize electroosmotic effects

Several coatings and coating variations were used in an attempt to flatten the cell profile. The effectiveness of methylcellulose as a coating was demonstrated by Herren.[62] An example profile from Herren's work is shown in Fig. 14. Goulet[63] was able to coat a Zetasizer cell with hydroxypropyl methylcellulose, Dow Methocel™ J75MS-N, which provided a slightly curved profile. This coating was applied by soaking the cell in a 0.1 % Methocel™ solution at pH 6. This coating lasted over three months. Coatings of Pierce SurfaSil™ and polyethylene glycol were found by Goulet to be ineffective.

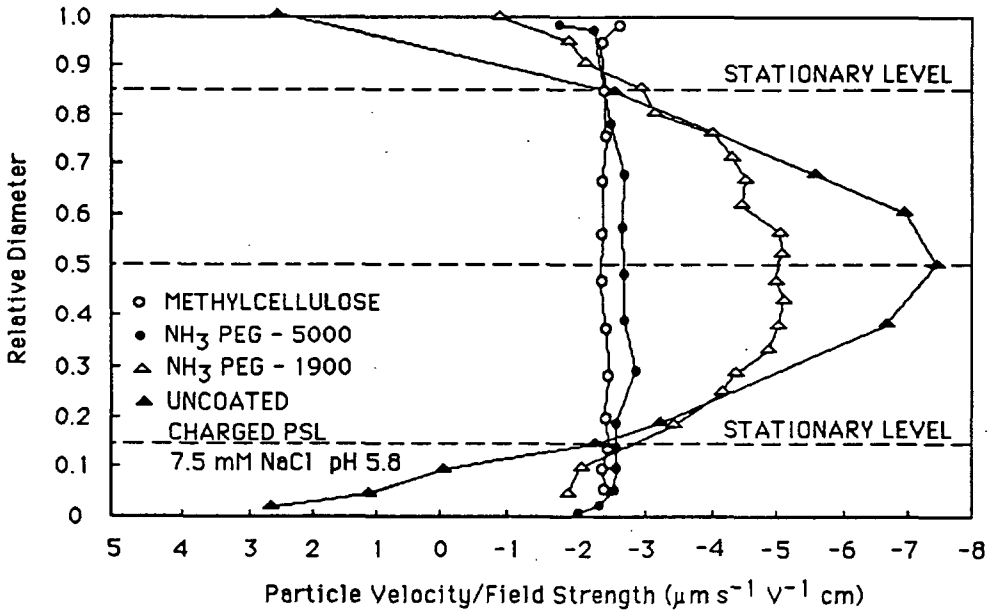

Figure 14. Degree of electroosmosis in uncoated and coated capillaries.[62]

Goulet's procedure was repeated in an attempt to coat another cell with Dow Methocel™. His procedure, however, was unsuccessful at pH 6.0 and pH 9.0. The literature has shown that methylcellulose coatings wash off within a day or two.[61,64] It is not known why Goulet's coating lasted three months.

It has been suggested that methylcellulose coatings will remain for a longer period of time if the glass or quartz cell is pretreated with a silane, such as Aldrich γ-glycidoxypropyltrimethoxysilane.[62,63] It is hypothesized by Nordt[61] that the silane forms covalent and hydrogen bonds with the glass as shown in Fig. 15. A reaction mechanism for the pretreatment and subsequent methylcellulose coating is given in Fig. 16.

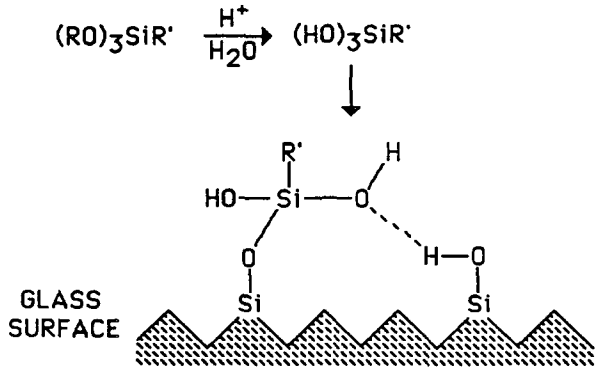

Figure 15. Silane attachment mechanism showing covalent and hydrogen bonding.[61]

Results of coating stability experiments

The latex used in the stability experiments was the standard latex 2-27-92. Coatings with methylcellulose in the absence of silane binder provided an effective but non-permanent reduction in electroosmosis. Use of the silane alone as a coating did not produce as flat a profile as desired. Pretreatment of the glass cell with silane followed by coating with methylcellulose proved to be quite effective (recall Fig. 12). These coatings generally lasted two months. The exact procedure for coating Zetasizer cells is given in Appendix V.

Several cells were coated with silane, dried, and kept in a desiccator until needed. The cells were then coated with methylcellulose and placed in the

Zetasizer. Profiles of the standard latex, as mentioned before, were run at the beginning of each day to ensure the proper operation of the Zetasizer and the stability of the cell coating.

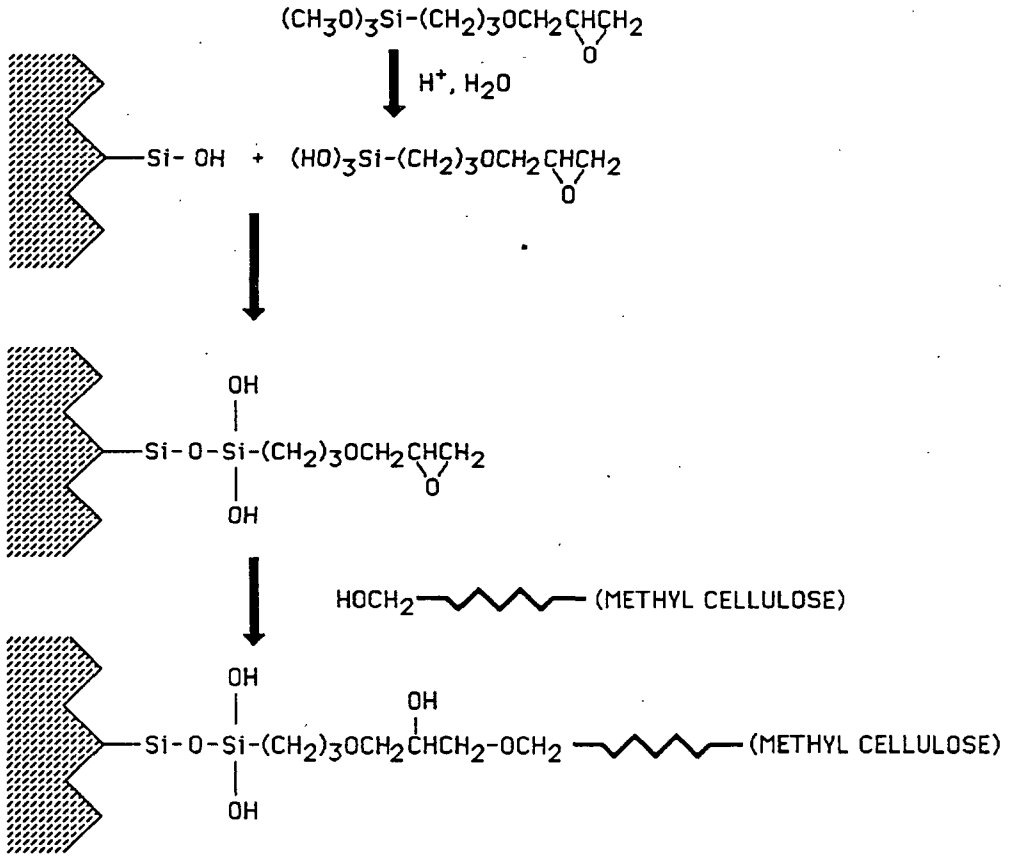

Figure 16. Reaction mechanism proposed by Nordt for the binding of methylcellulose to glass by silane.[61]

Determination of Retention

An absorbance method was first used to determine the concentration of latex in the whitewater samples. This method, however, included a bias toward higher retentions. This bias is explored in Appendix VI. Consequently, a gravimetric approach was pursued. This method was not without its problems. First and foremost was the measurement of dry weights of 0.03 g or less depending on the retention. To achieve these weights, 50-60 mL

samples of the whitewater were placed in Pyrex bottles which had a tare weight of approximately 100 g. Therefore, cleanliness and an accurate tare weight of the bottles were crucial.

Another problem associated with this method is the contribution to dry weight by the background electrolyte in the water. Therefore, all volumes of 0.01 M NaCl used for each sample and the whitewater sample wet weights were recorded so that the amount of salt in the whitewater sample could be calculated and subtracted from the whitewater sample dry weights. This correction for salt weight proved to be accurate to ±1% in experiments with samples of known salt and latex concentrations.

Reproducibility of retention measurements

The reproducibility of the retention experiments was determined by running sample 50-2-67 seven times with each test run in triplicate. The sample average retention for these seven trials was 65.4%. The standard deviation of the means was 9.1; therefore, the confidence interval about the sample mean was 65.4 ± 8.4 at a 95% confidence level. This interval is given as an error bar in each of the retention graphs presented later in the Retention Results section. This error is somewhat large, but considering the small weights obtained with the gravimetric method, this error is not unreasonable. The error will also decrease with decreasing retention since the weight in the whitewater increases giving larger dried weights. Thus, the rationale behind choosing the 50-2-67 sample was its high retention (higher error) and central location in the design.

The error within each sample was generally smaller. If the 21 individual determinations in the seven trials above are compared, the average is

again 65.4% and the standard deviation is 9.4. Hence at 95% confidence, the interval about the mean is 65.4 ± 4.3. This may be a better indication of the error involved in the gravimetric method, but statistically the interval of ±8.4 is strictly correct, since the reproducibility of the mechanism of retention is desired.

Particle Size

The Coulter Counter® (model TAII, Coulter Electronics, Inc.) was used to determine the particle size of treated and untreated latex samples. This instrument uses electrical resistance to measure particle volumes. As an aggregate or particle passes through the aperture (18 μm in this case), the resistance of the electrolyte background between the two electrodes is changed. The resulting voltage pulse is proportional to the aggregate volume. Particle volumes are then counted and collected in sixteen channels. The lower boundary of each channel is twice the volume represented at the lower boundary of the preceding channel. The number of particles in the aggregate can then be calculated using the volume of a single particle and the volume represented by each channel. The volume and number of singlets represented by each channel is shown in Table 2.

Table 2. Coulter Counter® floc sizes by channel for an 18 μm aperture.

Channel Number	Volume, μm^3	Radius of Equivalent Sphere, μm	Number of Singlets*
3	<0.065	0.500	1
4	<0.131	0.630	2
5	<0.262	0.794	3-4
6	<0.524	1.000	5-8
7	<1.047	1.260	9-13

* based on volume of 0.47 μm diameter sphere.

Because an 18 μm aperture was used, a 4% NaCl electrolyte background was required instead of the 1% generally used with larger apertures. The background electrolyte was also filtered 10 times through a 0.22 μm Millipore® filter to remove particulate impurities.

Before a sample is run, the instrument must be calibrated with a standard monodispersed polystyrene latex particle. The volume of this standard particle should fall in channel five or six. It is desired to have channels one, two, 15, and 16 open to collect any noise signals. These channels can then be easily subtracted out of the distribution without losses in actual particle size data. However, when the lower limit of an aperture is pushed, the data of interest may fall in channels two or three. The data should not be allowed to fall in channel one; when this occurs a smaller aperture should be used. If particle size data fall in the lower channels, background noise readings should be taken of the electrolyte alone. Once the noise level is determined, the sample can be run.

Designed Experimental Procedure

Three furnish fractions were required for the experimental runs--the fibers (1.2 od g), the latex to be treated, and the latex which remained untreated (latex total, 0.3 od g). The amount of treated and untreated latex depends on the conditions in the experimental design, which is given in Table 3 and Appendix VII. The design indicates the partitioning of the polymer dosage between the furnish fractions. The "treated latex" column indicates the weight of latex to be treated with Q5. The first entry, 0.06 od g, indicates that for each polymer dosage only 20% of the latex was treated. The remaining 0.24 od g latex was untreated.

The actual amount of polymer adsorbed onto the latex depended on the percentage dosage split between the fibers and fraction of latex to be treated. This split is given in Table 3 in the "latex, fiber" column under each polymer dosage. For example, the first entry under the 1.0 mg/od g dosage, *100, 0%*, indicates that 100% of the Q5 was adsorbed onto 20% of the total latex. Thus, a "polymer loading" of the sample, Φ, can defined by

$$\Phi = D\left(\frac{1.0\ g}{1000\ mg}\right)\left(\frac{1.5\ od\ g\ furnish}{0.3\ od\ g\ latex}\right)\left(\frac{1.0\ od\ g\ furnish}{L/100}\right)(1 - F) \qquad [12]$$

where,

D = polymer dosage, mg Q5/od g furnish
L = portion of latex treated, %
F = fraction of polymer dosage on fibers.

In words then, the polymer loading is the amount of Q5 adsorbed onto the treated latex fraction of the headbox furnish. The weight of Q5 used is the total dosage weight less the fraction adsorbed onto the fibers. Therefore, the polymer loading is an indication of the amount of polymer added to the oven-dried weight of treated latex. Polymer loadings for each run are given with the retention data in Appendix XIV.

A flow diagram showing the furnish fractions and mobility sampling points is given in Fig. 17. The distribution of Q5 between the latex and fiber fractions, as noted above, depend on the experimental design. Samples for electrophoretic mobility analysis, 10 mL each, were taken from the treated latex sample, the headbox latex or "fines" sample, and the whitewater sample. Thus after polymer treatment and EM sampling, the Britt jar contained 500 mL of furnish consisting of 80% fiber (1.2 od g) and 20% latex (0.3 od g).

Table 3. Experimental design.

TREATED LATEX	POLYMER DOSAGE		
	0.5 mg/g furnish	1.0 mg/g furnish	1.5 mg/g furnish
	latex, fiber	latex, fiber	latex, fiber
0.06 od g	100, 0%	100, 0%	100, 0%
(20%)	80, 20	80, 20	80, 20
	67, 33	67, 33	67, 33
	50, 50	50, 50	50, 50
	33, 67	33, 67	33, 67
0.15 od g	100, 0%	100, 0%	100, 0%
(50%)	80, 20	80, 20	80, 20
	67, 33	67, 33	67, 33
	50, 50	50, 50	50, 50
	33, 67	33, 67	33, 67
0.225 od g	100, 0%	100, 0%	100, 0%
(75%)	80, 20	80, 20	80, 20
	67, 33	67, 33	67, 33
	50, 50	50, 50	50, 50
	33, 67	33, 67	33, 67
0.30 od g	100, 0%	100, 0%	100, 0%
(100%)	80, 20	80, 20	80, 20
	67, 33	67, 33	67, 33
	50, 50	50, 50	50, 50
	33, 67	33, 67	33, 67

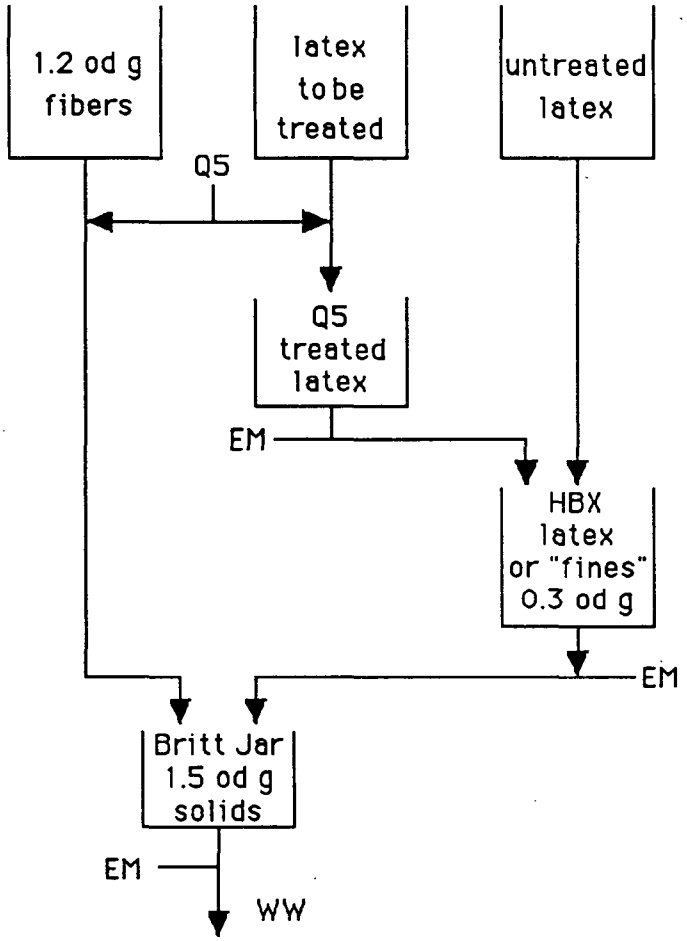

Figure 17. Experimental program for the treatment of furnish and electrophoretic mobility sampling points.

The conditions for an example experiment are listed in Table 4. This run was designated 75-3-67 where 75 indicated the percentage of latex treated with Q5, 3 indicated Q5 dosage in (lb/ton), and 67 indicated the fraction of the total dosage which was adsorbed onto the fibers. Thus the polymer loading for this experiment is

$$\Phi = (1.5)\left(\frac{1}{1000}\right)\left(\frac{1.5}{0.3}\right)\left(\frac{1}{75/100}\right)(1 - 0.67) = 0.0033 \text{ mg/od g treated latex.}$$

The correct amount of fiber for 1.2 od g (120 g @ 0.99% consistency) was weighed into a 400 mL polypropylene beaker and diluted to a total weight of 200 g. The latex suspension for the treated fraction (20.5 g @ 1.099% solids) and the latex for the untreated fraction (6.8 g @ 1.099% solids) were weighed separately into a 400 mL and 150 mL polypropylene beaker, respectively. These samples were diluted to total weights of 200 and 115 g, respectively. All samples were covered with Parafilm® to reduce evaporation and contamination.

Table 4. Example: conditions used for experimental run, 75-3-67.

Polymer Dosage	1.5 mg/g furnish (3 lb/ton, hence 3 in label)
Cotton Linter Solids (Consistency)	0.991%
Polystyrene Latex Solids	1.099%
Fraction of Dosage on Fibers	67%
Fraction of Latex Treated	75%
Electrolyte Background	0.01 M NaCl
pH	6.0 ± 0.05

The polymer solution was prepared such that 5 mL would correspond to a dosage of 1.5 mg/g. Since the fraction of polymer on the fibers is 67%, 3.3 mL Q5 were added to the fibers, and 1.7 mL Q5 were added to the latex fraction designated for treatment, in this case 75%. The fibers were treated first in the polymer delivery system which had been previously set to deliver 3.3 mL. After treatment in the polymer injection system, the fibers were mixed for one minute in the bottom jar. The treated fibers were removed from the polymer injection system and agitated at 200 rpm in the modified Britt jar used for retention measurements.

While the fibers were mixing in the Britt jar, the polymer delivery valve was adjusted to inject 1.7 mL into the latex sample. Following polymer injection, the treated latex sample mixed for one minute in the bottom jar of the polymer delivery system, after which a 10 mL sample was removed for electrophoretic mobility analysis. The balance of the sample was transferred from the bottom jar of the polymer injection system to a 400 mL polypropylene beaker. The untreated latex fraction in the 150 mL polypropylene beaker was then poured into the polypropylene beaker containing the treated latex to form the "headbox filler" sample. This mixture was allowed to mix at a constant rate with a magnetic stir bar for an additional two minutes.

While the headbox sample was mixing in the beaker, the 10 mL treated latex EM sample was diluted (approximately 5 mL in 150 mL water at pH 6.0 with an electrolyte concentration of 0.01 M NaCl) and injected into the Zetasizer IIC for analysis. After the two-minute mixing period for the headbox sample was completed, a 10 mL EM sample was removed and similarly diluted for electrophoretic mobility analysis. The remaining headbox sample was added to the Britt Jar containing the fibers as the mixer speed was quickly increased to 750 rpm.

After two minutes, the stopcock on the Britt Jar was opened and three whitewater samples (approximately 50 mL each) were collected after the first 50 mL of filtrate were discarded. A fourth whitewater sample was diluted for electrophoretic mobility measurement in the Zetasizer IIC. Latex retention was measured by gravimetrically determining the concentration of polystyrene in the whitewater. The three samples mentioned above were collected in pre-weighed, oven-dried 60 mL Pyrex bottles having ground glass lids. The lids were placed on each sample bottle after collection to minimize any evaporation losses.

The samples were then weighed to the nearest 0.0001 g. Upon removal of the lid, the bottles, including the lid, were placed in a forced air oven to dry at 105° C for at least five hours.

Latex retention was calculated from the amount of latex in the headbox (0.3 g) and the amount of latex in the dried whitewater samples. Determination of the weight of latex in each whitewater sample was complicated because the electrolyte in the water also contributed weight to each sample. This salt weight was subtracted from the dry weight since the initial salt concentration in the headbox, and the volume of the whitewater sample were both known.

The Zetasizer output data for the headbox, and whitewater samples of each run were entered into a computer for analysis and graphing. The data obtained from each run was a set of electrophoretic mobility distributions and averages for the treated, headbox, and whitewater latex samples and the retention under the stated design conditions.

CONDUCTANCE AND PH CONSIDERATIONS

Electrophoretic mobility has been shown to be dependent upon electrolyte concentration and pH.[8,65] For "simple" surfaces, increased electrolyte concentrations compress the double layer and cause mobilities to become less negative. This relationship, however, does not appear to be monotonic in tests with polystyrene latices.[66] The pH of the solution also contributes to changes in mobility depending upon the functional groups present on the particle surface. Variations in pH and conductance have been shown in biological systems, for example, to have such a pronounced effect on electrophoretic mobility that three-dimensional mapping or "fingerprinting" is required to quantify the

results.[44] Consequently, it was desired to keep these two variables, conductance and pH, constant in this work.

The specific conductance of each sample was maintained by making all dilutions and makeups with 0.01 M NaCl. The specific conductance, SC, was calculated for each sample from the voltage and current indicated by the Zetasizer IIC using Eq. 13.[63]

$$SC = 1000 \frac{I}{A} \frac{1}{V/L'} \qquad [13]$$

where

A = cell cross-sectional area, 0.13854 cm^2
L' = cell length between the voltage measuring electrodes, 5 cm
I = current
V = voltage.

A sampling of conductivities chosen randomly from all experimental runs is given in Appendix VIII.

Shaw[7] and Ma and co-workers[67] have shown that the mobility of polystyrene latex particles having sulfate functional groups is independent of pH in the range of 3-10. This trend was also seen in the present work in the pH range 6-10. The measured mobilities ranged from -6.4 to -6.7 (μm/s) / (volt/cm) with an average of -6.6 (μm/s) / (volt/cm) which is equivalent to the mobility previously reported at pH 6.0 for the latex used in this study (-6.59). As a precaution however, the pH was kept constant at 6.0 ± 0.05.

RESULTS AND DISCUSSION

ELECTROPHORETIC MOBILITY RESULTS

A linear relationship was found between headbox mobilities and the amount of polymer added. This relationship, Fig. 18, was also dependent on the percentage of latex treated. The polymer loading (abscissa) was defined as the weight of polymer added per dry weight of latex treated. At a given polymer loading, the average headbox mobility increased as more particles were treated. This was because the number of highly negative, untreated particles was decreasing. Since more particles were being treated, the average mobility would be expected to increase. The data in Fig. 18 were based on the weight of latex treated with Q5. The linear nature of the data can be seen more clearly in Fig. 19 where the 100% treated data line from Fig. 18 was expanded.

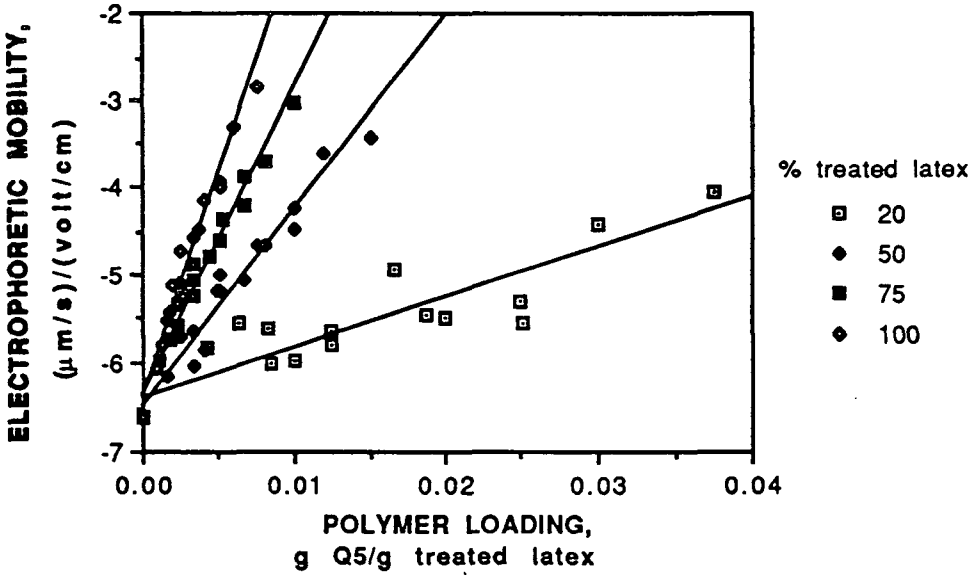

Figure 18. Headbox mobility vs. amount Q5 per treated latex weight.

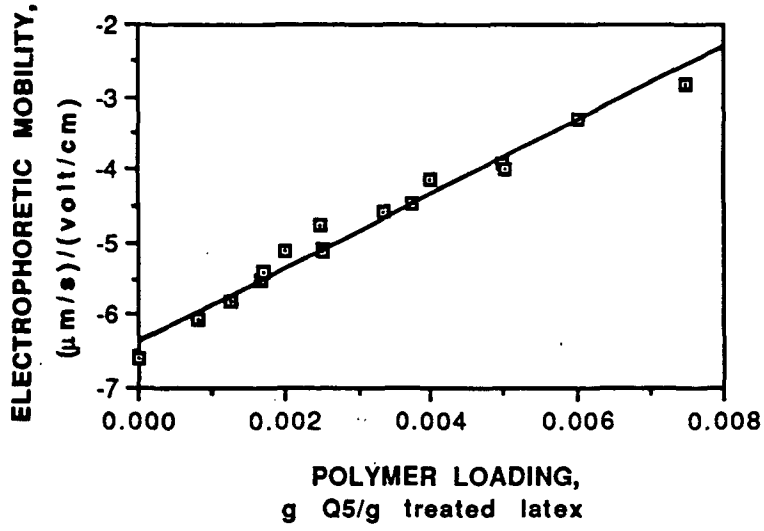

Figure 19. Enlargement of 100% treated data in Fig. 18.

Figure 20 resulted when the headbox mobility data in Fig. 18 and 19 were based on the total weight of latex. As the percentage of treated latex increased, the lines tended to approach the 100% treated line.

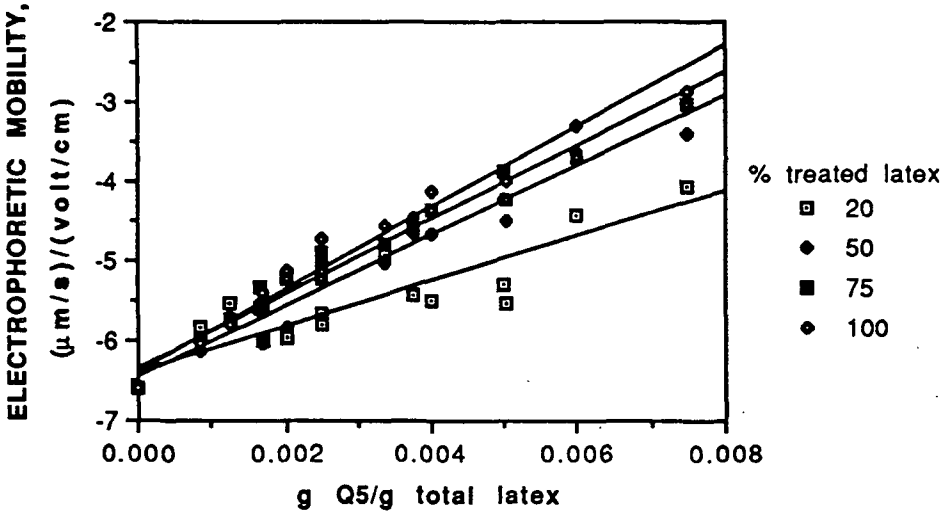

Figure 20. Headbox mobility vs. amount of polymer per total latex present.

Plotting the average mobility of the treated latex sample against polymer loading (Fig. 21) gave the range of mobilities within which this thesis investigated. Figure 21 also showed the response of the latex mobility with increasing amounts of adsorbed cationic polyacrylamide. It should be noted that the results in Fig. 21 were for the treated latex only. Figures 18-20 represent headbox data; hence, the samples in these figures contain added untreated latex (except for the 100% treated case). Consequently, the mobilities in Fig. 18-20 were more negative than those given in Fig. 21. This explained the presence of the positive values of mobility seen in Fig. 21 and not seen in the other figures.

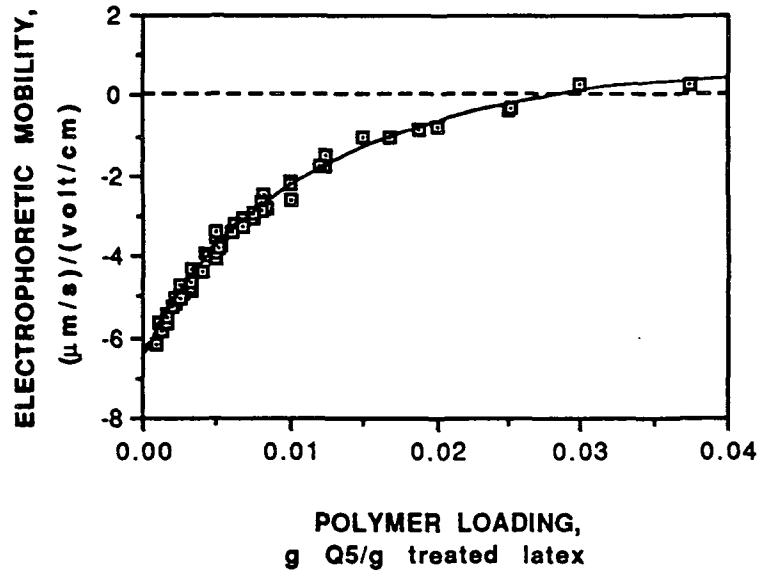

Figure 21. The effect of increasing polymer loading on the mobility of the treated latex sample.

The previous discussion centered on the average mobilities of the headbox and treated samples and how these averages were affected by Q5 adsorption. The following discussion involves the mobility distributions. The electrophoretic mobility distributions revealed which particles were

preferentially retained in the DDJ. An example set of distributions is seen in Fig. 22. In this sample 20% of the latex were treated with 33% of the total polymer dosage of 1.0 mg/g. That is, 67% of the dosage was placed on the fibers. The light-colored portions of the histogram depict the frequency of particles having a given mobility in the whitewater sample. The total frequency in each category is the headbox distribution. Both of these distributions were measured. The plotted values of the whitewater distribution were obtained by multiplying the measured frequencies by the factor (1-R), where R is the measured retention (the fraction of the latex retained in the DDJ). The darker sections represent the frequencies of those particles which were retained in the drainage jar. They were obtained by subtracting the whitewater frequency from the headbox frequency at each value of electrophoretic mobility. In this sample, the more negative particles were retained rather than the more positive ones.

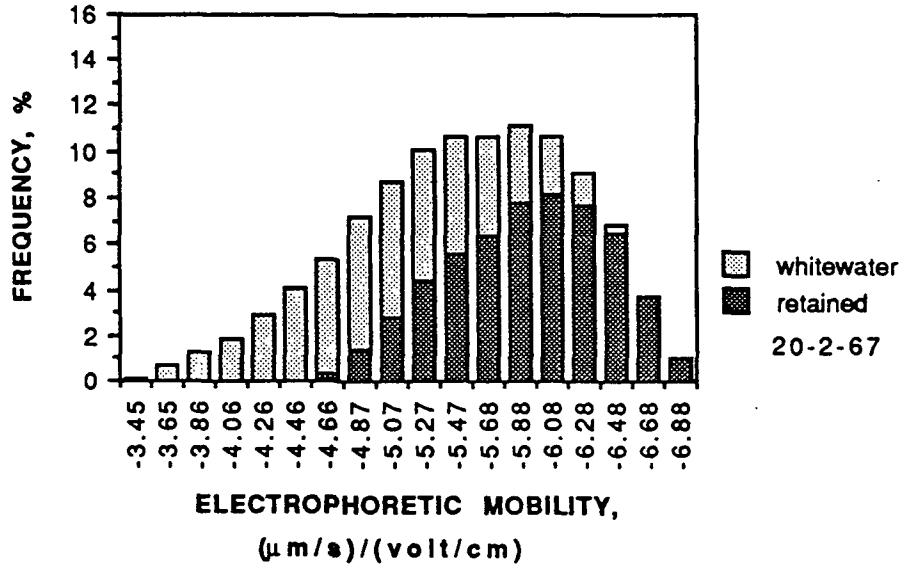

Figure 22. Mobility distributions for sample 20-2-67. Headbox distribution is the total frequency (the sum of whitewater and retained distributions).

The electrophoretic mobility distributions and averages of retained particles provided several interesting trends. In general, as more polymer was added to the fibers at the same percentage of treated latex, the average mobility of the retained particles became more negative. This trend is shown in Fig. 23 for all three dosages of polymer. When the percentage of treated latex was increased at the same polymer dosage level, the average mobility of the retained particles became less negative because more treated particles were retained (Fig. 24). The electrophoretic mobility distributions of all samples are given in Appendix IX. The averages can be found in Appendix X, and the standard deviations of the mobility distributions are given in Appendix XI.

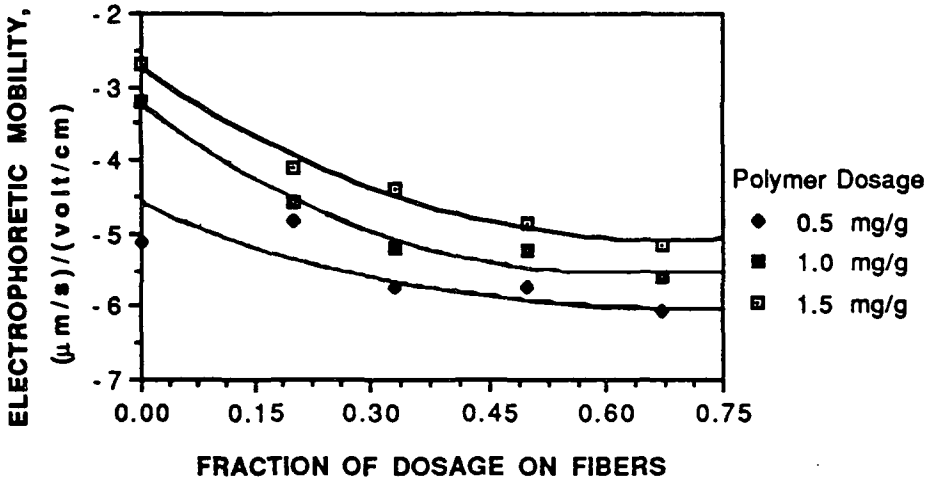

Figure 23. Effect of Q5 on mobility of retained particles at 75% treated latex level.

The preferential retention of more negatively charged particles at first was an unsettling result. It has been well documented that in some papermaking systems particles near their isoelectric point were retained better than those with higher charges.[12,38,68] This conclusion, however, was based on the mobility of the whitewater samples. It was assumed that the charged state of the long fiber fraction was either the same as the whitewater or unimportant.

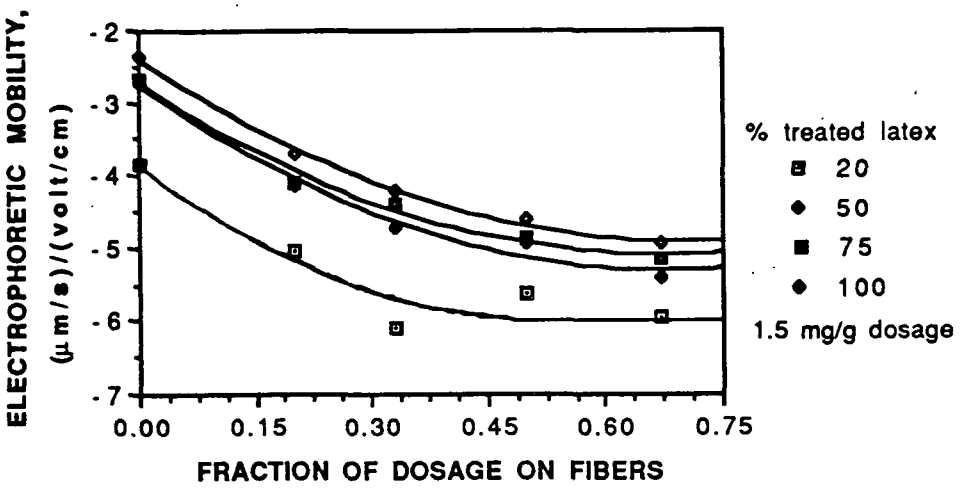

Figure 24. Effect of polymer partitioning on the mobility of retained particles at a constant polymer dosage.

In Fig. 25 and 26 the headbox, whitewater, and retained mobility distributions can be followed with increasing polymer dosage. Here the average mobility of the headbox, whitewater, and retained particles were -5.23, -5.27, and -5.10 (µm/s) / (volt/cm), respectively for 75-1-0 (a dosage of 0.5 mg/g). The average mobilities of the headbox, whitewater, and retained particles then changed to -3.04, -3.26, and -2.68 (µm/s) / (volt/cm), respectively, when the polymer dosage was increased to 1.5 mg/g (sample 75-3-0). Under these conditions, the retention changed from 15.2% to 22.3% with the 3-fold increase in Q5. So it appeared that for this sample, the retention increased with increasing (i.e. less negative) average mobilities. It was also apparent that the change in whitewater mobility with increasing polymer dosage did represent the trend seen in the headbox and retained sample mobilities.

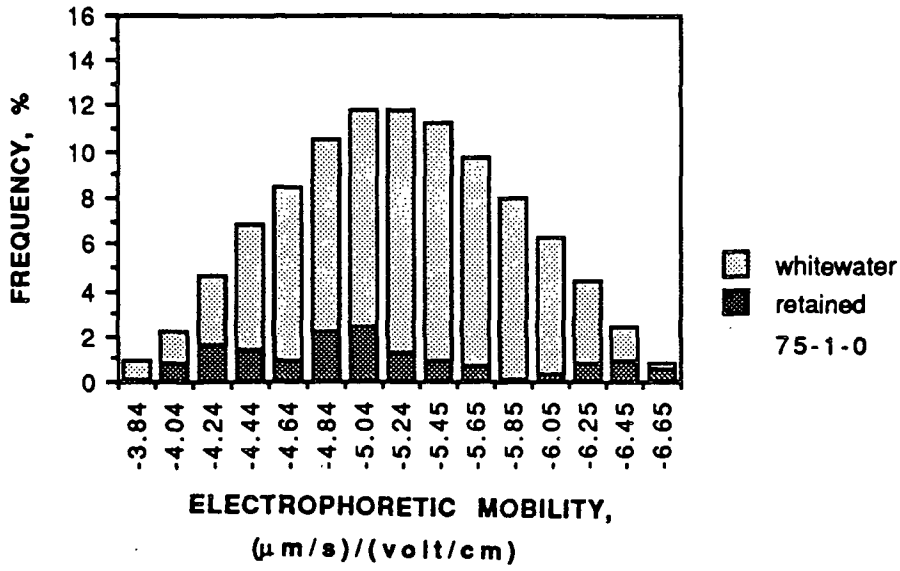

Figure 25. EM distributions for sample 75-1-0. Headbox distribution (total % frequency at each EM) is the sum of whitewater and retained distributions.

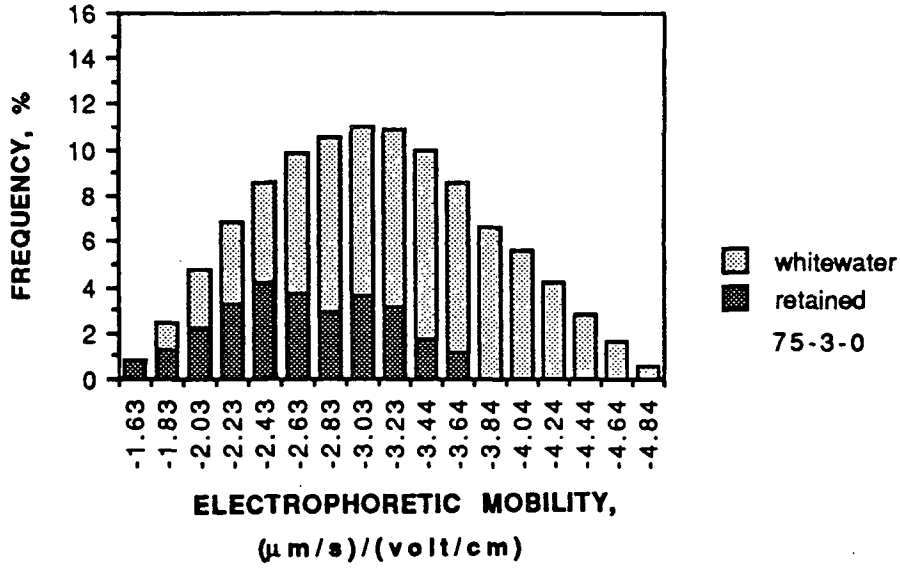

Figure 26. EM distributions for sample 75-3-0. Headbox distribution (total % frequency at each EM) is the sum of whitewater and retained distributions.

The retention of less highly charged particles was dependent upon whether the polymer was added to the fibers. This dependence was due to differences in polymer configuration when polymer was adsorbed onto the fibers versus the latex. The linters and latex should have different surface charge densities. Although the actual surface charge densities were not known, the mobilities of the two were quite different. The zeta potential of unmodified cotton linters was measured at -9.3 mV in 0.01 M NaCl by Herrington.[69] This corresponded to an electrophoretic mobility of approximately -0.75 (μm/s) / (volt/cm). This value of mobility would be expected to become more negative as the degree of oxidation was increased. Crow determined the mobility of the oxidized linters used in this study to be -1.0 (μm/s) / (volt/cm) in 0.01 M KCl.[51] Thus the zeta potential of the linters was much more positive than that of the latex (-6.6 (μm/s) / (volt/cm)).

Consequently, the polymer would be held tighter and closer to the latex surface than to the linters surface. Then the positive charges of the polymer would be more accessible to the bulk solution when adsorbed onto the fiber. This would explain why the more negatively charged particles were preferentially retained when polymer was adsorbed onto the fibers (Fig. 26 and 27). In these figures, the average mobility of those retained particles in sample 75-3-0 was -2.68 (μm/s) / (volt/cm) while the value for sample 75-3-50 was -4.85 (μm/s) / (volt/cm). This could also be viewed as the result of positive and negative charge interactions of the fiber and latex surfaces. The retention obtained in samples 75-3-0 and 75-3-50, 22.3 and 55.5%, respectively, also demonstrated that zero average zeta potential of the latex was not a prerequisite for increased retention.

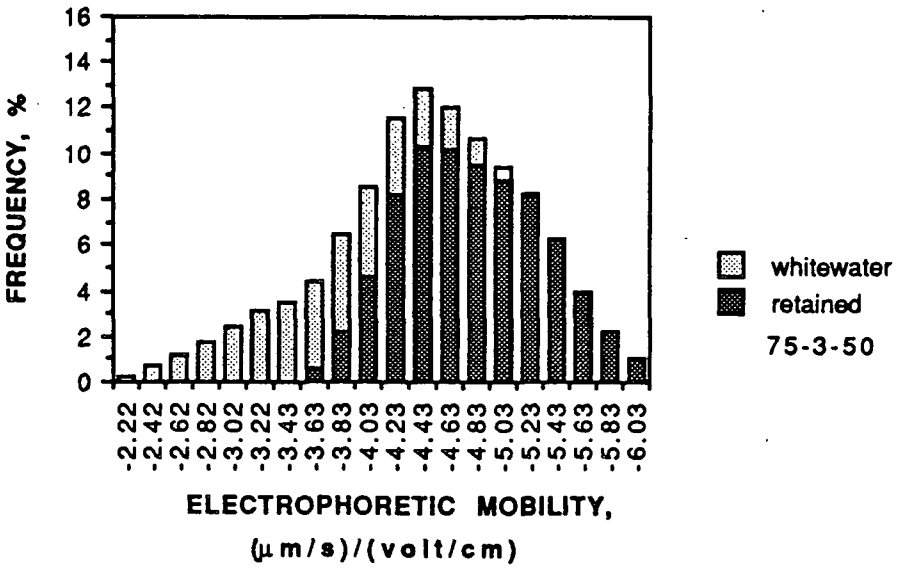

Figure 27. EM distributions for sample 75-3-50. Headbox distribution (total % frequency at each EM) is the sum of whitewater and retained distributions.

Several conditions existed in the design where the amount of polymer adsorbed on the latex was constant. The only change was whether or not the polymer was also added to the fibers. Such pairs, where the latex polymer loading was constant, were samples 20-1-0 and 20-2-50 and samples 100-2-0 and 100-3-33. In each case, the retention was much higher when the polymer was added to the fiber. The retention of sample 20-1-0 was 6.4% while the retention of sample 20-2-50 was 40.0%. This was due to the preferential retention of negative particles.

This preferential retention was evidenced by the headbox and whitewater samples. In each sample pair, the average headbox EM was the same value for each individual sample. For example, the average headbox EM of sample 100-2-0 was -3.93 (µm/s) / (volt/cm) and -3.95 (µm/s) / (volt/cm) for sample 100-3-33. The average whitewater EM for sample 100-2-0 was -3.99 (µm/s)

/ (volt/cm) when the fibers were untreated. Because all of the latex was treated, the headbox and whitewater mobilities were found to be similar as was expected. When polymer was added to the fibers in sample 100-3-33, the average whitewater EM was -3.02 (μm/s) / (volt/cm) which indicated a loss in the most negatively charged particles in the whitewater and the retention of these negative particles in the headbox.

The retention of sample 100-2-0 described above was 3.4%. Under the conditions of sample 100-3-33, the retention increased to 52.1%. Therefore, the retention was greatly increased even though the headbox mobilities were similar. This increase was brought about in part by the location of the polymer.

The increase in retention between 100-2-0 and 100-3-33 could also be attributed to an increase in polymer dosage. If the polymer dosage were kept constant, the retention would still change with polymer location. For example, sample 100-2-50 differed from 100-2-0 only in that half of the dosage was placed on the fibers. Consequently, the headbox and whitewater mobilities (-5.09 and -4.51 (μm/s) / (volt/cm), respectively) were more negative than those stated above for 100-2-0 (-3.93 and -3.99 (μm/s) / (volt/cm), respectively). The whitewater mobility was again more positive indicating the retention of negatively charged latex. A retention of 51.1% was obtained for sample 100-2-50. Hence, the location of polymer greatly affects the retention and the headbox and whitewater mobilities. As more polymer was directly adsorbed onto the fibers, increasingly negative particles were retained. As more polymer was adsorbed onto the latex, increasingly positive particles were retained. These observations showed that polymer treated latex particles were retained by attaching themselves to the fibers.

Reproducibility of mobility distributions

The average values of mobility were shown to be reproducible in an earlier discussion (see page 34). The mobility distributions, such as those given in Fig. 25-27, were also reproducible. An example was the 100-3-33 sample which was duplicated. The two sets of data are given in Table 4 and Fig. 28-29. Comparison of the headbox distributions showed that the frequencies of these two samples at a given mobility generally differed by less than 1.3%. The whitewater frequencies varied a maximum of 1.6% at any given value of mobility. The averages and standard deviations were similar. It should be noted that run 2 was a complete duplicate not a second measurement of the samples generated in run 1.

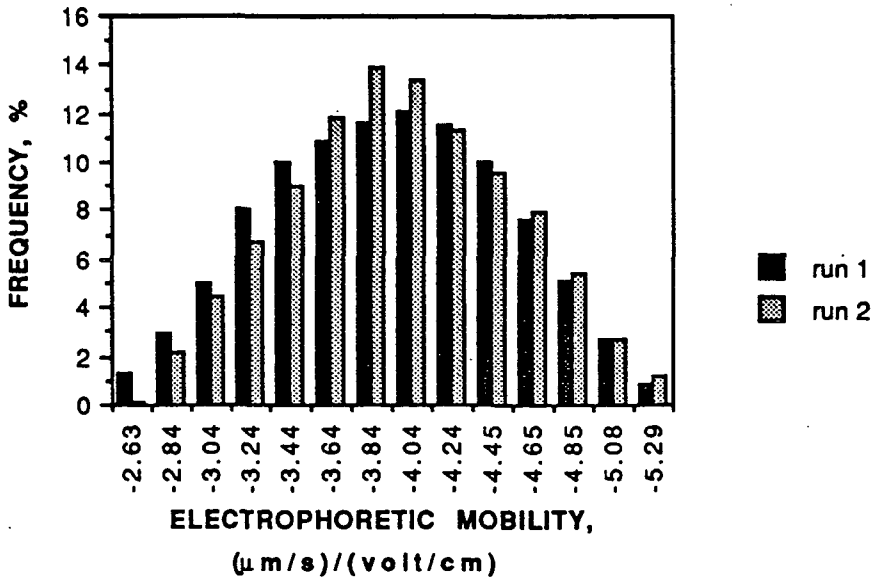

Figure 28. Headbox EM distribution comparison for sample 100-3-33.

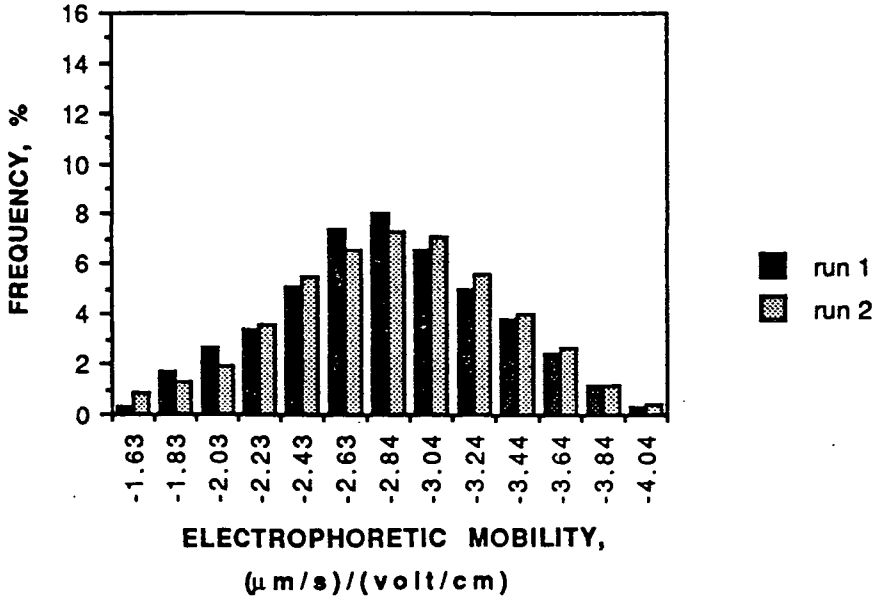

Figure 29. Whitewater EM distribution comparison for sample 100-3-33.

Table 5. Comparison of duplicate distributions.

Electrophoretic Mobility (μm/s) / (volt/cm)	Frequency, %			
	Headbox		Whitewater	
	run 1	run 2	run 1	run 2
-1.63	0.0	0.0	0.0	0.2
-1.83	0.0	0.0	0.8	1.7
-2.03	0.0	0.0	3.5	2.6
-2.23	0.0	0.0	5.5	4.0
-2.43	0.0	0.0	7.2	7.6
-2.63	1.3	0.1	10.6	11.5
-2.84	2.9	2.2	15.4	13.7
-3.04	5.0	4.4	16.7	15.1
-3.24	8.0	6.7	13.7	14.8
-3.44	10.0	9.0	10.4	11.7
-3.64	10.9	11.9	7.9	8.4
-3.84	11.7	13.9	5.1	5.5
-4.04	12.0	13.3	2.5	2.5
-4.24	11.6	11.4	0.8	0.8
-4.45	10.0	9.6	0.0	0.0
-4.65	7.6	7.9	0.0	0.0
-4.85	5.1	5.4	0.0	0.0
-5.08	2.7	2.8	0.0	0.0
-5.29	0.9	1.2	0.0	0.0
Avg. EM	-3.95	-4.00	-3.02	-3.06
Std. Dev. of Distribution	0.58	0.55	0.49	0.51

PARTICLE SIZE ANALYSIS

Mathematically, the change in headbox mobility with polymer can be predicted (recall Fig. 18); however, a theoretical or physical explanation must also be obtained to lend credibility to any model. Floc size is one physical property which is important to understand when developing a retention model. Therefore, treated, headbox, and whitewater samples were run on a Coulter Counter® Model TAII to determine the size distribution during each stage of an experimental run. Particle volume histograms of three sets of data are shown in Fig. 30-32. The data for these figures is given in Appendix XII. The ordinate in the particle size figures represents number frequencies.

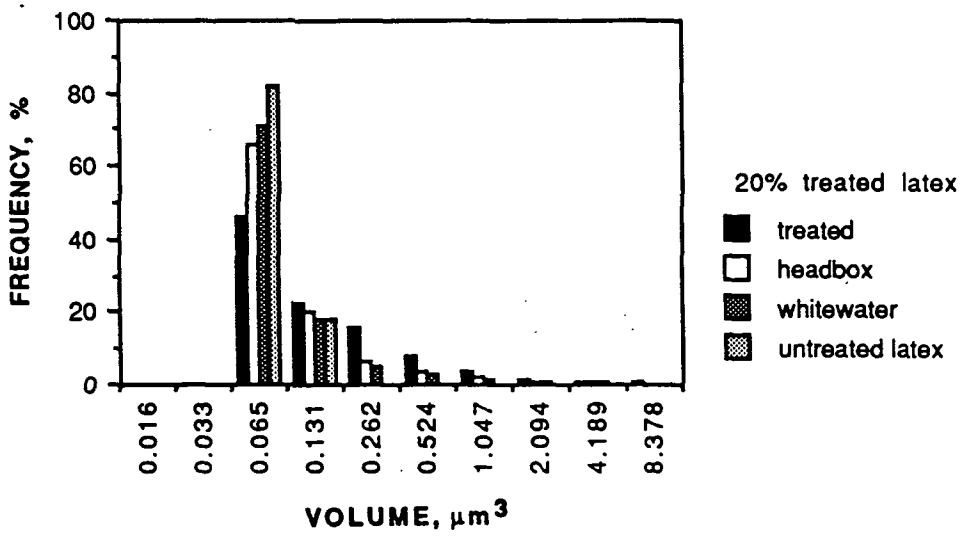

Figure 30. Particle size data for treated, headbox, and whitewater samples for run 20-3-0.

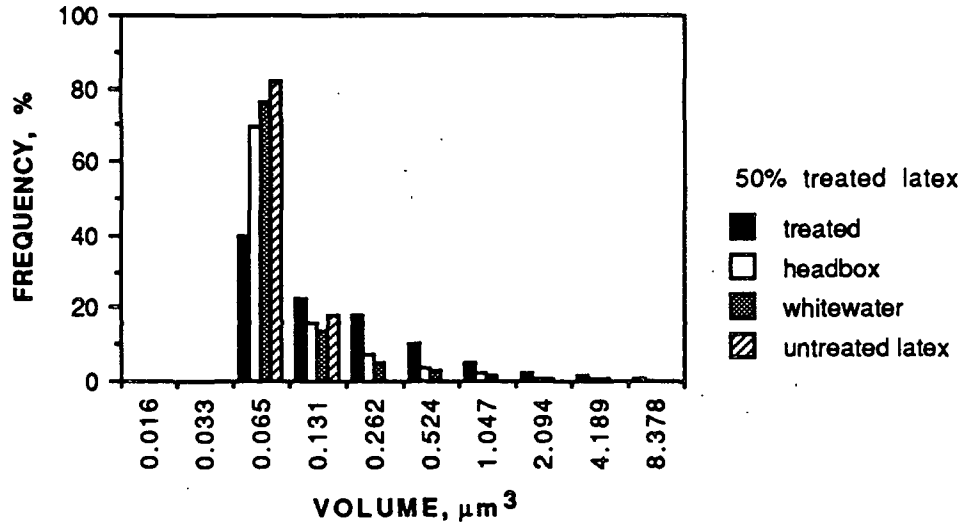

Figure 31. Particle size data for treated, headbox, and whitewater samples for run 50-3-0.

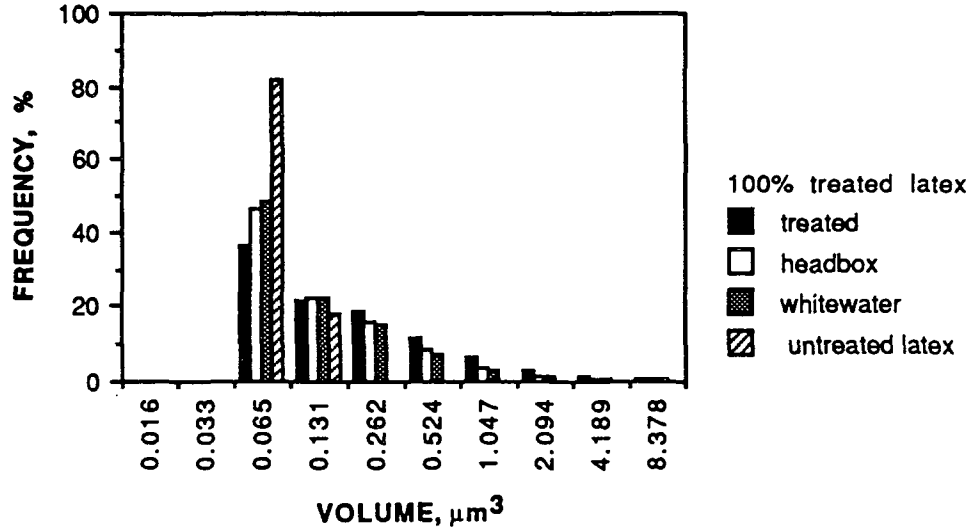

Figure 32. Particle size data for treated, headbox, and whitewater samples for run 100-3-0.

Table 2. Coulter Counter® floc sizes by channel for an 18 μm aperture.

Channel Number	Volume, μm^3	Radius of Equivalent Sphere, μm	Number of Singlets*
3	<0.065	0.500	1
4	<0.131	0.630	2
5	<0.262	0.794	3-4
6	<0.524	1.000	5-8
7	<1.047	1.260	9-13

* based on volume of 0.47 μm diameter sphere.

The previous three figures indicated several conditions which existed throughout the experiments of this thesis. First was the dominance of singlets in each sample even when the polymer dosage was the highest. The distribution of the untreated latex and Table 2 have been given for reference. The percentage of singlets was highest when the percentage of treated latex was lowest. This follows for the headbox and whitewater samples because more untreated latex, which was ~85% singlets, was added as the amount of treated latex diminishes.

High percentages of singlets were also seen in the treated samples. The total percentage change in singlets between 20-3-0 and 100-3-0 (about 10%), however, was half of the change seen between the headbox and whitewater samples (about 20%). The percentage of doublets was consistently near 20% for all samples. The formation of multiplets was also reflected in the standard deviation of the mobility distribution. As the percentage of treated latex increased, the percentage of singlets decreased and the standard deviation increased. The increase in standard deviation indicated floc formation. Even

though the samples were primarily singlets, any multiplet formation decreased the amount of polymer available for attachment of the latex to the fibers. The conditions found to promote the highest retentions are discussed in the following sections.

The mobility results discussed previously were supported by the particle size data given in Fig. 30-32. The reduction in mobility as more untreated latex was added to a sample was supported due to the high number of singlets. These particles still retained their original surface charge and caused the average mobility to become more negative as their numbers increased.

RETENTION MEASUREMENTS

Once the gravimetric procedure was fine tuned, experiments could be made to determine whether Davison's theory[35] applies to the current system. The retention experiments were run as part of a series of tests to determine whether corrections to the oven-dried weight were satisfactory. Correction was needed to account for the salt from the NaCl electrolyte background. A detailed explanation of the salt correction is given in Appendix XIII. First, a known concentration of latex diluted with 0.01 M NaCl was dried in weighing dishes. The theoretical "retention" of this sample should be 0% after salt correction. The value found was -0.2%. This indicated that the correction for the salt content of the samples was valid.

Second, several combinations of samples were then added to the DDJ to again check the procedures. Addition of the latex to the DDJ without polymer or fiber gave a retention of 0.5% where, again, 0% was expected. Fibers were then added with the latex, salt water background, and without Q5 polymer. A retention of -0.6% was obtained from this combination. The fiber was then

tested alone to see whether 100% retention could be obtained. In this case, a retention of 101.7% was the result. It was concluded, therefore, that the correction to remove the salt weight was satisfactory.

An experiment using the highest polymer loading (1.5 mg Q5/g latex treated) was chosen to test Davison's theory that retention in the DDJ is due to flocs too large to pass through the screen. To test this, the 20-3-0 sample was run without fibers to compare the retentions obtained with and without fibers. If Davison's theory is correct, the retention should be the same for both tests. A retention of 4.2% was obtained previously with fibers in the system. Gravimetrically, the retention without fibers was determined to be 1.6%. The 1.6% retained may include some latex loss due to particles attaching to the walls of the DDJ or in the polymer injection system or salt correction error, but it is evident that, for this system, removal of the fibers decreased retention. This supports the theory that particle attachment is a viable mechanism for particle retention in papermaking systems.

The above test was not the only experiment to test Davison's theory. In the other experiments, the polymer was added to the latex with an automatic pipet by directly injecting the Q5 into the DDJ or into a beaker-- common practice for retention aid studies. This method showed visibly large flocs due to the inadequate mixing characteristics at the point of addition. Retention was then measured without fibers present. Instead of a value of 1.6% or 4.1%, retentions as high as 20% were obtained for sample 20-3-0 under these conditions. Thus, the high values of retention obtained by Davison could have been caused by large flocs formed due to inadequate mixing characteristics at the point of polymer addition. Fast polymer injection actually formed visibly larger flocs than slower,

more deliberate polymer addition. Thus, it was determined that changes in the method of polymer addition drastically affected the retention obtained in a DDJ.

If polymer adsorption is considered irreversible,[70] the retention aid will not migrate to uniformly cover the surface of all the particles in a suspension. Uniform coverage is only approached as the mixing efficiency increases at the point of addition. Hence, the mechanisms which involve adsorption of fines and filler onto fibers depend on the conditions under which the retention aid is added. Therefore, polymer injection systems, such as the one used in this study, are needed to accurately study retention mechanisms and mill processes.

RETENTION RESULTS

The retention results presented in this section are those obtained gravimetrically. A compilation of the numerical data is given in Appendix XIV. The data are represented graphically in Fig. 33-36. Each figure represents retentions at different percentages of treated latex, that is 20, 50, 75, and 100%, respectively. The trends are similar for each figure indicating that retention is relatively independent of the fraction of latex treated with Q5. As more latex is treated, the retention does not consistently increase or decrease. The lines presented are computer-generated, best-fit quadratic polynomials.

The following discussion of Fig. 33 applies to the other figures as well. The variable on the abscissa is given as polymer loading in g Q5/od g treated latex. The variation in polymer loading for each curve is an effect of adding different amounts of polymer to the fibers. As more polymer is adsorbed onto the fibers, there is less polymer available for the latex at a given total dosage.

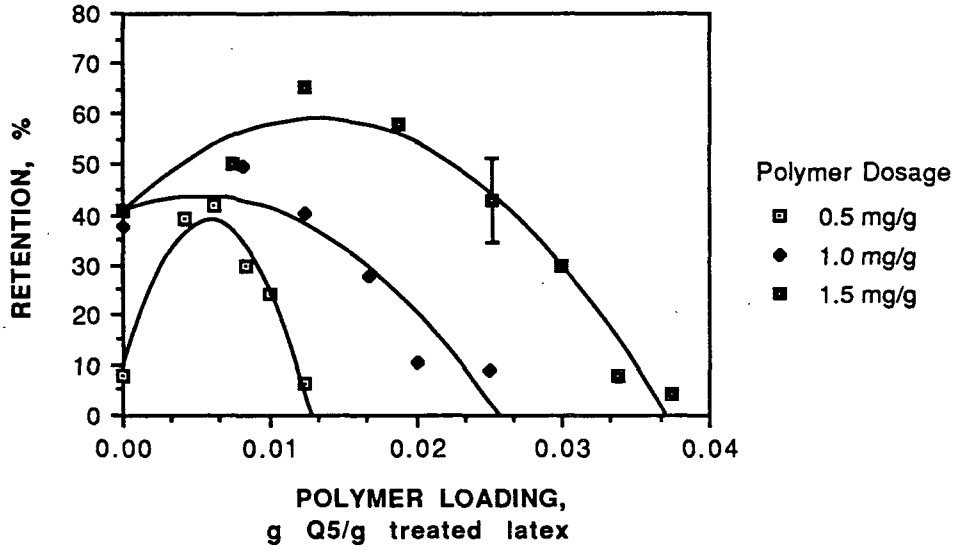

Figure 33. Retention vs. polymer loading for 20% treated latex series at three dosage levels, 0.5, 1.0, and 1.5 mg Q5/od g furnish. The error bar shown is the 95% confidence interval.

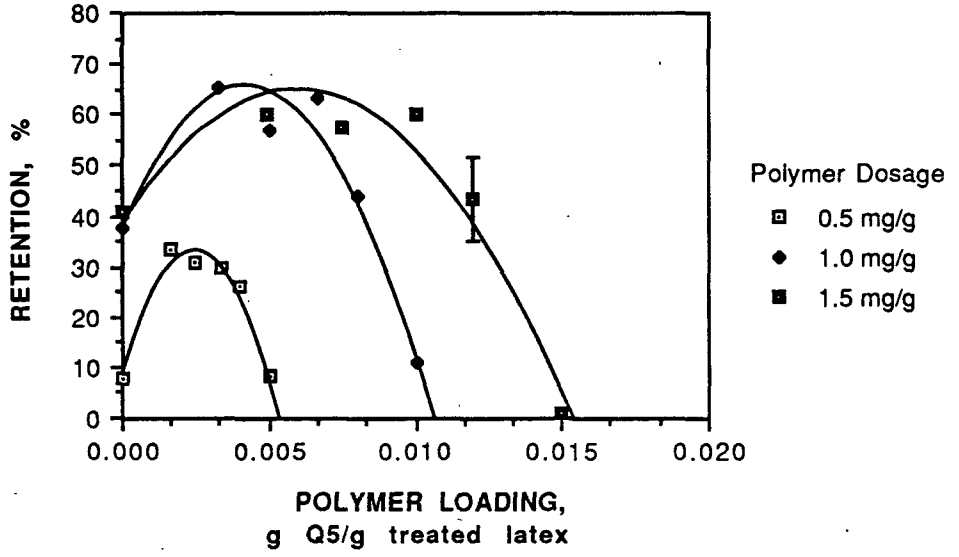

Figure 34. Retention vs. polymer loading for 50% treated latex series at three dosage levels, 0.5, 1.0, and 1.5 mg Q5/od g furnish. The error bar shown is the 95% confidence interval.

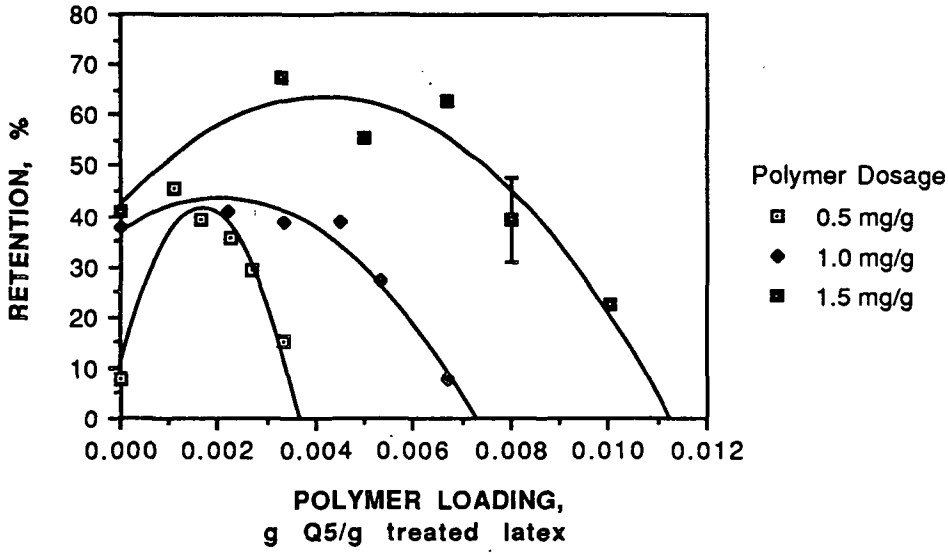

Figure 35. Retention vs. polymer loading for 75% treated latex series at three dosage levels, 0.5, 1.0, and 1.5 mg Q5/od g furnish. The error bar shown is the 95% confidence interval.

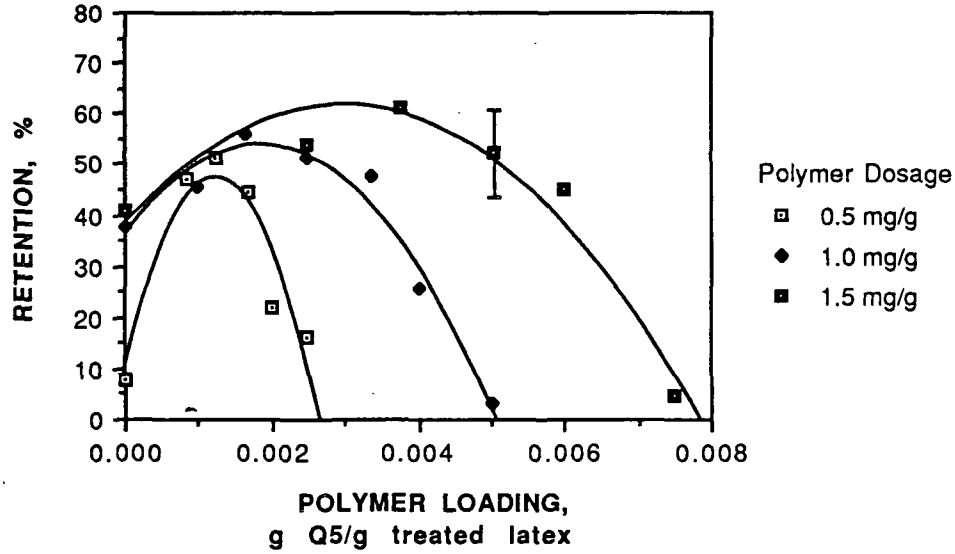

Figure 36. Retention vs. polymer loading for 100% treated latex series at three dosage levels, 0.5, 1.0, and 1.5 mg Q5/od g furnish. The error bar shown is the 95% confidence interval.

When all of the polymer was adsorbed on the fibers (polymer loading equals zero), the retention increased with polymer dosage. However, the percent increase in retention decreased as the dosage increased. Therefore, the retention was approaching a maximum. This maximum would occur when the latex began to cover more than half of the fiber surface. As more latex attached itself to the fiber, increases in retention were diminished because the area available on the fiber for more latex particles decreased. This maximum, however, depended upon the shear and contact time.

A word of caution must be given for the analysis of Fig. 33-36. Each point in the graph is also a function of the amount of polymer on the fibers of the sample. Hence, the point with the error bar in Fig. 33 has 0.025 g Q5/od g latex treated. It has a retention of approximately 42% when 33% of the dosage (1.5 mg/od g in this case) is added to the fibers. The other point at a loading of 0.025 g Q5/od g latex treated at a dosage of 1.0 mg/od g has a retention of 9%. But this sample has no polymer adsorbed onto the fibers. Therefore, even though these two points have the same polymer loading, they are not directly comparable except for the average headbox mobility as noted in Fig. 18.

For a given dosage, the fraction of the polymer on the fibers increases from right to left. The order is 0, 20, 33, 50, 67, 100% dosage on fibers. Several curves also have points with 10 and 80% dosage on the fibers in order to fill in a more complete picture of the relationship. If the retention data in Fig. 33 for 0.5 and 1.5 mg/od g dosages were plotted against the fiber treatment or the fraction of the dosage added to the fibers, Fig. 37 would result. As more polymer is diverted to the fibers, the retention increases until a maximum is reached between 50-60% polymer addition to the fibers irrespective of the percentage of

treated latex. Note the inverse relationship between polymer loading and the fraction of the dosage added to the fibers.

A three dimensional representation of the data is also given in Fig. 38 which includes the fraction of polymer adsorbed onto the fibers. If retention is plotted versus fraction of dosage on fibers and total dosage, a surface diagram emerges. This figure illustrates the increase in retention with increasing polymer dosage. The most dominant feature of the figure, however, is the trend seen earlier of a maximum retention near a 50% dosage split between the fibers and latex. And as seen earlier, this trend is independent of the fraction of latex treated (recall Fig. 33-36). Figure 37 also shows that the poorest retention occurs when there is no polymer on the fibers. This would indicate that there is little polymer available to bridge the particles to the fibers or that the polymer has reached a final configuration which does not promote heteroflocculation.

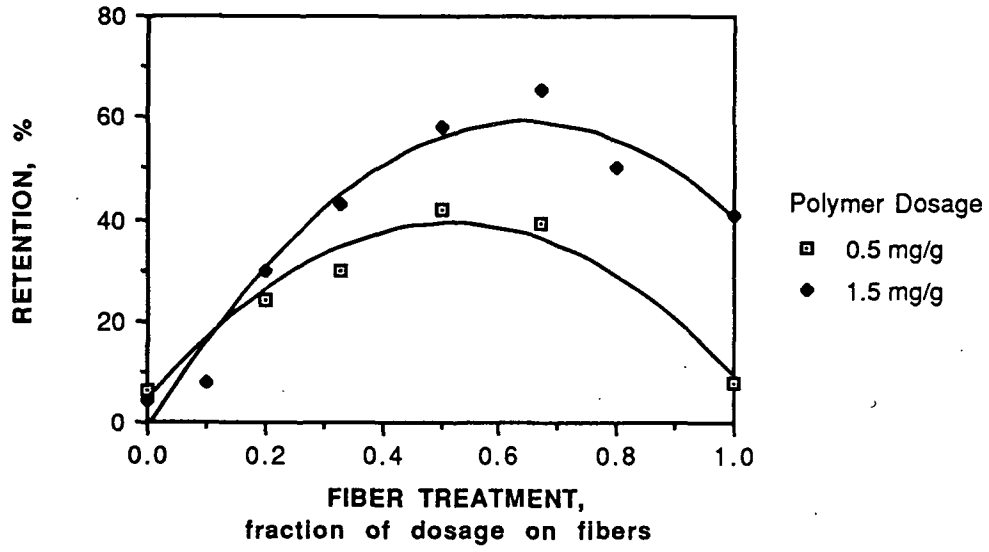

Figure 37. Retention plotted against fraction of dosage on fibers.

In one case, 20-3-0, the dosage was sufficient to cause the average EM of the treated sample to become slightly positive (0.30 (μm/s) / (volt/cm)). This situation is similar to the tests of Das and Lomas.[41] They used pretreated fines as flocculants. Fines whose charge was reversed by polymer addition were termed "super flocculants" because the retention increased dramatically when these particles were added into a furnish. In the present system, the addition of these so-called super flocculants did not achieve higher retentions. The retention was 4.2% for sample 20-3-0. At lower polymer dosages which did not produce charge reversal, the retentions were 6.4 and 8.9% for 20-1-0 and 20-2-0, respectively. Perhaps the amount of overdosing was not sufficient to cause such increases as seen by Das and Lomas.

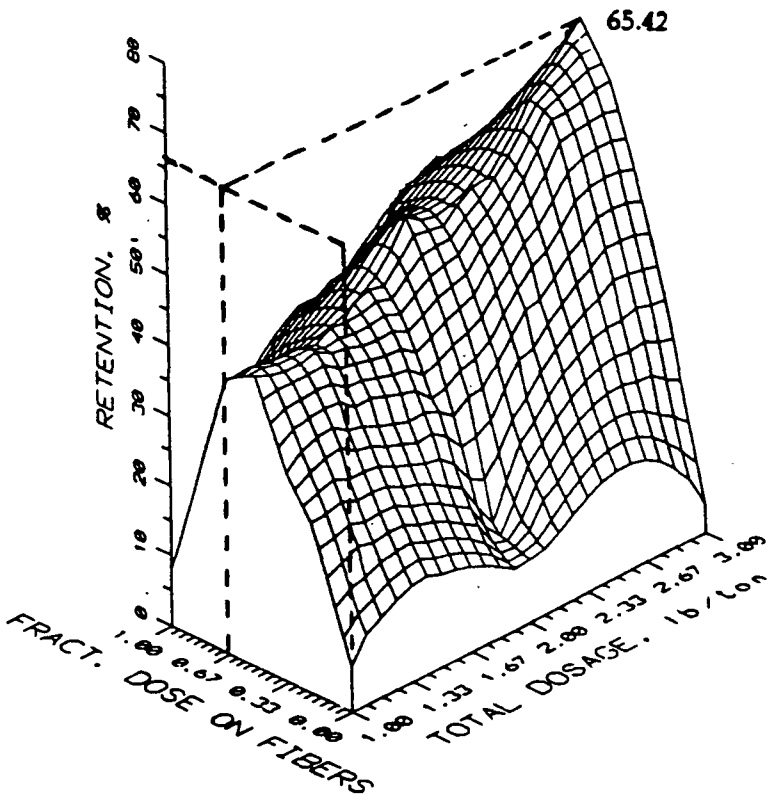

Figure 38. Three-dimensional representation of retention vs. dosage and amount of dosage adsorbed onto the fibers for the 20% treated latex case.

From the previous discussion, there seemed to be a difference between polymer treated latex and polymer treated fibers such that the treated fibers were more instrumental in increasing retention. Gregory[21,71] extensively studied the adsorption and flocculation of high charge density polymers. His conclusions were that low or high molecular weight, high charge density polymers flocculate according to a patch type mechanism. This hypothesis was based on the time of coagulation determined from Smoluchowski theory.[5] For Gregory's system, the time for the particle concentration to be halved was approximately 150 s.

Wågberg and co-workers[72] showed that when a high molecular weight cationic polyacrylamide was used as a flocculating agent, polymer chains initially adsorbed with very few polymer segments attached to cellulosic fibers. After more time had passed, the polymer reconformed giving a flatter configuration as many of the positive sites were drawn closer to the negative particle surface. This conclusion was based on decreasing charge group availability observed beyond 60 s after polymer addition.

To determine the number of available charged groups on the polyacrylamide, Wågberg first reacted the polymer with NaBr to displace the chloride ion associated with the quaternary ammonium groups. When the polymer adsorbed onto the carboxymethylated pulp fibers, bromide was released. The availability of charged groups then was determined by noting the concentration of bromide ion released during absorption. From these availability experiments, Wågberg concluded that much of the polymer was still in a coiled state during the first 60 s; hence, during the early stages of adsorption, bridging was possible. Wågberg also showed that this reconformation time increased as the charge density of the fiber decreased.[72] Since the polymers used

by Wågberg were of high charge density, the patch mechanism was operating after the polymer reached its equilibrium configuration.

Gregory and Sheiham[71] also stated that "non-equilibrium" flocculation similar to that observed by Wågberg also occurred if the particle concentration and polymer molecular weight were high. For non-equilibrium flocculation, it was possible that the polymer chains had not yet reached their final configuration when a particle collision occurred; consequently, bridging between the two colliding particles was the flocculation mechanism. For the high and low molecular weight, high charge density polymers used by Gregory, the time available for non-equilibrium flocculation or bridging was estimated at less than one second. Gregory concluded that non-equilibrium flocculation was most likely to occur when the particle concentration was greater than 1×10^{11} particles/mL.[71]

In the present study, however, the polymer used was a high molecular weight, low charge density polyacrylamide. This type of polymer has been theorized to flocculate with a bridging mechanism.[20,32] There was evidence in the present work that bridging was occurring in the fiber-latex system. The use of Smoluchowski theory provided a coagulation time of less than one second for the 100% treated latex sample. This time was generated from Eq. 14:[5]

$$T_{1/2} = 3\eta / 4kTn_o \qquad [14]$$

where,

$T_{1/2}$ = time for initial number of particles to be halved
η = viscosity
k = Boltzmann's constant
T = absolute temperature
n_o = number concentration.

For the case where water was the medium of dispersion and where the temperature was 298°K, Eq. 14 then became

$$T_{1/2} = 2 \times 10^{11}/n_o. \qquad [15]$$

The number concentration of the latex used in Eq. 15 was 5.5×10^{12} particles/mL which is larger than 1×10^{11} indicating bridging, according to Gregory.[71]

The adsorption characteristics of the polymer onto the cotton linters were also of importance. Polymer adsorbed onto the oxidized cotton linters used in this study was in its final equilibrium configuration before any latex was added. The linters had a conductometric charge of 30 μeq/g as compared with 214 μeg/g which was the lowest charged fiber used by Wågberg.[72] Because of the relatively low fiber surface charge, the polymer would be expected to remain in a more "extended" coil when adsorbed onto the fiber surface. The loops and tails associated with the polymer when adsorbed onto the higher charge density latex surface would be expected to be smaller or more compact.

The time required for a polymer to reach its final configuration was investigated by Cohen Stuart and Tamai.[73] These researchers determined the thickness relaxation time of adsorbed neutral polymers on glass. This time was commensurate with the time required for the polymer to reach its equilibrium configuration. Polymer was injected into a glass capillary every two minutes. The hydrodynamic thickness was tracked by measuring the streaming current in the capillary and then calculating the thickness. The polymer reached its final configuration in less than two minutes. The data indicated that most of the polymer actually reached equilibrium in less than one minute. The positively charged polymer and the negatively charged fiber used in the present study

would suggest an even faster equilibrium time. To ensure an equilibrium polymer configuration on the fiber and latex in this thesis, mixing times of one and two minutes (three minutes total per sample) were chosen because 90% of the Q5 was adsorbed onto the fibers during that time.

Since bridging was occurring, and since the time frame involved can be approximately stated, a physical picture of the retention data can be presented. The mobility distributions showed that addition of polymer only to the latex fraction resulted in random particle retention; that is, particles with a particular charge did not seem to be preferentially retained. Those particles which were trapped inside the fluid boundary layer around the fiber were retained. The trapping of particles in this boundary layer was proposed by van de Ven.[74] Because the fibers and many of the latex particles (depending on the percentage of treated latex) were still negative, the retention values were low and far from optimum.

Better retention was found when polymer was partitioned onto the fiber fraction. Because of the lower surface charge density of the fibers, the adsorbed polymer chains were in a more "extended" coil when in their equilibrium configuration. Consequently, the positive charges on the polymer were more available to attract the latex particles because the polymer loops and tails reached out further beyond the double layer.

Van de Ven[75] has stated that heteroflocculation or particle attachment between particles of unequal size can be favored over homoflocculation. In general, homocoagulation, where no polymeric bridging agent is present, is favored when double layer effects are absent so that

coagulation is only caused by van der Waals forces. Van der Waals forces, however, only cause homocoagulation when the particles reach a minimum separation distance, d_{min}.[75] When electrostatic forces are present, that is, when a flocculation aid is present, the double layer and van der Waals forces are negligible; consequently, d_{min} is increased. This increase in d_{min} is a function of the molecular weight of the flocculation aid. High molecular weight polymers, such as the Q5 used in the present study, extend beyond the double layer such that d_{min} is no longer applicable. Since d_{min} is no longer a factor, heteroflocculation is possible.[75]

Heteroflocculation becomes dominant when the shear rate in the system is high or when large particles such as fibers are present.[75] Bonds formed between equally sized particles are easily broken under these conditions; bonds formed between unequally sized particles are not easily broken.[75] Hence, treated latex particles formed aggregates which were easily broken. The presence of some doublets was noted in the particle size data. However, large numbers of latex aggregates were not seen indicating the unfavorability of homoflocculation. When latex aggregates were destroyed by shear, the polymer chains were broken which caused the coil size to diminish. This reduction in chain length also contributed to a reduction in polymer bridging.

The bonds between the latex particles and the fibers were stronger and were protected by the large mass of the fibers. Therefore, heteroflocculation or particle attachment was the dominant flocculation mechanism. Hence, adsorbed polymer on the surface of the fiber was more efficient than polymer adsorbed on the latex in effecting retention due to the extended coil and due to the dominance of heteroflocculation which produced stronger bonds. Consequently, retention was higher when polymer was added to the fibers.

Maximum retention values, however, were found when polymer was located on the fibers as well as the latex. The highest retention values occurred when 50-60% of the polymer dosage was added to the fibers. The latex when attached to the fibers did not cover the entire surface. At a retention of 67%, 53% of the fiber surface was covered with latex particles. This coverage was determined from the projected area of one latex particle, the number of attached latex particles, and the available fiber surface area. A retention of 67% would require that 0.2 od g of latex was attached to the fibers. If the latex density is taken as 1.0 g/cm^3, the volume of latex retained was 2.0×10^{11} μm^3. This volume corresponds to 3.7×10^{12} latex particles (0.47 μm diameter). Each particle projects an area of 0.1735 μm^2; therefore, the total projected area was 6.4×10^{11} μm^2. Recall that the fiber surface area was 1.0 m^2/g. So the area associated with 1.2 od g fibers is 1.2×10^{12} μm^2. The coverage can now be calculated to be $(6.4 \times 10^{11} / 1.2 \times 10^{12}) \times 100\% = 53.5\%$.

Retentions generally peaked in the 60-67% range because the fiber surface area available for particle attachment was decreasing. The retention also was dependent on the contact time between the fibers and latex as mentioned earlier. For a contact time of two minutes, the maximum retention was 67%. The maximum retention was independent of the polymer dosages used in this study.

The dependence on the availability of fiber surface area also applied to situations where polymer was only added to the fibers. In this case (also discussed on page 71), the retention was lower than 67% because after the available polymer on the fiber surface was bridged with untreated latex particles, there were no treated latex particles to attach to the polymer-free surface area

remaining on the fiber. Consequently, about 40% retention was gained by treating only the fibers, and an additional 25% retention was gained by splitting the dosage between the fibers and the latex.

When latex particles were treated with half of the dosage and the other half of the dosage was on the fibers, retention increased to the maximum value because both the treated and untreated particles could be retained on the fiber surface. The treated particles attached themselves to a negative fiber site; the untreated latex attached themselves to the polymer on the fiber surface. This result was also predicted by Deason.[76] The most efficient bridging was predicted to occur when the particle surface was half covered by polymer. Deason's calculations showed that homoflocculation between small particles (the latex) was not statistically favored when larger particles were present. But, the collection of colloidal particles by larger particles (such as fibers) was favored.

Retention decreased when more than 50-60% of the dosage was placed on the fibers. This increase in polymer coverage would then reduce the number of negative sites available for treated latex particles. The number or "degree" of treatment of treated particles decreased, however, as more polymer was added to the fibers. Consequently, the additional increase in retention caused by attachment of polymer treated latex was reduced.

Recalling Fig. 33-36, the retention did not decrease to zero when more polymer was added to the fibers (an increase in adsorbed polymer on the fiber corresponds to a decrease in polymer loading) because of the high percentage of untreated latex particles which could still be retained. Figures 33-36 also showed that the retention increased with total polymer dosage when the percentage of treated latex was constant.

Partitioning the polymer retention aid succeeded in differentiating two degrees of bridging. The first and lower degree of bridging occurred when the latex was treated with Q5. Here, the polymer coil was held more tightly to the particle which reduced d_{min}, the minimum separation distance for flocculation. The polymer coil was also reduced in size and effectiveness when latex-latex flocs were broken due to the shear in the system. The second and more efficient bridging occurred when polymer was adsorbed onto the fibers. The "extended" nature of the adsorbed polymer coil also increased the bridging efficiency. Thus, the polymer located on the fiber was able to more effectively capture the untreated latex particles.

In summary, the mechanism of retention observed in this model system can be described in the following manner. In each sample, the percentage of singlets was high due to two factors: untreated latex particles were present and homoflocculation between the latex particles was not favored. These singlets were retained by particle attachment to the cotton linters. Heteroflocculation occurred via bridging. Bridging, however, was affected by the location of the polymeric retention aid such that two degrees of bridging were identified. Polymer chains adsorbed onto the fiber surface provided more efficient bridging of latex particles which increased the latex retention. Less efficient bridging occurred when the retention aid was located only on the latex.

Optimum retention occurred when approximately half of the polymer dosage was adsorbed onto the latex and half adsorbed onto the fibers. Under these conditions, some polymer treated particles were retained on untreated areas on the fiber surface, and retention was higher than the condition where the polymer was only on the fibers. As more polymer was added to the

fibers, there were fewer treated latex particles to bridge to these untreated areas on the fiber surface. Consequently, the retention dropped from the optimum to the value seen when the polymer was only located on the fibers.

The effect of the percentage of treated latex on retention seemed to be minimal; therefore, the major variables of interest were the fractional dosage on the fibers, the total dosage, and the electrophoretic mobility. These were the variables explored in the statistical model.

STATISTICAL ANALYSIS

Current theories regarding the effects of retention aids on retention deal with properties such as dosage and whitewater zeta potential or mobility. If the tests were run in a dynamic drainage jar, the stirrer speed and thus shear rate, time of agitation, and jar geometry also were used as variables to study and to explain the system. In this study, all of these variables were kept constant except dosage and whitewater mobility. Correlating retention with these two variables using multiple analysis of variance yielded Eq. 16:

$$R = -30.124 + 14.279\ D - 8.216\ EMW \qquad [16]$$

where,

R = retention
D = polymer dosage
EMW = whitewater electrophoretic mobility.

A measure of the accuracy of the model was given in the coefficient of determination, r^2. In this case, the r^2 value was 0.143; therefore, the model did not in this case accurately represent the data.

Depending on the mixing conditions, method of polymer addition, and concentration of sample in the drainage jar, the location of polymer within the sample will change. A second statistical model, Eq. 17, was developed by including the location of polymer in the system--

$$R = -15.973 + 137.345\ F - 111.471\ F^2 + 8.508\ LT + 7.683\ D - 0.964\ EMW \qquad [17]$$

where,

F = fraction of dosage on fibers
LT = percent treated latex.

The variables of interest were fraction of dosage on fibers, % latex treated, whitewater mobility, and total polymer dosage. This equation was developed by testing the relationship's response to quadratic and logarithmic functions of each variable. From this analysis, only the fraction of the dosage on the fibers exhibited a significant quadratic response. Addition of this term increased the r^2 to a value of 0.811. The effectiveness of this equation can be seen in Fig. 39 where the calculated retentions are plotted against the measured values. From an F-ratio, it also was determined Eq. 17 represented the data better than Eq. 16. The F-ratio for the polymer location equation, Eq. 17, is 46.4, versus 4.8 for Eq. 16.

The next question was whether the standard deviation of the whitewater mobility distribution affected the empirical relationship. Addition of the standard deviation did not increase the level of correlation of the equation as measured by r^2. The F-ratio of the model also decreased from the previous 46.4 to 37.9. Thus, the standard deviation of the distribution was not significant when predicting retention. The use of an adjusted r^2 instead of the usual r^2 to test the regression equations was not necessary because of the large number of total degrees

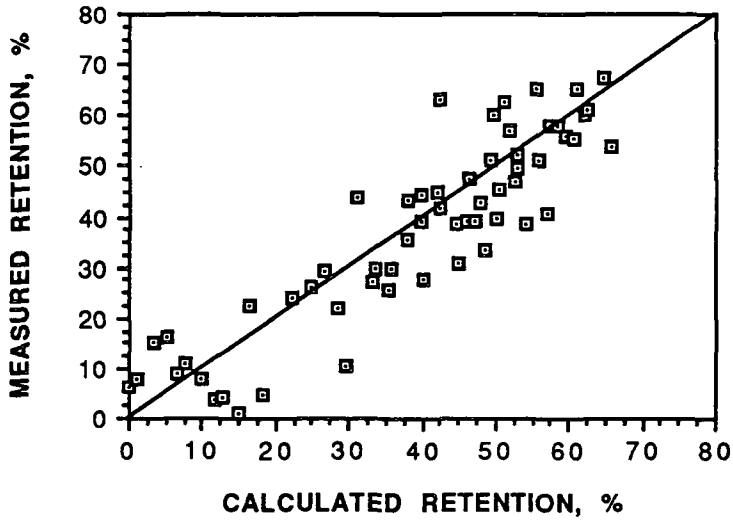

Figure 39. Representation of model fit. Line drawn is 1:1.

of freedom. Hence the addition of terms to the regression equation did not bias the correlation.

Since average headbox mobilities were shown (Fig. 18) to correlate with polymer dosage, the effects of headbox EM on Eq. 17 were investigated. A comparison showed very little difference between the headbox EM and whitewater EM equations. Hence, an *a priori* knowledge of the average headbox mobility did not significantly improve the empirical retention calculated from the average whitewater mobilities. The AVOVA tables for the regressions presented above can be found in Appendix XV.

From the preceding discussion, the most significant variables contributing to retention, in descending order of significance as determined by the t-statistic (see Appendix XV), were fraction of polymer dosage adsorbed onto long fibers, total polymer dosage, percentage of latex treated with polymer, and whitewater or headbox average EM.

Both whitewater and headbox average mobilities are listed as important variables. Use of the headbox EM would be preferred because the average headbox mobility can be predicted based on polymer dosage and location. However, the whitewater regression compared very well with the headbox equation. The fact that the whitewater mobility can be determined easily in the paper mill favored the whitewater mobility regression. Until headbox mobilities can be measured without removing the long fiber, the whitewater values will continue to be used and will continue to provide meaningful results.

CONCLUSIONS

Several conclusions were drawn from this thesis. The headbox electrophoretic mobility is a function of the polymer dosage and the percentage of latex treated. Prediction of headbox mobility in a real papermaking system is still elusive because the percentage of latex treated is an unknown that is related to the mixing conditions during polymer addition.

The mixing conditions at the point of addition were found to have a large effect on the retention determined with a dynamic drainage jar. If the polymer was added under poor mixing conditions, the retention aid created large aggregates due to locally high polymer concentrations which yielded unusually high retentions. Retention of these large flocs may be undesirable depending on the end use of the paper. Retention values obtained under these conditions would not accurately predict the retention on a paper machine because of the shear and mixing at the point of polymer addition. Hence, to accurately predict commercial scale responses, the mixing conditions during polymer addition must also be considered when running retention or retention aid studies in a dynamic drainage jar.

Particle size and retention analysis also showed that latex particle attachment is an important mechanism in retention. The floc sizes encountered in this study were generally not greater than quadruplets, which easily passed through the 76 μm screen in the DDJ. This and other retention experiments with and without fibers proved that Davison's large floc retention mechanism was not operating under the conditions of this study.

Particle attachment was shown to be affected by the partitioning of the polymeric retention aid throughout the furnish. Electrophoretic mobility distributions graphically demonstrated which particles were preferentially retained in the DDJ. As more polymer was directly adsorbed onto the fibers, increasingly negative particles were retained. As more polymer was adsorbed onto the latex, increasingly positive particles were retained. These observations showed that polymer treated latex particles were retained by attaching themselves to the fibers. When the polymer was preferentially added to the fibers, the more negative particles were drawn toward the polymer loops and tails near the fiber surface but outside the double layer. These results indicated that the location of polymer is a critical factor in determining which particles attach onto larger fibers, thus being retained.

From the above observations, two forms of bridging were identified. The first type resulted when a polymer treated particle attached to a fiber. The compact polymer coil on the particle surface did not efficiently produce fiber-latex bridges. This compact nature was due to the high charge density of the latex and due to the formation and subsequent breakage of latex-latex bonds. The highest bridging efficiency resulted from heteroflocculation between polymer treated fibers and the latex. This was due to the lower charge density of the fibers which allowed the polymer coil to remain in a more extended state, thereby more effectively attracting the latex.

The latter form of particle attachment did provide enhanced particle retentions. As the amount of polymer added to the cotton linters increased, the retention increased to a maximum which occurred between 50 and 60% addition onto the fibers. This rise in retention revealed that preferential adsorption of the

retention aid onto the long fiber fraction of a papermaking furnish was desirable. The retention then fell as more polymer was adsorbed onto the fibers.

Retention can be empirically determined by

$$R = -15.973 + 137.345\ F - 111.471\ F^2 + 8.508\ LT + 7.683\ D - 0.964\ EMW. \qquad [17]$$

The average whitewater EM was used because it can be measured in the paper mill. When the standard deviation of the EM distribution was added to the regression, the correlation of the model was not enhanced; therefore, the mobility distribution was not a significant variable in this model papermaking system.

SUGGESTIONS FOR FUTURE RESEARCH

More research is needed to quantify the decrease in absorbance of a polymer flocculated polystyrene latex suspension. Latex particles are used as model particles in many systems such as papermaking and wastewater treatment systems. This includes the use of these particles to gain fundamental as well as practical understanding. Previous turbidity and absorbance data in the literature may be in error if flocculation was polymer-induced.

Another area of research should be to partition the polymer in a furnish consisting of fibers and fiber fines. With this system the weak acid content of the pulp can be included in the analysis. The weak acid content of fibers has been shown by Goulet[77] to affect the electrokinetic characteristics of the fibers. Hence, an even better understanding of the relationship between retention and electrokinetics will be the result.

If Coulter's DELSA system is available, it would also be interesting to note whether Brownian motion affects the EM distribution of a papermaking system. It would also be interesting then to compare those results with the results obtained on the Zetasizer. Sanders[10] has done some work, but more is still needed.

The Zetasizer might also be useful in an experiment which investigates polymer transfer. A set of EM experiments could be run on a mixture of latices containing particles with two different dosages of polymer. The resulting EM distributions may show bimodality or a single peak indicating polymer movement.

PRACTICAL IMPLICATIONS

The mixing conditions at the point of polymer addition is a matter which has been seriously overlooked in the paper industry. Many retention aids are evaluated by squirting them into a DDJ. When a retention aid is injected into the DDJ many of the fibers, filler, and fines are overdosed due to inadequate mixing at the point of addition. This overdose is difficult to reproduce and is in itself undesirable. Hence, I would recommend a standard polymer addition into the DDJ which is more reproducible and more indicative of machine conditions so that retention aid testing and evaluation may be done objectively.

ACKNOWLEDGEMENTS

I would like to take this opportunity to acknowledge the guidance and support of my advisory committee: Dr. Robert Halcomb, Dr. Jeffrey Lindsay, and my chairman, Dr. Robert Stratton. I would also like to thank Dr. Frank Etzler who joined my committee near the completion of the thesis. My highest regards and respect go to Bob Stratton for being there and listening whenever I needed to talk. Bob's constant optimism and support helped to smooth the rocky road of research.

Thanks are due to the member companies of the Institute of Paper Chemistry without whose support this thesis would not have been possible. I am also grateful for the help of the faculty, staff, and students at the Institute. Those deserving special mention are Sally Berben, Norm Colson, Don Gilbert, Mike Goulet, Chris Luettgen, and Mike Mischuk. The cooperation of Peter Vichos of Coulter Electronics is gratefully acknowledged.

Extra special thanks go to my parents, sister, grandparents, and my wife, Melisse, for their never-ending love and support in all my endeavors.

SYMBOLS and ABBREVIATIONS

in order of appearance

Ψ_o	=	surface potential, mV
Ψ	=	potential, mV
Ψ_δ	=	potential at Helmholtz plane, mV
δ	=	thickness of the Stern layer
κ	=	Debye-Hückel parameter, 1/m
e	=	electronic charge
z_i	=	electrolyte valency of ion "i"
N_A	=	Avogadro's number
c_i	=	concentration of ion "i", moles/L
ε	=	dielectric constant of medium
ε_o	=	permittivity of free space, farad/m
k	=	Boltzmann's constant
T	=	absolute temperature
ζ	=	zeta potential, mV
EM	=	electrophoretic mobility, $(\mu m/s)/(V/cm)$
η	=	viscosity, Ns/m^2
a	=	radius of curvature, m
$f(\kappa a)$	=	function related to particle shape in Henry equation
od g	=	oven-dried weight in grams
R_θ	=	Rayleigh ratio
M	=	molecular weight
B	=	second virial coefficient
c_2	=	solute concentration
i_s	=	scattering per unit volume
I_o	=	intensity of light incident
r	=	radial distance to the point of observation
θ	=	scattering angle
$\tilde{n}$	=	refractive index
λ_o	=	wavelength of incident light
$P(\theta)$	=	Rayleigh-Gans-Debye form factor

SYMBOLS and ABBREVIATIONS (cont.)

ν	=	frequency
v	=	relative transmitter velocity
k′	=	scattering vector
WWF	=	latex solids in whitewater
HBXF	=	latex solids in headbox
Q5	=	cationic polyacrylamide coploymer retention aid used in this study
DDJ	=	dynamic drainage jar (Britt Jar)
Φ	=	polymer loading, mg Q5/od g treated latex
D	=	retention aid dosage
F	=	fraction of dosage adsorbed onto cotton linters
L	=	percentage of latex treated
A	=	cell cross-sectional area
L′	=	cell length
I	=	current
V	=	voltage
R	=	retention in empirical equations
EMW	=	average electrophoretic mobility of whitewater sample
EMH	=	average electrophoretic mobility of headbox sample

LITERATURE CITED

[1] Schmut, R. Zeta potential in the paper industry. Industrial and Engineering Chemistry 56(10): 28-33 (Oct. 1964).

[2] Penniman, J. G. New state-of-the-art automatic microelectrophoresis instrumentation. TAPPI Papermakers Conf. (Chicago) Proc.: 43-48 (April 18-20, 1977).

[3] Smith, M. K. Surface charges on mechanical pulp fibers and their effects on drainage and retention on newsprint machines. The Second International Seminar on Paper Mill Chemistry (New York) Proc.: (September 11, 1978).

[4] Verway, E. J. W.; Overbeek, J. T. G. Theory of the Stability of Lyophobic Colliods. Elsevier, New York, 1948.

[5] Kruyt, H. R. Colloid Science, Vol. 1, Elsevier, New York, 1952.

[6] Dukhin, S. S.; Derjaguin, B. C. Equilibrium double layer and electrokinetic phenomena. *in* Surface and Colloid Science, (E. Matijevic, ed.), Vol. 7, Wiley-Interscience, New York, 1974.

[7] Shaw, D. J. Introduction to Colloid and Surface Chemistry, 3rd Edition, Butterworths, London, 1980.

[8] Hunter, R. J. Zeta Potential in Colloid Science. Academic Press, London, 1981.

[9] Strazdins, E. Factors affecting the electrokinetic properties of cellulose fibers. Tappi 55(12): 1691-1695 (December, 1972).

[10] Sanders, N. D.; Schaefer, J. H. Zeta potential distributions in pulp/pcc mixtures. TAPPI Papermakers Conf. (Washington, D. C.) Proc.: 43-48 (April 10-12, 1989).

[11] Hiemenz, P. C. Polymer Chemistry: The Basic Concepts. Marcel Dekker, New York, 1984.

[12] Arno, J. N.; Frankle, W. E.; Sheridan, J. L. Zeta potential and its application to filler retention. Tappi 57(12): 97-100 (Dec. 1974).

[13] Nichols, P. W. The use of polyacrylamides to improve the retention and drainage of both fibers and fillers in groundwood sheets. TAPPI Papermakers Conf. (New Orleans) Proc.: 181-188 (April 14-16, 1986).

[14] Yeh, Y.; Cummins, H. Z. Applied Physics Letters. 4: 176-78 (1964).

[15] Drain, L. E. The Laser Doppler Technique. Wiley, New York, 1980.

[16] Coulter Electronics, Inc. Coulter DELSA 440, 1988. 10 p.

[17] Israelachvili, J. N. Intermolecular and Surface Forces. Academic Press, New York, 1985.

[18] Bleier, A.; Matijevic, E. Interactions of monodispersed chromium hydroxide with polyvinyl chloride latex. J. Colloid and Interface Science. 55(3): 510-524 (1976).

[19] James, R. O.; Homola, A.; Healy, T. W. Heterocoagulation of amphoteric latex colloids. J. Chemical Society, Faraday Trans. I: 1436 (1977).

[20] LaMer, V. K.; Healy, T. K. Adsorption-flocculation reactions of macromolecules at the solid-liquid interface. Reviews of Pure and Applied Chemistry. 13: 112-133 (1963).

[21] Gregory, J. Rates of flocculation of latex particles by cationic polymers. J. Colloid and Interface Science 42(2): 448-456 (1973).

[22] Kasper, D. R. Theoretical and Experimental Investigations of the Flocculation of Charged Particles in Aqueous Solutions by Polyelectrolytes of Opposite Charge. Doctoral Dissertation. Pasadena, CA, California Institute of Technology, 1971.

[23] Brecht, W.; Holzhey, F. Influence of groundwood quality on paper opacity and the show-through and penetration of printing ink. Papier 22(10A): 726 (1968).

[24] Robinson, J. V. Optical properties of paper as affected by wet end chemistry. Tappi 59(2): 77 (1976).

[25] Clark, J. d'A. Controlling the quality of mechanical pulps. Cellulose Chem. Technol. 2(1): 105 (1968).

[26] Hergert, R. E.; Waech, T. G. Newsprint furnish solids retention. Tappi 62(11): 79-81 (1979).

[27] Unbehend, J. E. The "dynamic retention/drainage jar" increasing the credibility of retention measurements. Tappi 60(7): 110-112 (July, 1977).

[28] Haslam, J. H.; Steele, F. A. The retention of pigments in paper. Tappi Papers 19: 249 (1936).

[29] Hubbe, M. A. How do retention aids work? TAPPI Papermakers Conf. (Chicago) Proc.: 389-398 (April 11-13, 1988).

[30] Williams, D. G.; Swanson, J. W. Particle retention in papermaking systems. Tappi 49(4): 147-151 (1966).

[31] Britt, K. W. Retention of additives during sheet formation. Tappi 56(3): 83-86 (March, 1973).

[32] Britt, K. W. Mechanisms of retention during paper formation. Tappi 56(10): 46-50 (October, 1973).

[33] Stratton, R. A. Effect of agitation on polymer additives. Tappi J. 66(3): 141-144 (March, 1983).

[34] Franco, R. P.; Stratton, R. A. unpublished work, 1978.

[35] Davison, R. W. Mechanism of fine particle retention in paper. Tappi J. 66(11): 69-72 (Nov. 1983).

[36] Davison, R. W. personal communication. February, 1989.

[37] Abson, D.; Bailey, R. M.; Lenderman, C. D.; Nelson, J. A.; Simons, P. B. Predicting the performance of shear-sensitive additives. Tappi 63(6): 55-58 (June, 1980).

[38] Gess, J. M. Drainage/retention using the G/W system (II). TAPPI Papermakers Conf. (New Orleans) Proc.: 307-309 (April 14-16, 1986).

[39] Han, S. T. Retention of small particles in fiber mats. Tappi 47(12): 782 (1964).

[40] Lindström, T. Some fundamental chemical aspects on paper forming. *in* Fundamentals of Papermaking (Baker and Punton, eds.) Vol. I. Mech. Eng. Publns. Ltd., London, 1989: 311-412.

[41] Das, B. S.; Lomas, H. Flocculation of paper fines. I. Adsorption of and flocculation by polyelectrolytes. II. Study of the nature of the solid surface and soluble impurities. Pulp and Paper Mag. of Canada 74(8): 95-100 (August, 1973).

[42] Temming, H. Temming Linters. Technical Information on Cotton Cellulose. Gluckstadt, Germany, Peter Temming AG, 1966.

[43] MacLaurin, D. J.; Ward, K. Literature Survey on Cotton Linters as a Papermaking Fiber. Project 1708-A. Appleton, WI, The Institute of Paper Chemistry, 1954.

[44] Marlow, B. J.; Fairhurst, D. Electrophoretic fingerprinting and the biological activity of colloidal indicators. Langmuir, 4: 776-780 (1988).

[45] Russo, P.; Mustafa, M.; Cao, T.; Stephens, L. Interactions between polystyrene latex spheres and a semiflexible polymer, hydroxypropylcellulose. J. Colloid and Interface Science 122(1): 120-137 (March, 1988).

[46] Kitahara, A.; Ushiyama, H. Flocculation in mixed latices. J. Colloid and Interface Science 43(1): 73-77 (April, 1973).

[47] Bøhmer, E. Filling and loading. *in* Pulp and Paper Chemistry and Chemical Technology (Casey, J. P., ed.) Vol. III, 3rd ed. New York, Wiley-Interscience, 1981: 1516.

[48] MacDonald, R. G., ed. Pulp and Paper Manufacture, Vol. II, 2nd ed. New York, McGraw-Hill, 1970: 22.

[49] Arnson, T. R. The Adsorption of Complex Aluminum Species by Cellulosic Fibers from Dilute Solutions of Aluminum Chloride and Aluminum Sulfate. Doctoral Dissertation. Appleton, WI, The Institute of Paper Chemistry, 1980.

[50] Proxmire, P. R. The Influence of Aluminum Salts on the Retention of Titanium Dioxide When Using Cationic Polyelectrolyte as a Retention Aid. Doctoral Dissertation. Appleton, WI, The Institute of Paper Chemistry, 1988.

[51] Crow, R. D.; Stratton, R. A. The chemistry of aluminum salts in papermaking II: Influence on the adsorption of a cationic polyelectrolyte. *in* Papermaking Raw Materials (Punton, ed.) Vol. II. Mech. Eng. Publns. Ltd., New York, 1985: 895-916.

[52] Swanson, J. W.; Steber, A. J. Fiber surface area and bonded area. Tappi 42(12): 986-994 (Dec. 1959).

[53] Stone, J. E.; Nickerson, L. F. A dynamic nitrogen adsorption method for surface area measurements of paper. Pulp and Paper Magazine Canada 64: T155-T161 (1963).

[54] Ingmanson, W. L.; Whitney, R. P. The filtration resistance of pulp slurries. Tappi 37(11): 523-8 (1954).

[55] Goodwin, A. R.; Hearn, J.; Ho, C. C.; Ottewill, R. H. Studies on the preparation and characterization of monodisperse polystyrene latices. III. Preparation without added surface active agents. Colloid and Polymer Science 252: 464-471 (1974).

[56] Labib, M. E.; Robertson, A. A. The conductometric titration of latices. J. Colloid and Interface Science 77(1): 151-161 (Sept., 1980).

[57] Carlson, J. unpublished data, 1978.

[58] Malvern Zetasizer IIC user manual. Malvern Instruments Ltd, Malvern, Worcestershire, England, January, 1988.

[59] Oja, T.; Bott, S. paper presented at 63rd ACS Colloid Symposium (Seattle): (June, 1989).

[60] Taylor, J. T. personal communication, 1989.

[61] Nordt, F. J.; Knox, R. J.; Seaman, G. V. F. Elimination of electroosmotic flow in analytical particle electrophoresis. in Hydrogels for Medical and Related Applications. (Andrade, J. D., ed.) ACS Symposium Series, No. 31, American Chemical Society, New York, 1976. p. 225-240.

[62] Herren, B. J.; Shafer, S. G.; van Alstine, J.; Harris, J. M.; Snyder, R. S. Control of electroosmosis in coated quartz capillaries. J. Colloid and Interface Science 115(1): 46-55 (January, 1987).

[63] Goulet, M. T. personal communication, 1988.

[64] Patterson, W. J. Development of polymeric coatings for control of electroosmotic flow in ASTP MA-011 electrophoresis technology experiment. National Aeronautics and Space Administration, Technical Memorandum, NASA TMX-73311, U. S. Govt. Printing Office, Washington, D. C., 1976.

[65] Healy, T. W.; White, L. R. Ionizable surface group models of aqueous interfaces. Adv. Colloid and Interface Science 9: 303-345 (1978).

[66] Midmore, B. R.; Hunter, R. J. The effect of electrolyte concentration and co-ion type on the ζ-potential of polystyrene latices. J. Colloid and Interface Science 122(2): 521-529 (April, 1988).

[67] Ma, C. M.; Micale, F. J.; El-Aasser, M. S.; Vanderhoff, J. W. The relationship between the electrophoretic mobility and the adsorption of ions on polystyrene latex. ACS Symposium Series, No. 165, American Chemical Society, New York, 1988. p. 251-262.

[68] Lindström, T.; Söremark, C.; Heinegård, C.; Martin-Löf, S. The importance of electrokinetic properties of wood fibers for papermaking. Tappi 57(12): 94-96 (Dec. 1974).

[69] Herrington, T. M. The surface potential of cellulose. *in* Papermaking Raw Materials (Punton, ed.) Vol. I. Mech. Eng. Publns. Ltd., New York, 1985: 165-181.

[70] Hesselink, F. Th. On the theory of polyelectrolyte adsorption. J. Colloid and Interface Science 60(3): 448-466 (July, 1977).

[71] Gregory, J.; Sheiham, I. Kinetic aspects of flocculation by cationic polymers. British Polymer J. 6(1): 47-59 (1974).

[72] Wågberg, L.; Ödberg, L.; Lindström, T.; Aksberg, R. Kinetics of ion-exchange reactions during adsorption of cationic polyelectrolytes onto cellulosic fibers. J. Colloid and Interface Science 123(1): 287-295 (May, 1988).

[73] Cohen Stuart, M. A.; Tamai, H. Thickness relaxation of poly(ethylene oxide) on glass as a function of segmental binding energy. Langmuir 4: 1184-1188 (1988).

[74] van de Ven, T. G. M. Physicochemical and hydrodynamic aspects of fines and filler retention. *in* Fundamentals of Papermaking (Baker and Punton, eds.) Vol. I. Mech. Eng. Publns. Ltd., London, 1989: 471-494.

[75] van de Ven, T. G. M. Effects of polymer bridging on selective shear flocculation. J. Colloid and Interface Science 81(1): 290-291 (May, 1981).

[76] Deason, D. M. Statistical model for bridging efficiency in polymeric flocculation. *in* Flocculation in Biotechnology and Separation Systems (Attia, ed.) Elsevier Science Publishers B. V., Amsterdam, 1985: 21-30.

[77] Goulet, M. T. The Effect of Pulping, Bleaching, and Refining Operations on the Electrokinetic Properties of Wood Fiber Fines. Doctoral Dissertation. Appleton, WI, The Institute of Paper Chemistry, 1989.

[78] Wigsten, A. L. Polymer Adsorption and Flocculation of Particles in Turbulent Flow. Doctoral Dissertation. Appleton, WI, The Institute of Paper Chemistry, 1983.

[79] Kerker, M. The Scattering of Light and Other Electromagnetic Radiation. Academic Press, New York, 1969.

APPENDIX I

CARBOXYL CONTENT OF COTTON LINTERS

Methylene blue determinations procedure: (adapted from TAPPI T237 su-63)

1. To a 60 mL polypropylene bottle, add a sample of fiber. The amount of fiber depends on an estimate of the number of equivalents of carboxyls per 100 g of the sample (use a range of sample weights- ±20% of estimated sample weight).
   Example:

$$\text{equivalents} = \frac{(5 \times 10^{-6}\ \text{M})\ (100)}{(\text{weight in grams})}$$

   Estimate 0.016 equivalents; therefore, 0.03 g fiber required. Test range would then be 0.024-0.036 g.
2. Add 10 mL of methylene blue (MB) buffer solution. This solution is made from 50 mL of 2 millimolar MB solution and 50 mL buffer stock solution.
3. Dilute sample in polypropylene bottle with distilled water to 30 mL.
4. Mix 24 hours in a 25° C water bath.
5. Centrifuge the bottles until a clear supernatant is obtained.
6. Add 5 mL of supernatant to a 50 mL volumetric flask.
7. Add 5 mL 0.1 M HCl.
8. Dilute with distilled water to 50 mL.
9. Measure absorbance at 620 nm.
10. Filter the fibers, dry, and weigh to determine the actual weight of fibers used in the test.
11. Calculate the concentration of the supernatant from the calibration curve: (1×10^{6})(absorbance) =(0.043768)(concentration)
12. Determine the weight of sample which gave a 50% consumption of MB.
13. Find equivalents from equation in step 1 and report as milliequivalents/ 100 od g fiber.

Example calculation:

Sample wt	30 mL Sample wt.	absorbance	initial concentration	final concentration	% consumption
0.49 od g	0.03002 L	0.199	3.30×10^{-4} g/L	4.54×10^{-5} g/L	0.8637

$$\text{initial concentration} = \frac{(0.001\ \text{g/L})\ (0.01\ \text{L})}{0.03002\ \text{L}}$$

Final concentration = (concentration from step 11) x 10

$$\%\ \text{consumption} = \frac{(\text{initial conc.}) - (\text{final conc.})}{(\text{initial concentration})}$$

Weight correction due to MB adsorbed onto fibers:
-to each sample, 0.003739 g of MB was added.
So, the weight of MB on fibers = 0.003739(% Consumption)
the corrected weight = 0.49-0.003739(0.8637) = 0.0458 g

meq/100 g = $(5 \times 10^{-6})(100)(1000)/$(od weight in grams at 50% consumption)

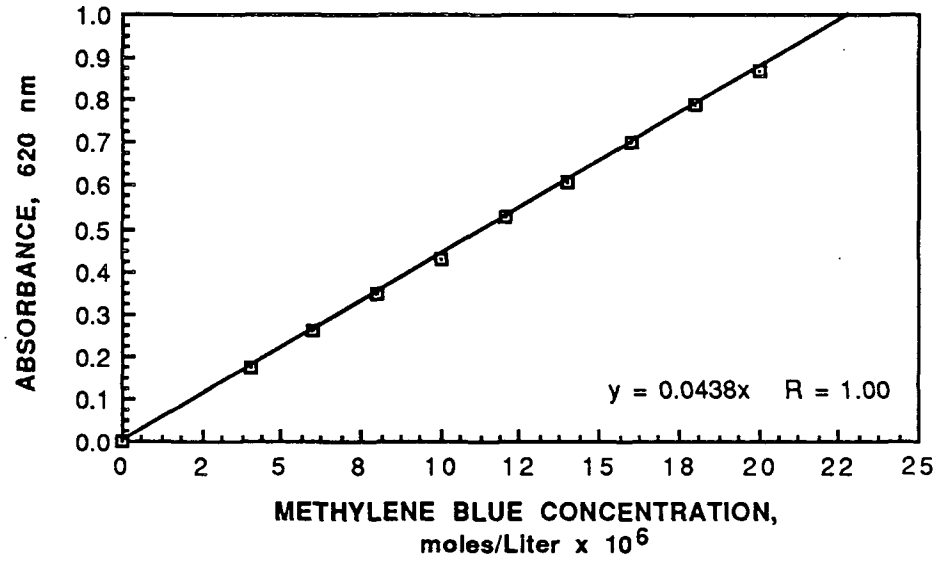

Figure A1. Methylene blue dye calibration curve.

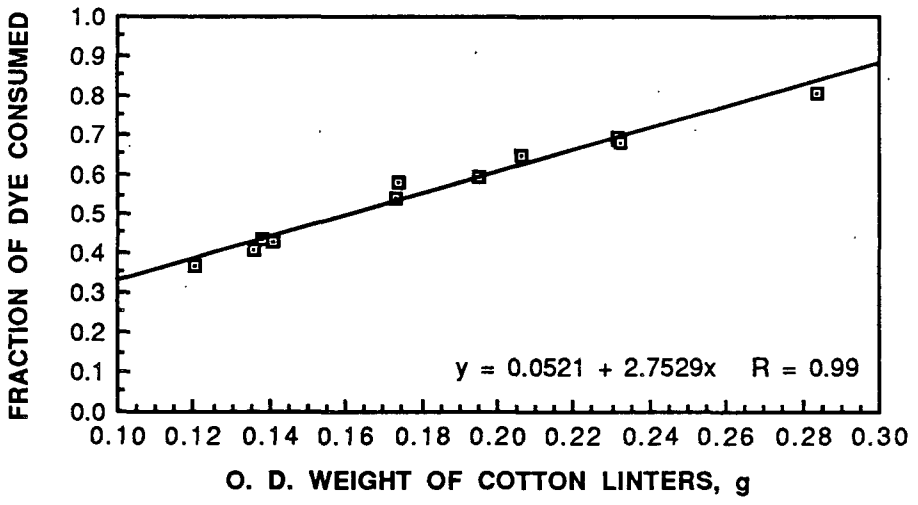

Figure A2. Consumption of methylene blue vs. fiber weight.

APPENDIX II

PROCEDURE FOR PREPARATION OF MONODISPERSED POLYSTYRENE LATICES

The following basic recipe was based on the methods presented in reference 53.

1. Place 2100 mL distilled water into a 5-liter round-bottomed three-necked flask (See Fig. A3).
2. The initial pH of the water is adjusted to 11.0.
3. Place the flask in a heater and heat to 80° C.
4. As the water solution is heating, bubble nitrogen through one port into the liquid to remove any oxygen contamination. A condenser and thermometer can be placed on the other port on the flask to reduce evaporation and monitor temperature. The exit gas from the condenser should be bubbled through a beaker of water to prevent oxygen from re-entering the system. Allow the N_2 to bubble for at least 10 min.
5. The center port should be fitted with a ground glass stirrer with teflon paddle adjusted to 350 rpm. A curved stirrer paddle was used to conform to the rounded flask. Begin agitation.
6. Remove the condenser or N_2 injector and add 144.97 g of styrene (152.6 mL) and then replace the fitting. Allow the mixture to equilibrate for 15 min while continuing agitation.
8. Dissolve 1.3647 g of potassium persulfate in 100 mL distilled water in a 150 mL Pyrex beaker. Add the initiator via the condenser port and wash the beaker with 47 mL distilled water to give a total volume of 2400 mL.
9. Allow the polymerization 4 hours to come to completion or until large amounts of coagulum is formed.
10. When the reaction is complete, allow the system to stand without mixing for several minutes. This allows any unreacted monomer to rise to the surface. The latex should then be filtered through a filter packed with glass wool to remove both unreacted monomer and any coagulum formed.
11. The latex is cleaned in approximately 200 mL batches using an ultrafiltration cell. Large particles are first screened out with a 5 μm polycarbonate membrane. Washing is accomplished by diafiltration. This is done with the Amicon XM-300 membrane. Each batch is washed with 2000 mL of distilled water which is allowed to pass through the membrane while the latex cannot penetrate the 0.037 μm pores in the membrane.

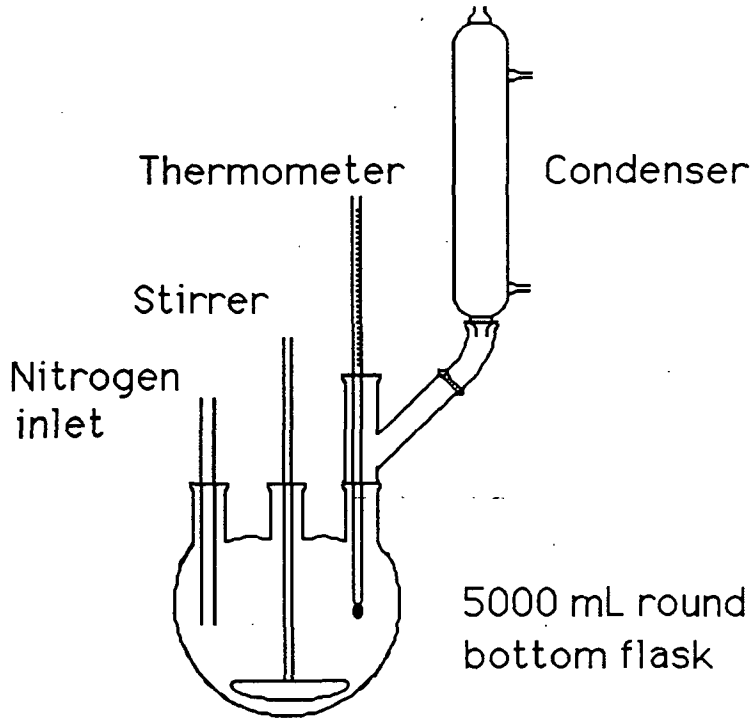

Figure A3. Apparatus for the preparation of polystyrene latex.

APPENDIX III

CHARACTERIZATION OF THE LATEX

Conductometric Titration Procedure

1. After polymerization of the polystyrene, 200 mL of uncleaned latex (approximately 4% solids) were passed through a 5 μm membrane in the Amicon ultrafiltration cell to remove any large particles formed during the polymerization.
2. Continuing with the cleaning procedure as outlined previously, 2100 mL of distilled water were washed through the latex to remove soluble contaminants. An XM-300 membrane was used in the ultrafiltration cell. The volume of latex was maintained at 200 mL to maintain the percent solids of the sample.
3. Without removing the sample from the filtration cell, approximately 600 mL of 0.0005 M HCl were allowed to pass through the sample to protonate the sulfate surface groups.
4. Again without removing the sample, 4000 mL of distilled water were passed through the sample to wash out the remaining HCl.
5. The latex was then removed from the cell and placed in a glass bottle.
6. 70 mL of latex were placed in a 100 mL three-necked round bottom flask. Another 10 mL were used to determine the percent solids of the sample.
7. Nitrogen was bubbled through the sample in the flask for one hour to remove any CO_2 contamination. The latex was continuously stirred with a teflon magnetic stir bar.
8. The nitrogen was then placed above the level of the sample to provide a nitrogen blanket.
9. Conductivity was measured through a side port with a Cole-Parmer 5800-20 conductivity probe connected to a Cole-Parmer 5800-00 Solution Analyzer. Conductivity was measured with the stirrer off.
10. The third port was used to introduce 0.02478 N NaOH in 0.05 mL increments.
11. Between the NaOH additions, the sample was allowed to mix for one minute before the conductivity was measured. NaOH was added until a plot of conductivity vs. mL NaOH increased linearly (after approximately 1.5 mL).
12. A plot of conductivity vs. meq of NaOH was made, and the two linear portions extrapolated to give the end point.

13. Acid content was calculated from: $\frac{\text{(meq NaOH at end point)(100)}}{\text{(\% solids of latex)(mL latex sample)}}$

14. Steps 6-13 were repeated for the rest of the latex sample.

Table A1. Conductometric Titration Data.

Run 1		Run 2	
meq NaOH	Conductance	meq NaOH	Conductance
0.00000	14.58	0.00000	14.50
0.00124	14.95	0.00124	14.85
0.00248	14.20	0.00248	14.10
0.00372	13.79	0.00372	13.21
0.00496	12.95	0.00496	12.54
0.00620	12.34	0.00620	11.99
0.00743	11.64	0.00743	11.34
0.00867	11.21	0.00867	10.88
0.00991	10.51	0.00991	10.04
0.01115	9.88	0.01115	9.63
0.01239	9.22	0.01239	8.80
0.01363	8.74	0.01363	8.25
0.01487	8.28	0.01487	7.85
0.01611	8.14	0.01611	7.89
0.01735	8.37	0.01735	8.13
0.01859	8.72	0.01859	8.65
0.01982	9.50	0.01982	9.20
0.02106	10.66	0.02106	10.76
0.02230	12.21	0.02230	12.59
0.02354	14.08	0.02354	14.82
0.02478	16.23	0.02478	16.82
0.02602	18.89	0.02602	18.68
0.02726	20.20	0.02726	22.00
0.02850	24.10	0.02850	24.20
0.02974	27.30	0.02974	27.40
0.03098	30.00	0.03098	29.90
0.03221	33.10	0.03221	35.70
0.03345	35.10	0.03345	37.50
0.03469	39.80	0.03469	40.10
0.03593	42.10	0.03593	43.50
0.03717	44.40	0.03717	46.70
0.03841	48.50	0.03841	49.50

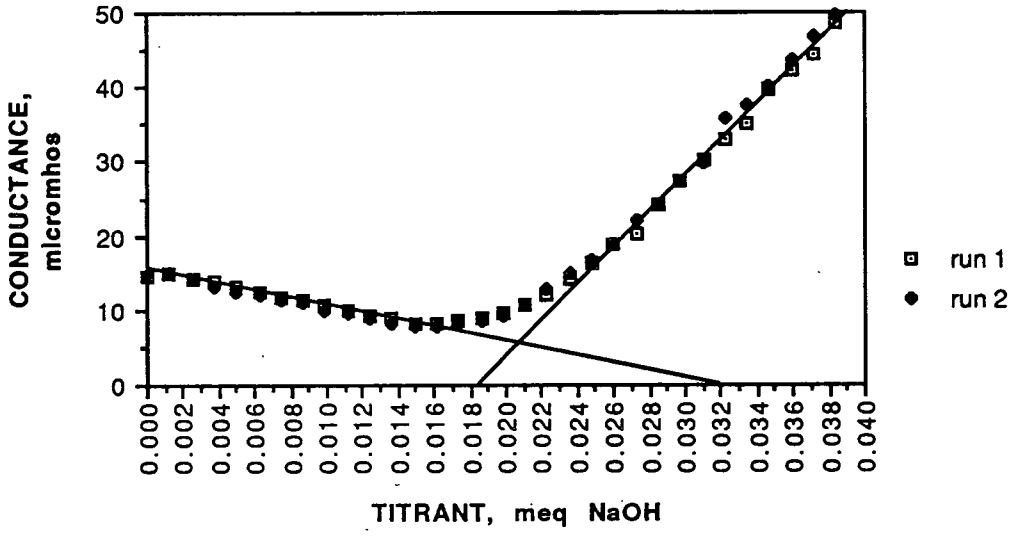

Figure A4. Conductometric titration curves for two separate runs.

Particle Size Determination

The particle size was determined by three methods: (1) measurement by hand from a scanning electron micrograph (SEM), (2) measurement with a Hewlett-Packard Dymec Model Dy-7092 Data Recording System from a SEM negative, and (3) measurement with the Zetasizer using the PC4 cell.

Method one consisted of measuring single particles by hand from several scanning electron micrographs at 20,000 X. A standard scale was also photographed at 20,000 X. The actual particle diameter was obtained from a ratio of the measured diameter to the standard scale length. The average diameter from 20 particles was 0.46 μm with a standard deviation of 0.026 μm. An example SEM is shown in Fig. A5.

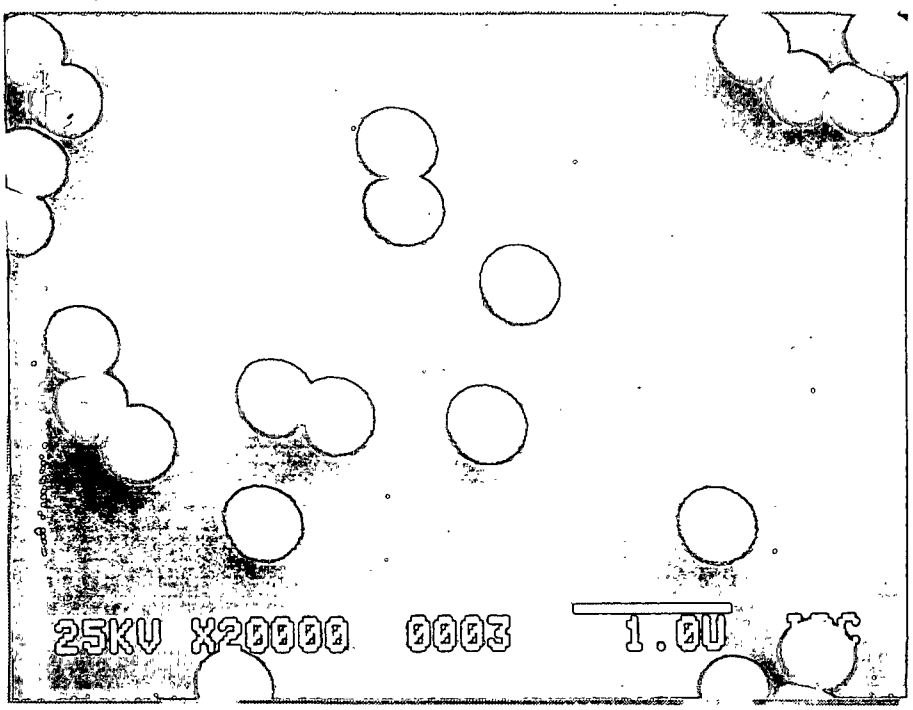

Figure A5. A scanning electron micrograph used for particle size determination.

The second method consisted of recording the x,y coordinates corresponding to the edges of single particles with the Hewlett-Packard Dymec Model Dy-7092 Data Recording System. The diameters were then calculated from the distance between the two points. The x,y coordinates were obtained by shining light through the film negative. The average particle diameter was calculated to be 0.419 μm with a standard deviation of 0.037 μm. The edges of smaller particles are generally harder to distinguish which probably lead to increased error. Shadows on the negative also became more evident as the magnification decreased.

Method three used the Zetasizer IIc. The analysis was done at pH 4.5 and 0.01 M NaCl background at 25° C using one laser beam and the PC4 cell. The results from the PC4 cell are given in Fig. 34. The z-average particle size was

0.4832 μm with a standard deviation of 0.0642 μm. The standard deviation was low and, the polydispersity was 0.018 which indicated a monodispersed sample. An average value from the first and last method, 0.47 μm, was taken as the particle diameter.

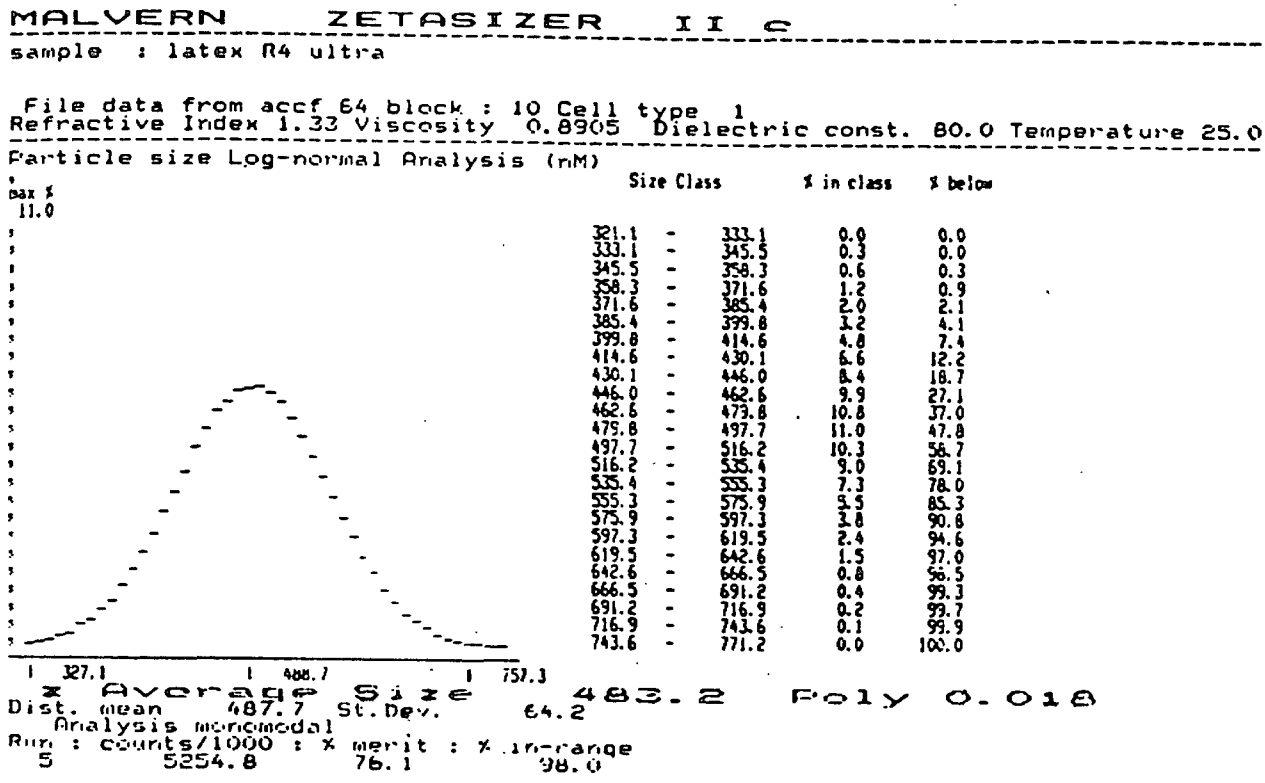

Figure A6. Particle size output from the Zetasizer for the latex used in this study.

APPENDIX IV

PROCEDURE TO DETERMINE ADSORPTION VS. TIME RELATIONSHIP

This procedure uses a modified form of the colloid titration to determine the amount of polyacrylamide remaining in solution.[79] This test is probably an underestimate because the potassium polyvinyl sulfate will also bind with segments of Q5 present in the loops and tails.

1. To the Britt jar add 1.2 od g cotton linters after adding enough water to bring total volume to 500 mL.
2. Mix the furnish with a mixer speed of 750 rpm for a period of two minutes.
3. Add the appropriate dosage of polymer to the jar and start the stopwatch.
4. When sample time has expired, drain the Britt jar-- waiting 10 s before collecting a sample for measurement. Therefore, the contact time of polymer is the sample time plus 10 s.
5. Collect a 40 mL sample and centrifuge if there are cotton linter fines present.
6. Add 5 mL 2.0 mg/L potassium polyvinyl sulfate, then 5 mL 11 mg/L o-toluidine blue. Shake.
7. Measure absorbance at 625 nm and compare with calibration curve, Fig. A7, to calculate amount of polymer present in white water.

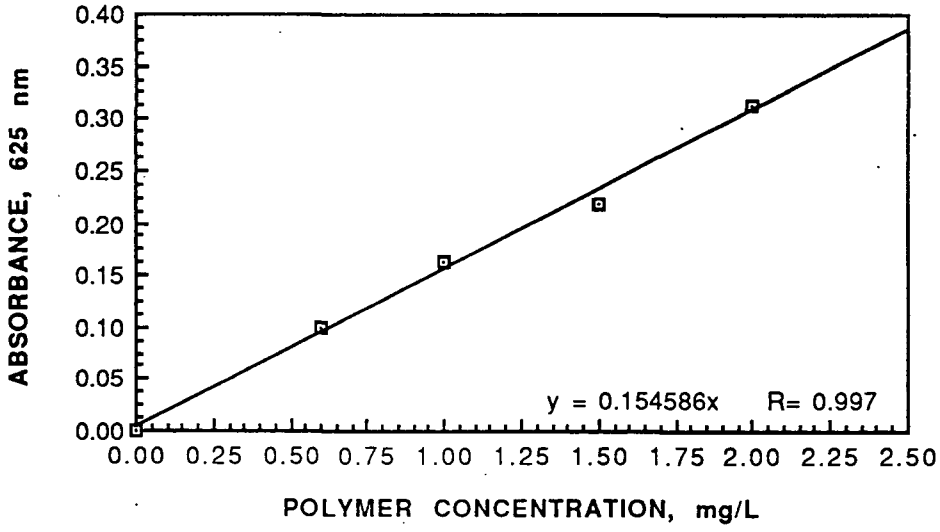

Figure A7. Colloid titration calibration curve.

APPENDIX V

ZETASIZER CELL COATING PROCEDURE

1. The cell was cleaned, dried in an oven, and cooled before coating.
2. The cell was pretreated with γ-glycidoxypropyltrimethoxysilane by plugging one end of the cell with a rubber stopper and filling it with undiluted silane. The silane was allowed to remain in the cell for 10 min.
3. The capillary was drained and step 2 repeated.
4. After draining the second time, the cell was washed lightly with distilled water acidified with glacial acetic acid. The pretreated cell was then placed in an oven and dried. Several cells can be pretreated and kept in a desiccator until needed; the desiccator is crucial as moisture in the air will destroy the active bonding sites for the methylcellulose.
5. A 250 mL solution of 0.1% Dow Methocel™ (coated polymer beads) was prepared and allowed to mix for five minutes. The methylcellulose was then released from the special coating by adjusting the pH to 9.0 with ammonium hydroxide. The coating allows easier dissolution of the methylcellulose.
6. The cell was placed in the Methocel™ and allowed to stand one hour. The cell was then removed, rinsed with distilled water, and inserted into the Zetasizer cell holder.

APPENDIX VI

RETENTION BY ABSORBANCE

The first method examined to determine the concentration of latex in the whitewater, and thus, the retention used the UV absorbance of polystyrene. A suspension of latex was placed in a quartz cell and the absorbance measured with a Perkin-Elmer 320 Spectrophotometer set at a wavelength of 275 nm. A calibration curve was made using untreated latex. The retention values obtained with this calibration curve were not realistic. Noting that only one calibration curve was used for untreated and treated samples, calibration curves were made for each polymer loading to determine the effect of Q5 on the calibration curve. Theoretically, these curves should represent the same line. Figure A8 shows that this is not the case. The result of this decrease in absorbance with polymer present was to bias the retention results upward since apparently less latex was in the whitewater.

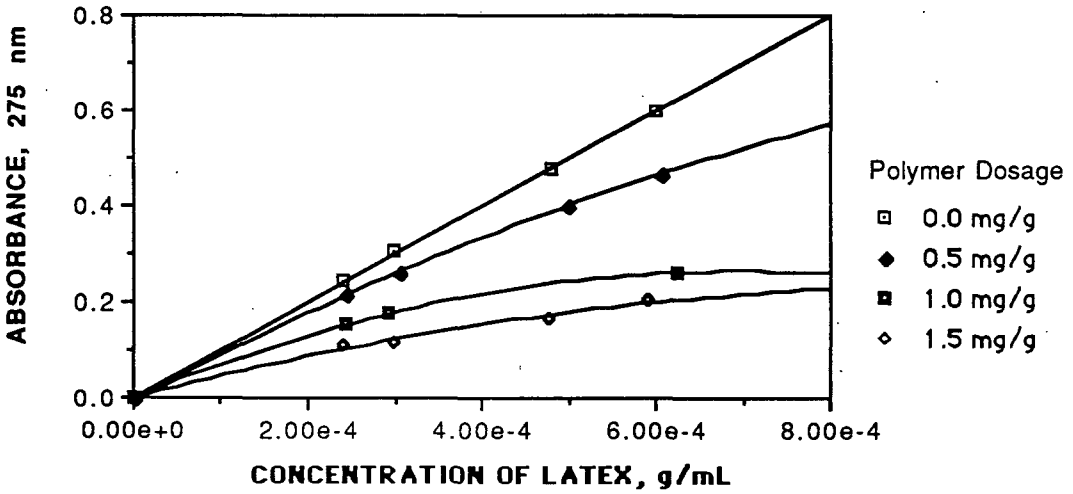

Figure A8. The effect of Q5 on the UV absorbance of polystyrene.

This decrease in absorbance could be the result of Rayleigh scattering within the polymer treated samples. Earlier in the literature section, it was stated that Rayleigh-Gans-Debye theory could be used if the quantity $(4\pi R/\lambda)(\tilde{n}_2/\tilde{n}_1 - 1)$ was much less than one. Unfortunately, in the present system, this assumption does not hold since this quantity equals 2.18. Therefore, in the strictest sense Mie theory should be used. But, Mie theory is dependent upon the scattering angle.[80] Therefore, Rayleigh-Gans-Debye theory will still be used here to determine the relative changes in scattered light at all angles that might be expected in a system of aggregating spheres. The theory is used with the knowledge that the values calculated are not absolute.

Rayleigh-Gans-Debye theory predicts that the intensity of scattering will increase with mass squared.[80] Hence, an increase in the mass of the light scatterer will increase the apparent absorbance. This quadratic response is not seen in Fig. A8. In fact, the response is the opposite of what is expected.

There are two possible reasons for this strange behavior. One is that the latex is being adsorbed onto the surface of the polypropylene beakers and quartz cell used in the analysis. This possible adsorption loss was tested using three types of beakers--glass, polyethylene glycol treated glass, and polypropylene. Treated latex samples of known concentration were placed in each of the beakers and diluted in a second beaker of the same type. These diluted samples were then tested on the spectrophotometer. The value of absorbance measured from each sample was constant indicating that latex adsorption was not a problem.

The second reason for the change in absorbance could be the formation of flocs. Large changes in the number concentration and particle size distribution caused by any such aggregation were not detected with the Coulter Counter.® The particle size data presented earlier in this thesis did not show large flocs but a high percentage of singlets in the whitewater samples. Consequently, more data are required to explain this odd absorbance relationship.

APPENDIX VII

EXPERIMENTAL DESIGN

GRAMS TREATED FINES	POLYMER DOSAGE		
	0.5 mg/g furnish	1.0 mg/g furnish	1.5 mg/g furnish
	fines, fiber	fines, fiber	fines, fiber
0.06 g	100, 0%	100, 0%	100, 0%
(20%)	80, 20	80, 20	80, 20
	67, 33	67, 33	67, 33
	50, 50	50, 50	50, 50
	33, 67	33, 67	33, 67
0.15 g	100, 0%	100, 0%	100, 0%
(50%)	80, 20	80, 20	80, 20
	67, 33	67, 33	67, 33
	50, 50	50, 50	50, 50
	33, 67	33, 67	33, 67
0.225 g	100, 0%	100, 0%	100, 0%
(75%)	80, 20	80, 20	80, 20
	67, 33	67, 33	67, 33
	50, 50	50, 50	50, 50
	33, 67	33, 67	33, 67
0.30 g	100, 0%	100, 0%	100, 0%
(100%)	80, 20	80, 20	80, 20
	67, 33	67, 33	67, 33
	50, 50	50, 50	50, 50
	33, 67	33, 67	33, 67

APPENDIX VIII

CONDUCTIVITY RESULTS

The effectiveness of the control of conductivity is shown in Fig. A9. The 76 randomly chosen sample runs shown have a mean of 1163.22 μmhos/cm, a standard deviation of 13.04 μmhos/cm, and, hence, a 95% confidence interval around the mean of 1163.22 ± 2.98 μmhos/cm.

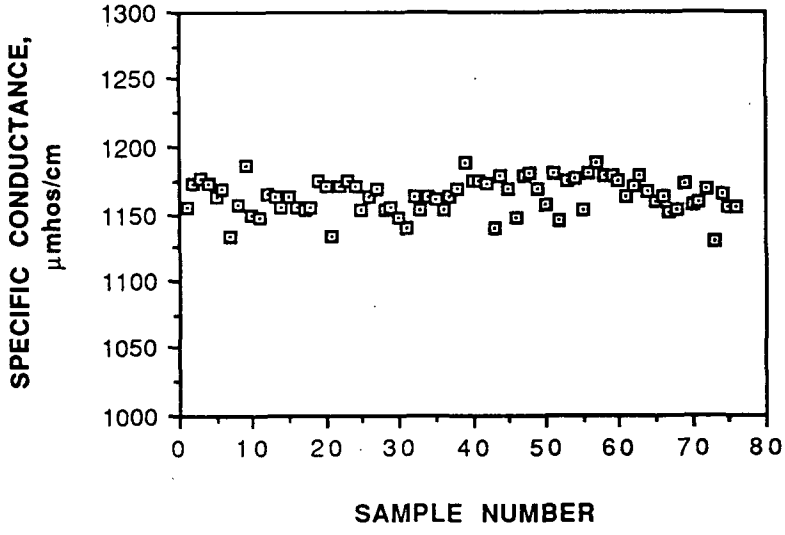

Figure A9. Constancy of specific conductance as shown by 76 randomly chosen samples.

APPENDIX IX

ELECTROPHORETIC MOBILITY DISTRIBUTIONS

To obtain the following electrophoretic mobility distributions, the individual headbox and whitewater distributions had to be placed on the same basis. The Zetasizer provides each distribution as a frequency distribution totalling 100%. If these distributions were converted to a mass basis, they could be directly compared. The whitewater distribution would then be a fractional part of the headbox distribution, and as such, it could be subtracted from the headbox distribution to give the mobility distribution of the retained particles. Therefore, all of the headbox samples were assumed to be the frequency distribution of 100% of the mass. The whitewater frequencies were then reduced by the fraction of mass in the whitewater sample as determined by the retention. In this way, the whitewater distribution of each sample could be subtracted from the corresponding headbox distribution.

For example, if the retention of a given sample was 60%, each frequency in the whitewater distribution would be multiplied by 0.40. The frequency in each mobility channel of the whitewater distribution would then be subtracted from the frequency of the corresponding mobility channel in the headbox distribution. This difference would represent the frequency distribution of the remaining 60% of the mass or the retained particles. Hence, the headbox frequency distribution for each value of mobility is the sum of the whitewater and retained frequencies for that particular value of electrophoretic mobility.

Therefore, the distributions that follow are presented such that the headbox frequencies total 100% of the mass, the whitewater frequencies total 100% minus the percent retention, and the retained particle frequencies total the percent retention.

Polymer Dosage: 0.5 mg/g or 1.0 lb/ton

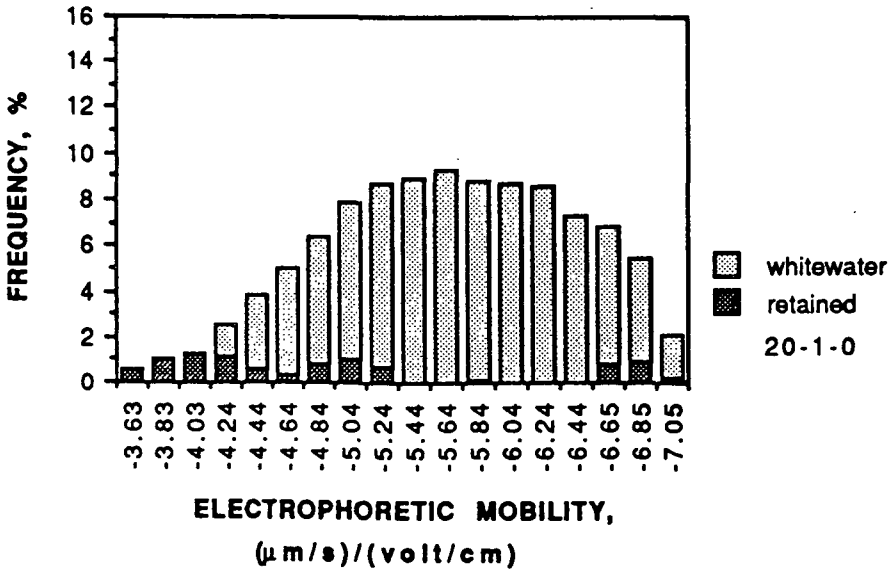

Figure A10. EM distributions for sample 20-1-0. Headbox distribution (total % frequency at each EM) is the sum of whitewater and retained distributions.

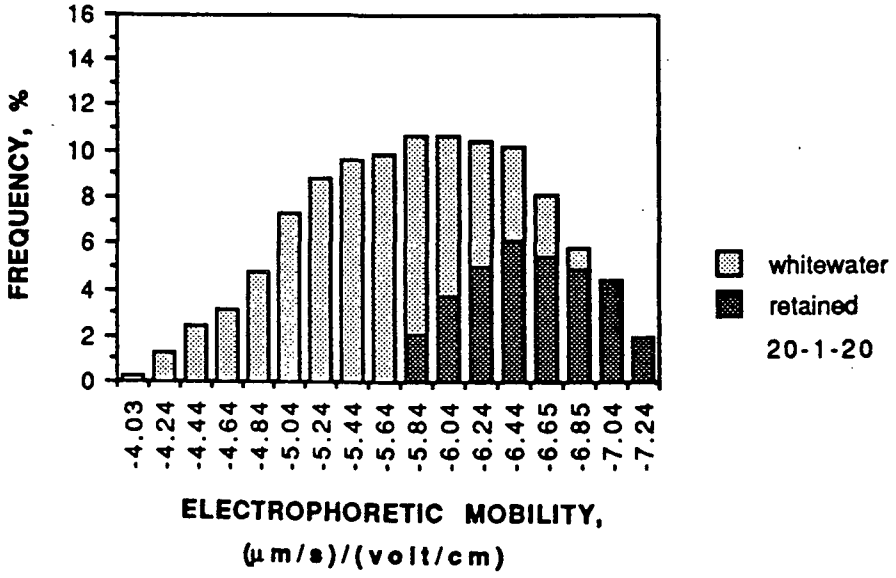

Figure A11. EM distributions for sample 20-1-20. Headbox distribution (total % frequency at each EM) is the sum of whitewater and retained distributions.

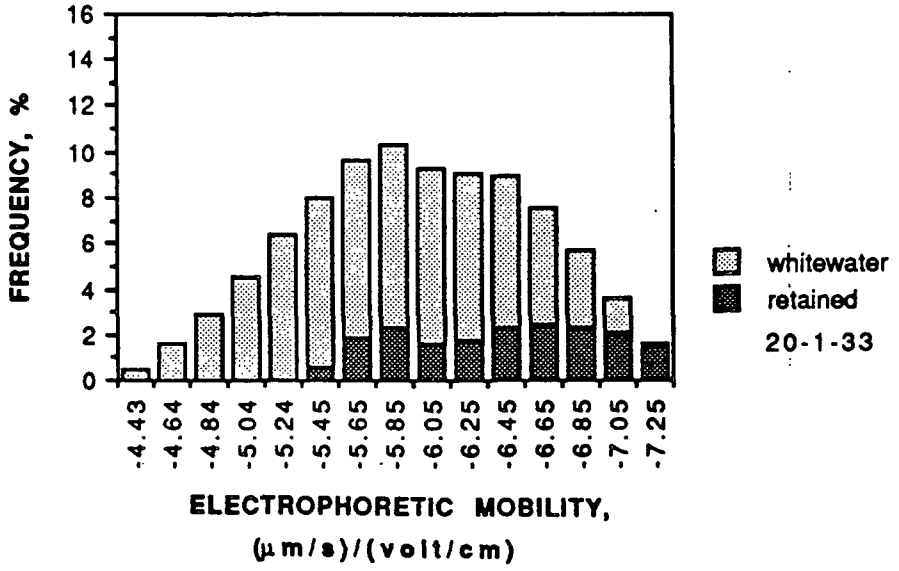

Figure A12. EM distributions for sample 20-1-33. Headbox distribution (total % frequency at each EM) is the sum of whitewater and retained distributions.

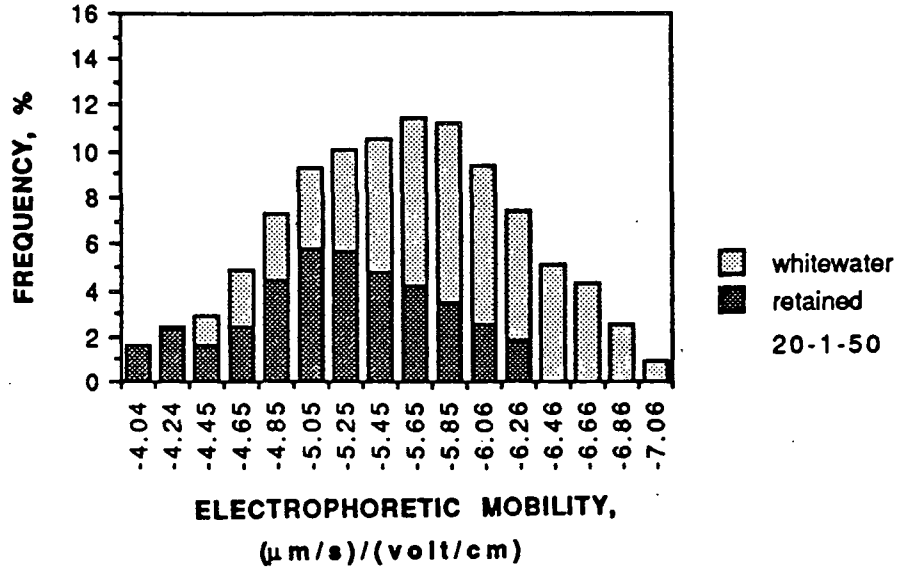

Figure A13. EM distributions for sample 20-1-50. Headbox distribution (total % frequency at each EM) is the sum of whitewater and retained distributions.

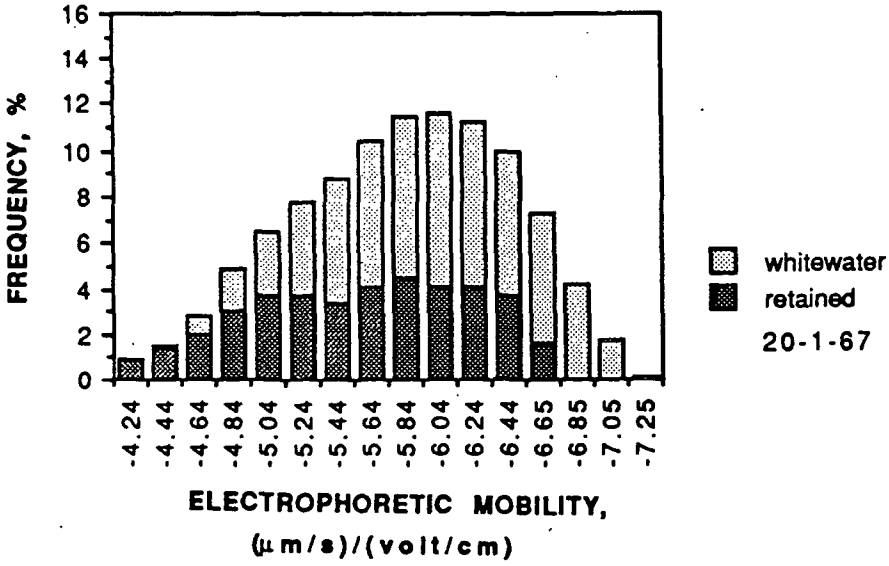

Figure A14. EM distributions for sample 20-1-67. Headbox distribution (total % frequency at each EM) is the sum of whitewater and retained distributions.

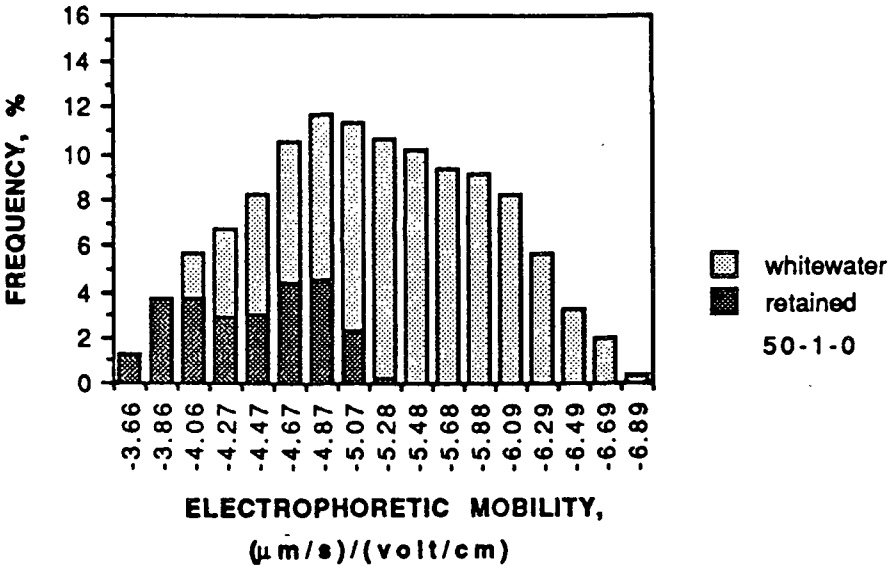

Figure A15. EM distributions for sample 50-1-0. Headbox distribution (total % frequency at each EM) is the sum of whitewater and retained distributions.

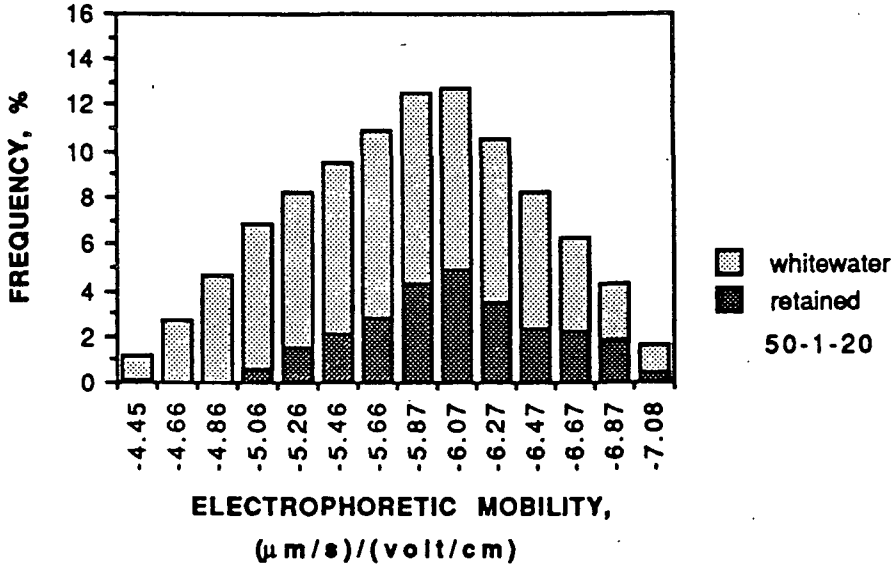

Figure A16. EM distributions for sample 50-1-20. Headbox distribution (total % frequency at each EM) is the sum of whitewater and retained distributions.

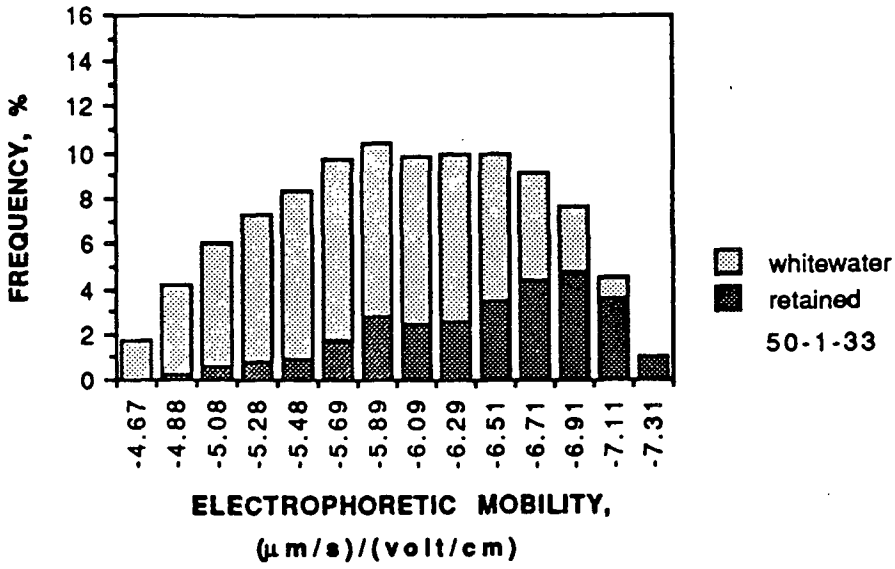

Figure A17. EM distributions for sample 50-1-33. Headbox distribution (total % frequency at each EM) is the sum of whitewater and retained distributions.

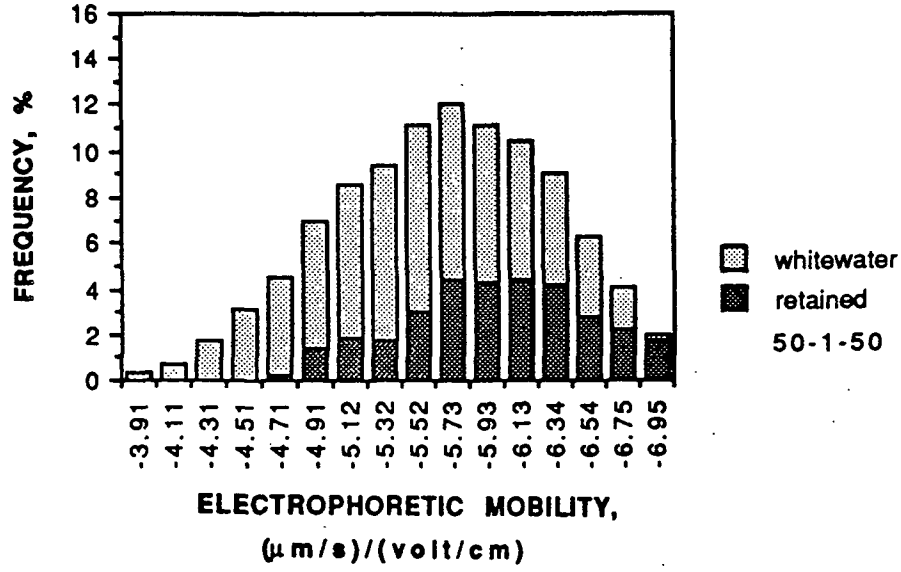

Figure A18. EM distributions for sample 50-1-50. Headbox distribution (total % frequency at each EM) is the sum of whitewater and retained distributions.

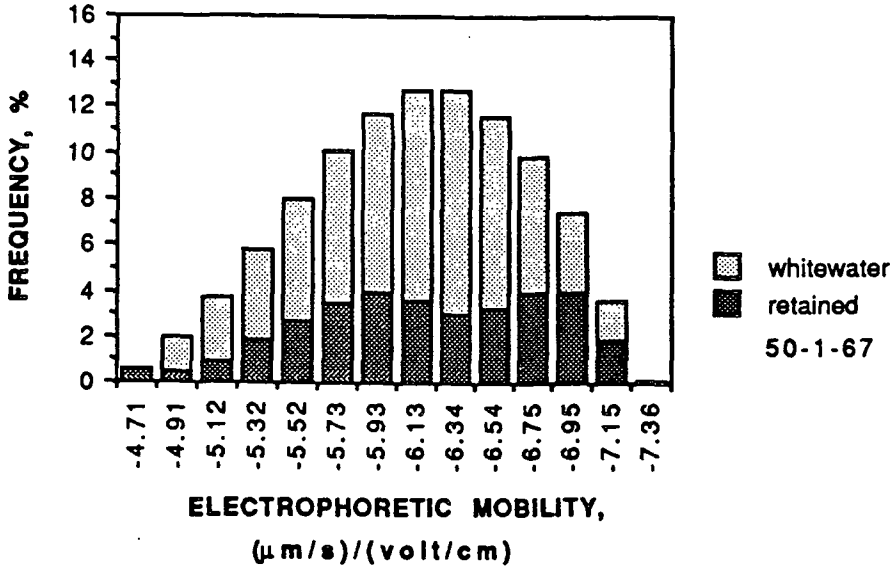

Figure A19. EM distributions for sample 50-1-67. Headbox distribution (total % frequency at each EM) is the sum of whitewater and retained distributions.

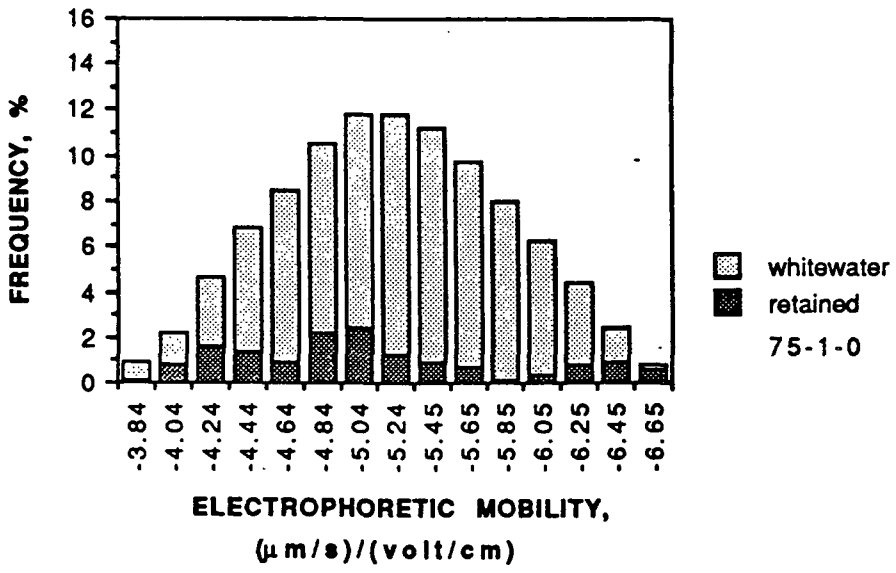

Figure A20. EM distributions for sample 75-1-0. Headbox distribution (total % frequency at each EM) is the sum of whitewater and retained distributions.

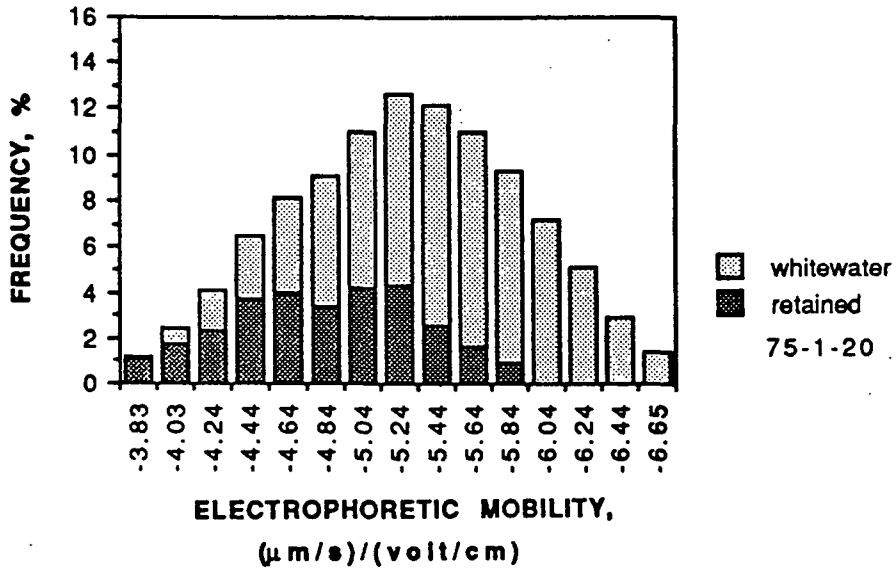

Figure A21. EM distributions for sample 75-1-20. Headbox distribution (total % frequency at each EM) is the sum of whitewater and retained distributions.

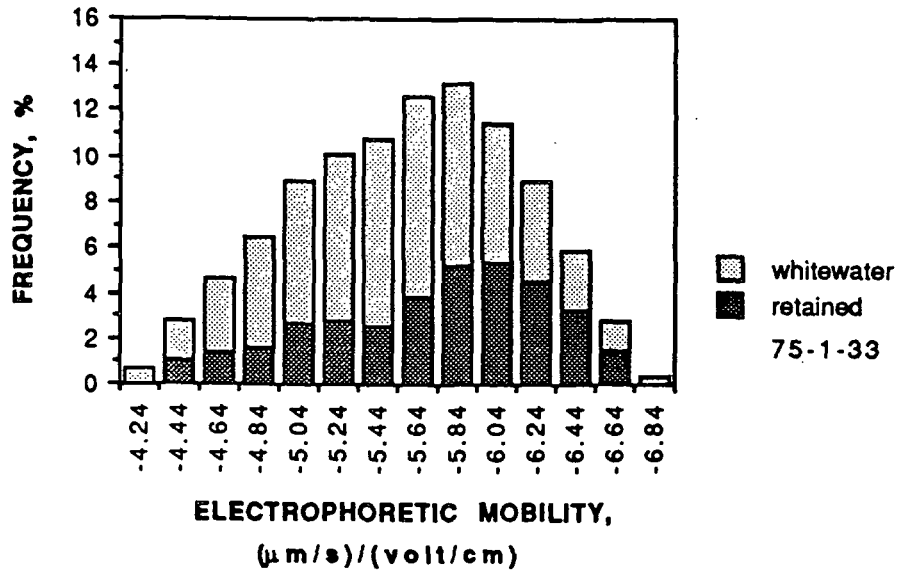

Figure A22. EM distributions for sample 75-1-33. Headbox distribution (total % frequency at each EM) is the sum of whitewater and retained distributions.

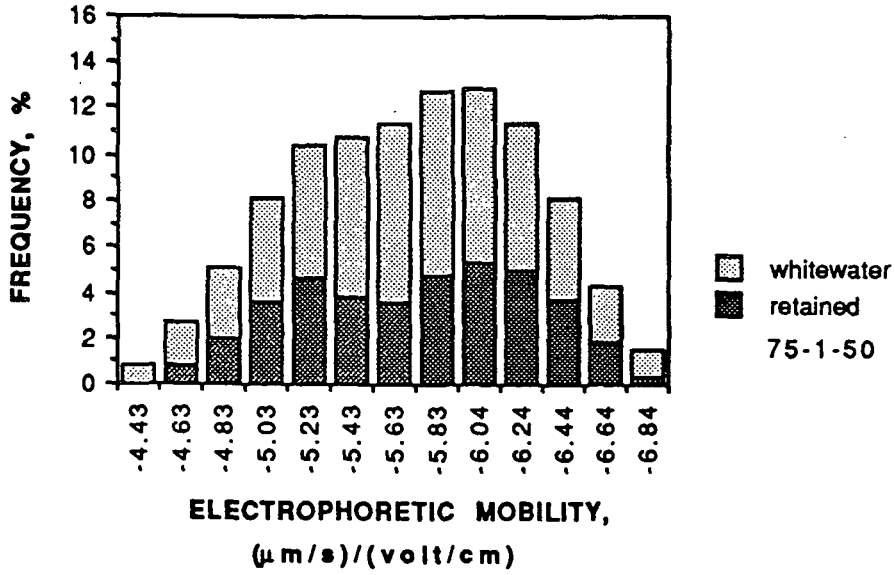

Figure A23. EM distributions for sample 75-1-50. Headbox distribution (total % frequency at each EM) is the sum of whitewater and retained distributions.

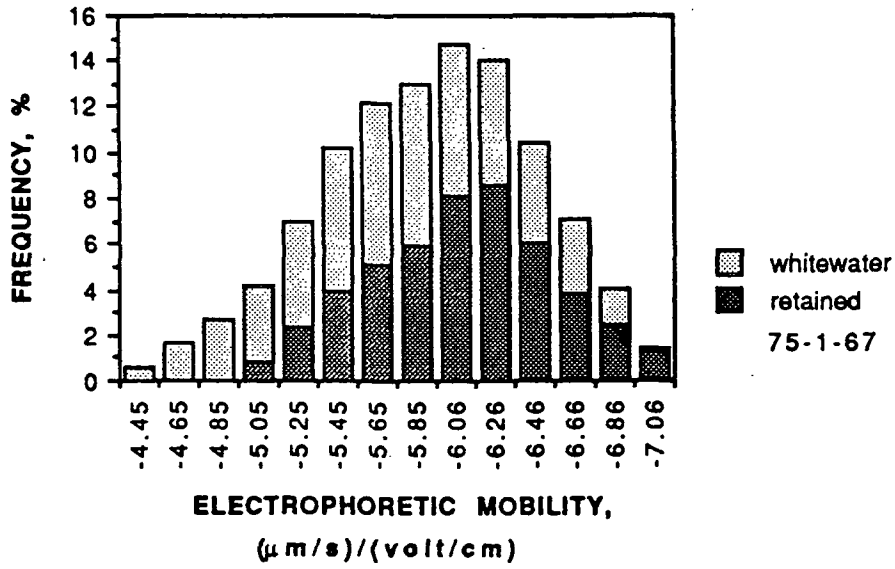

Figure A24. EM distributions for sample 75-1-67. Headbox distribution (total % frequency at each EM) is the sum of whitewater and retained distributions.

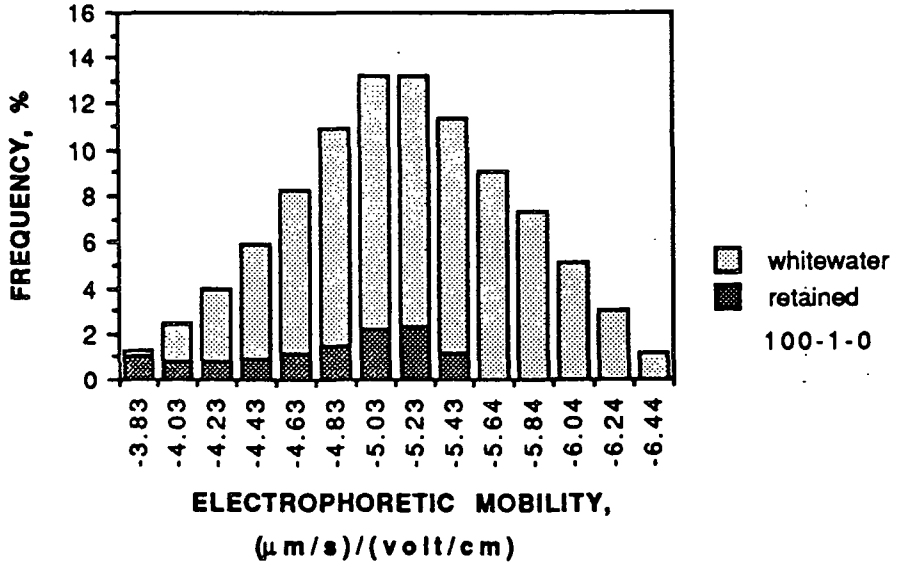

Figure A25. EM distributions for sample 100-1-0. Headbox distribution (total % frequency at each EM) is the sum of whitewater and retained distributions.

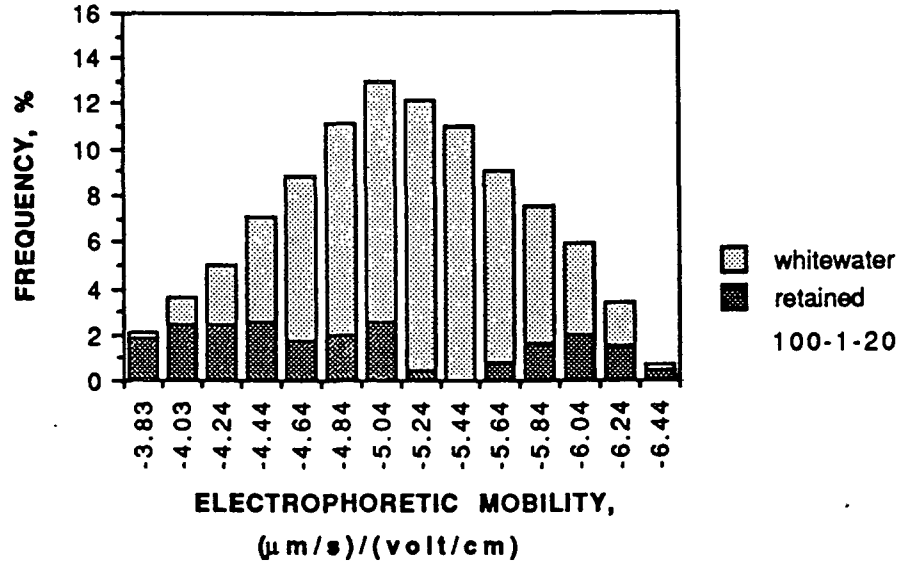

Figure A26. EM distributions for sample 100-1-20. Headbox distribution (total % frequency at each EM) is the sum of whitewater and retained distributions.

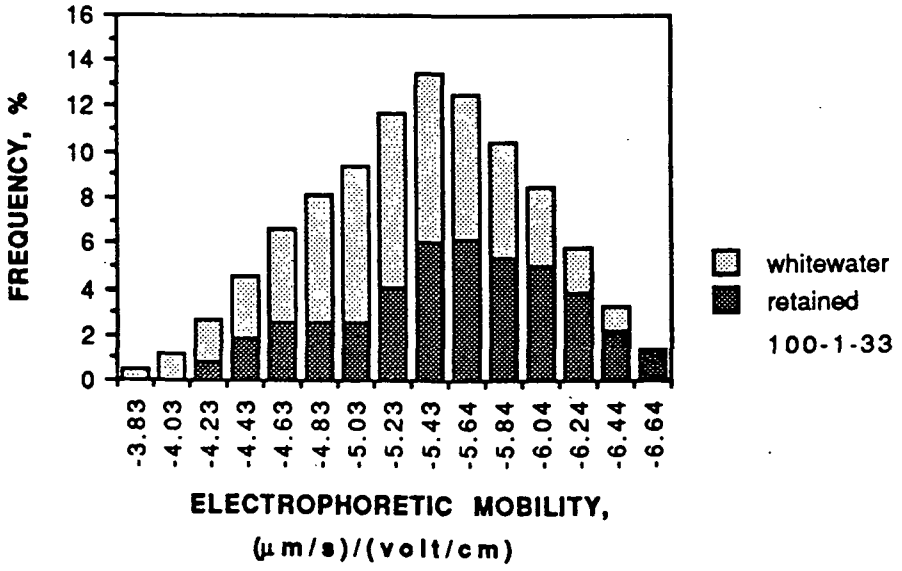

Figure A27. EM distributions for sample 100-1-33. Headbox distribution (total % frequency at each EM) is the sum of whitewater and retained distributions.

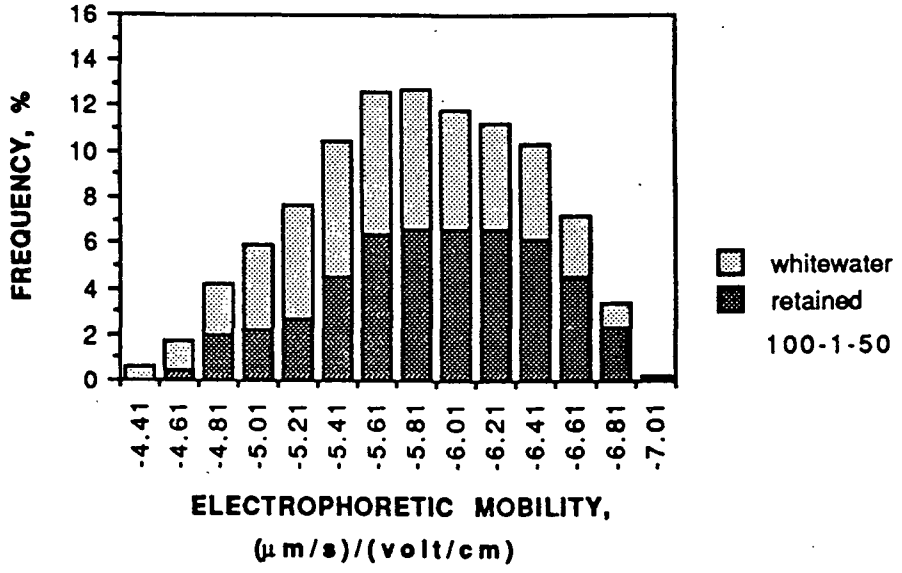

Figure A28. EM distributions for sample 100-1-50. Headbox distribution (total % frequency at each EM) is the sum of whitewater and retained distributions.

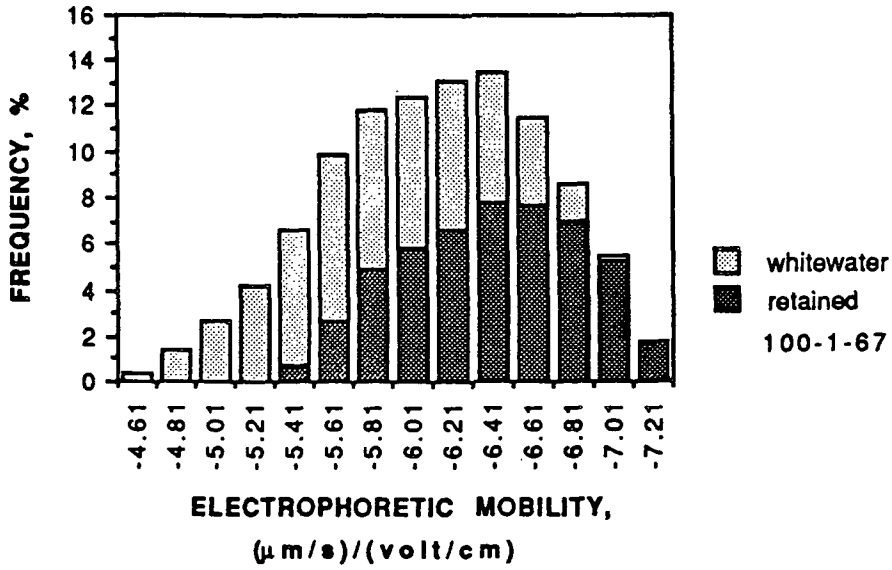

Figure A29. EM distributions for sample 100-1-67. Headbox distribution is the sum of whitewater and retained distributions.

Polymer Dosage: 1.0 mg/g or 2.0 lb/ton

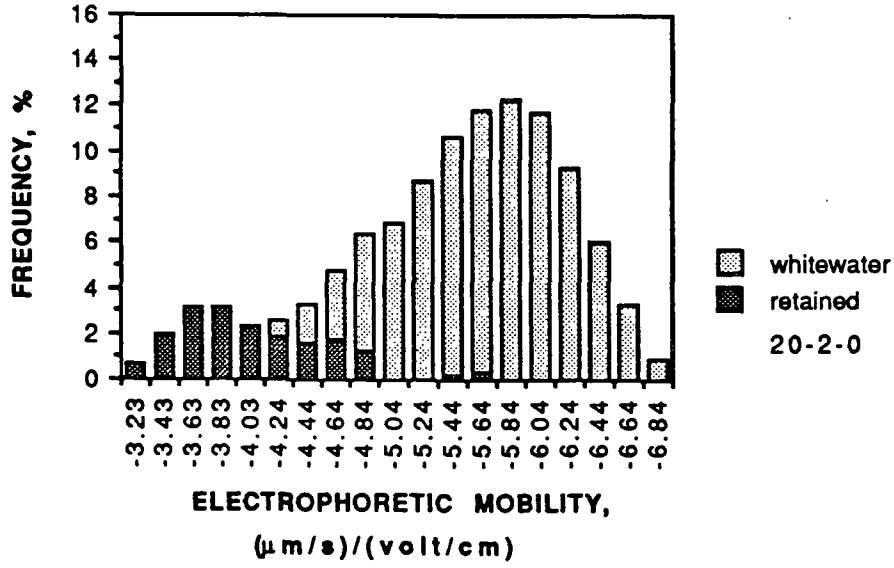

Figure A30. EM distributions for sample 20-2-0. Headbox distribution (total % frequency at each EM) is the sum of whitewater and retained distributions.

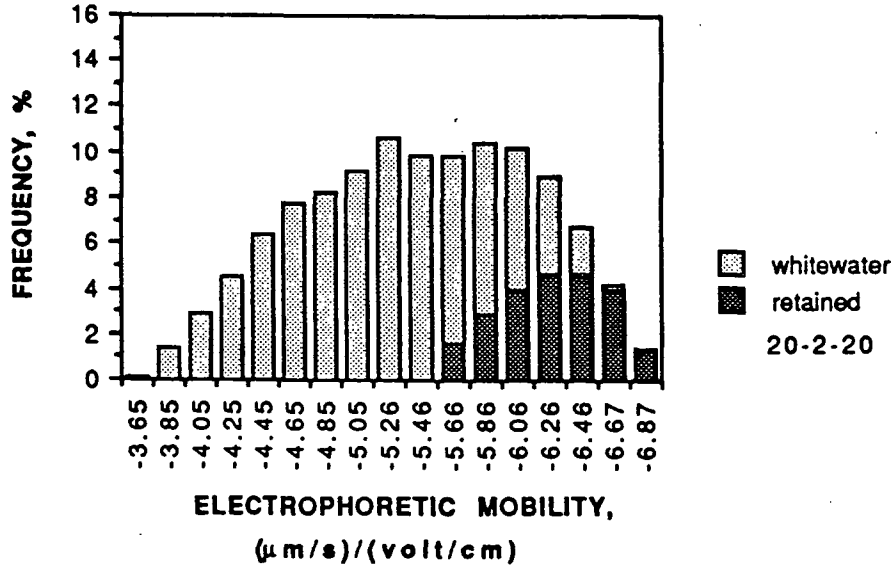

Figure A31. EM distributions for sample 20-2-20. Headbox distribution (total % frequency at each EM) is the sum of whitewater and retained distributions.

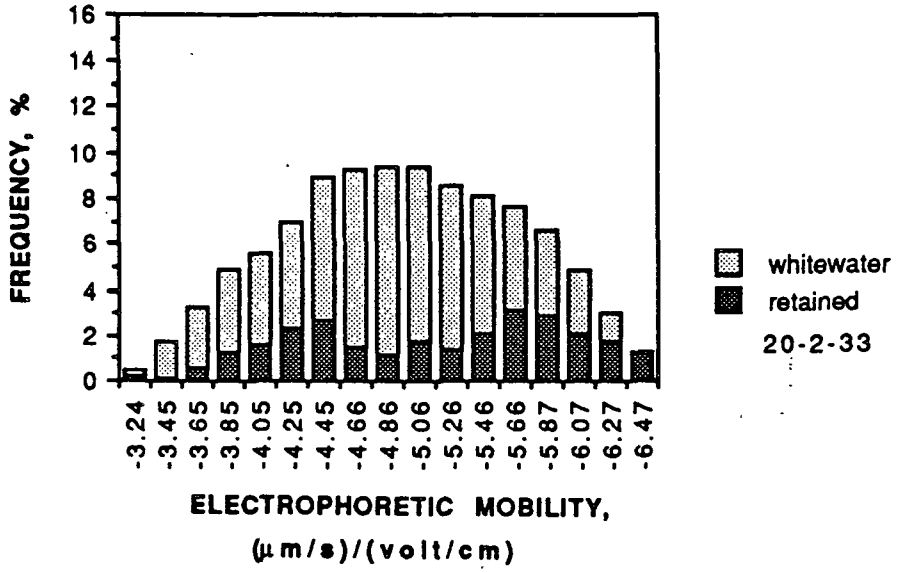

Figure A32. EM distributions for sample 20-2-33. Headbox distribution (total % frequency at each EM) is the sum of whitewater and retained distributions.

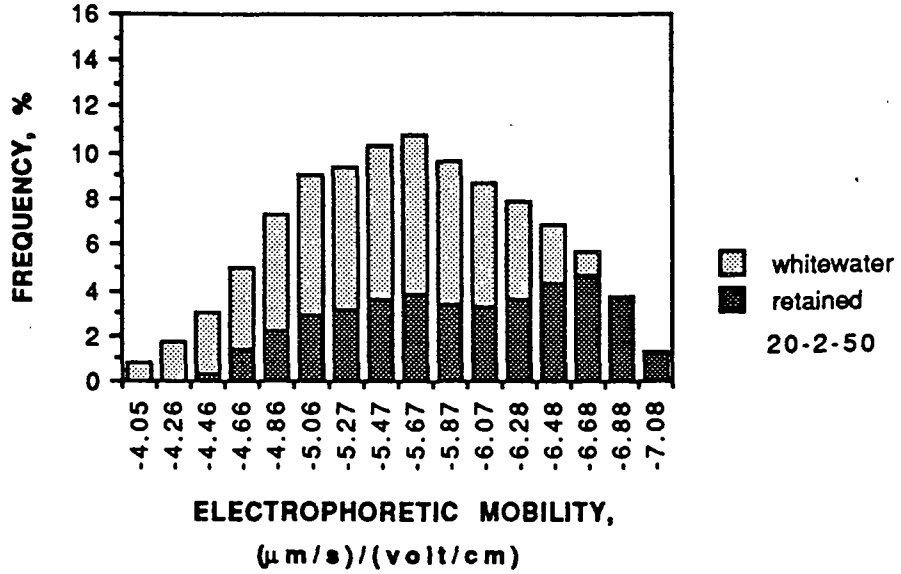

Figure A33. EM distributions for sample 20-2-50. Headbox distribution (total % frequency at each EM) is the sum of whitewater and retained distributions.

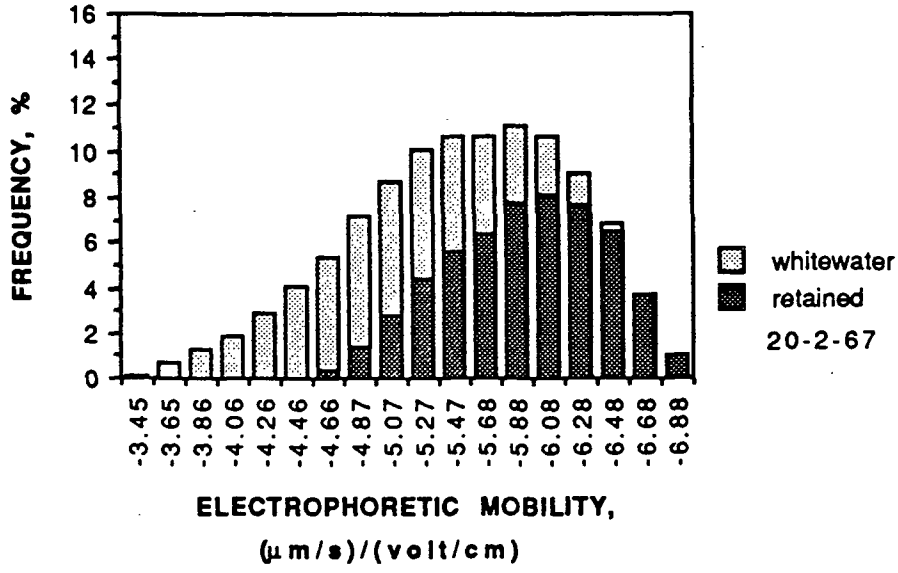

Figure A34. EM distributions for sample 20-2-67. Headbox distribution (total % frequency at each EM) is the sum of whitewater and retained distributions.

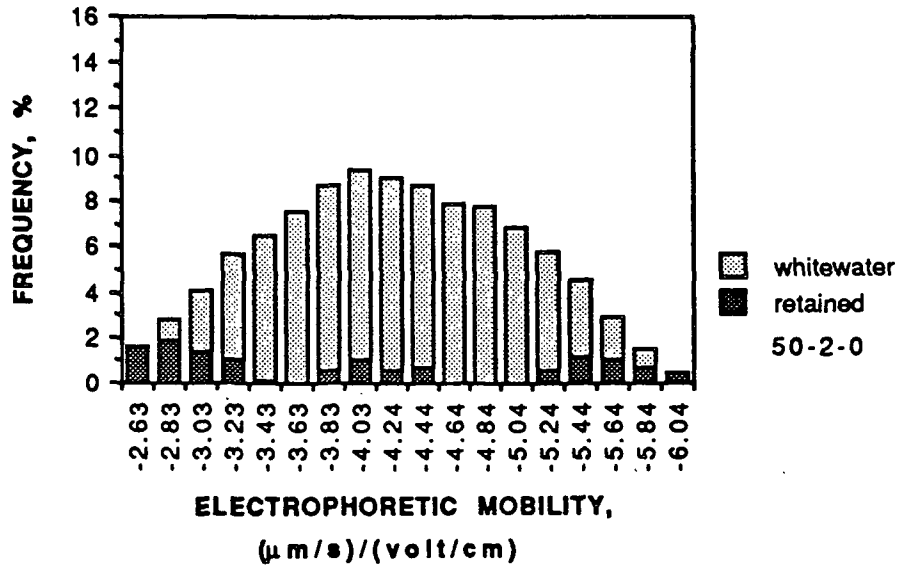

Figure A35. EM distributions for sample 50-2-0. Headbox distribution (total % frequency at each EM) is the sum of whitewater and retained distributions.

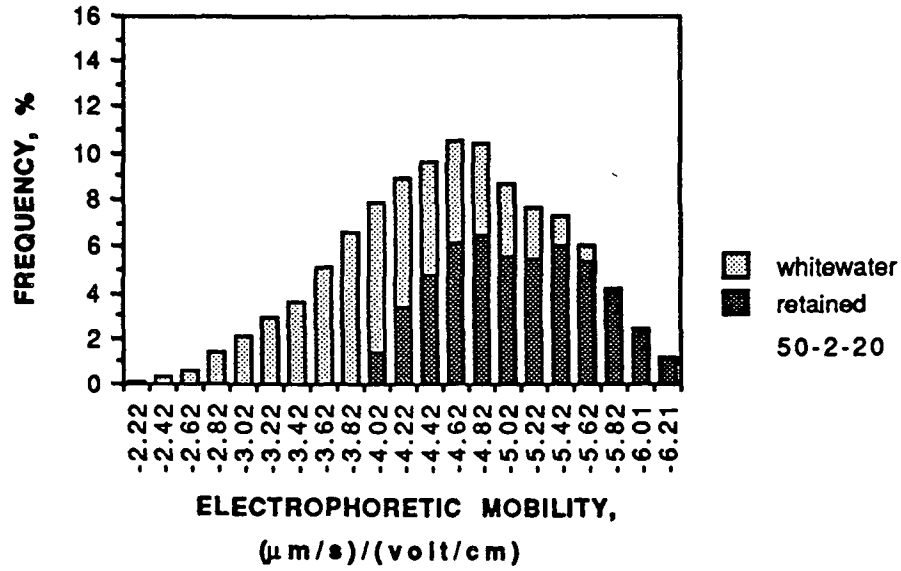

Figure A36. EM distributions for sample 50-2-20. Headbox distribution (total % frequency at each EM) is the sum of whitewater and retained distributions.

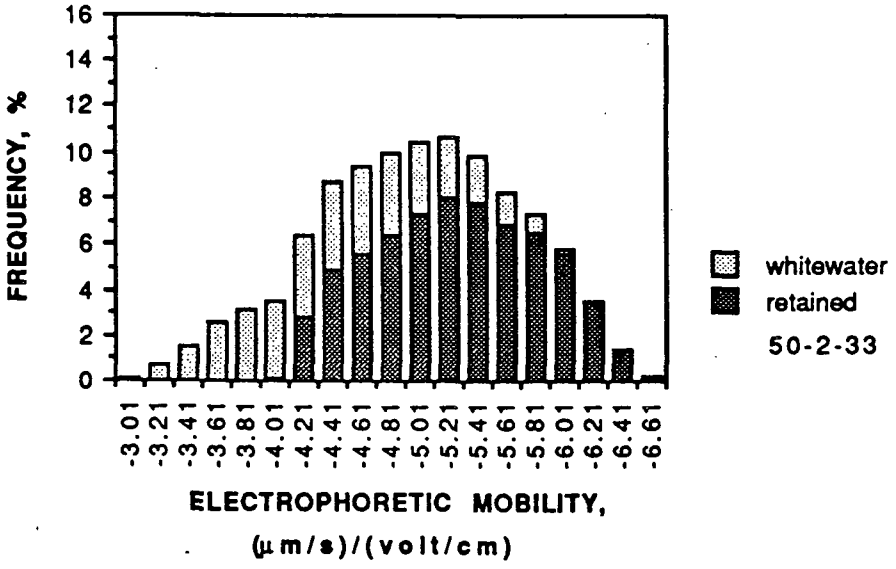

Figure A37. EM distributions for sample 50-2-33. Headbox distribution (total % frequency at each EM) is the sum of whitewater and retained distributions.

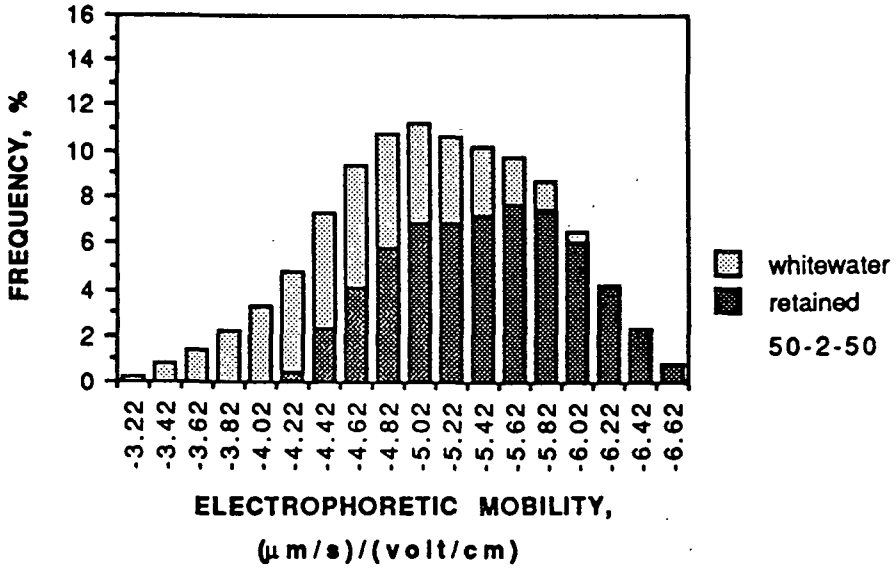

Figure A38. EM distributions for sample 50-2-50. Headbox distribution (total % frequency at each EM) is the sum of whitewater and retained distributions.

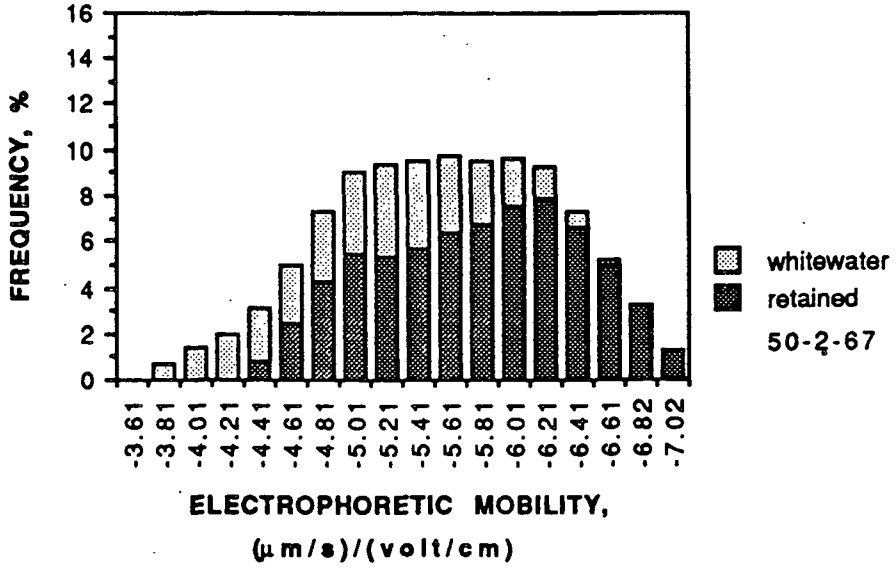

Figure A39. EM distributions for sample 50-2-67. Headbox distribution (total % frequency at each EM) is the sum of whitewater and retained distributions.

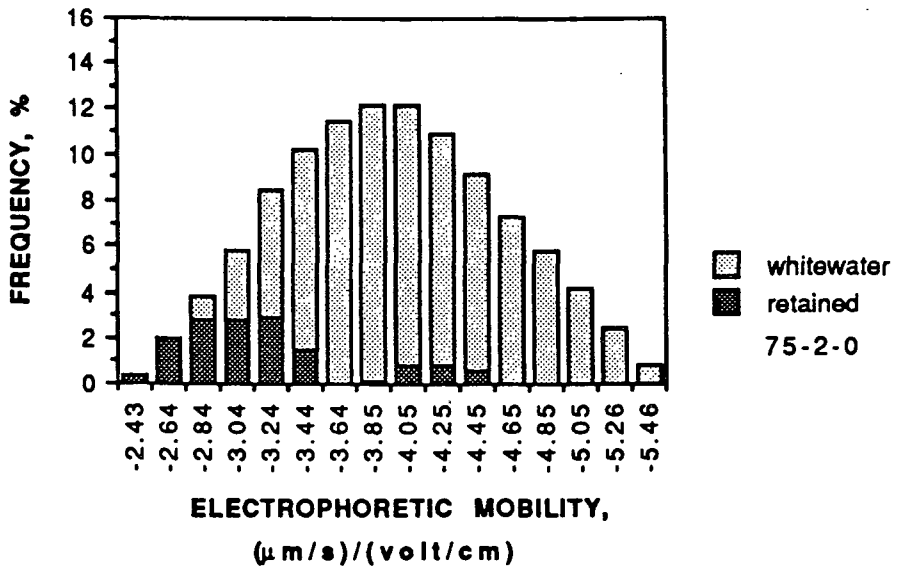

Figure A40. EM distributions for sample 75-2-0. Headbox distribution (total % frequency at each EM) is the sum of whitewater and retained distributions.

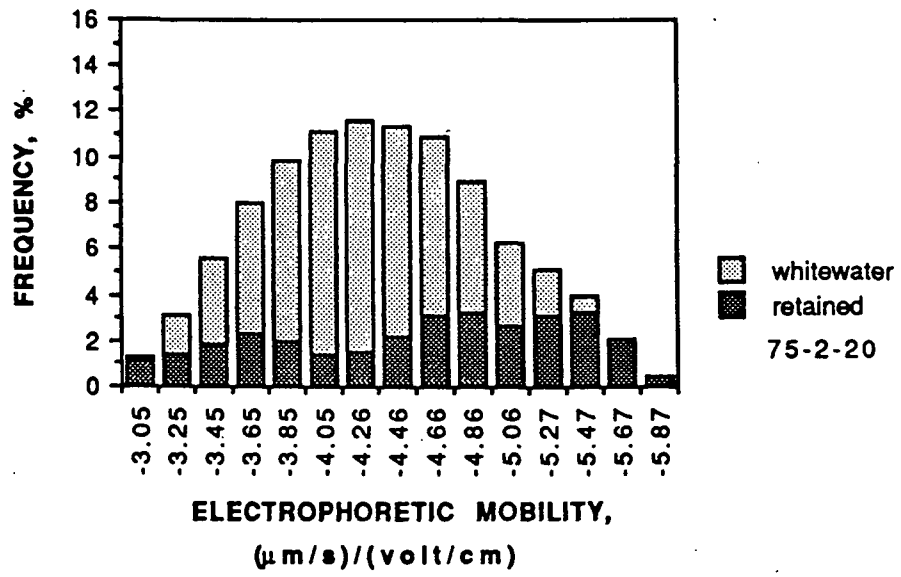

Figure A41. EM distributions for sample 75-2-20. Headbox distribution (total % frequency at each EM) is the sum of whitewater and retained distributions.

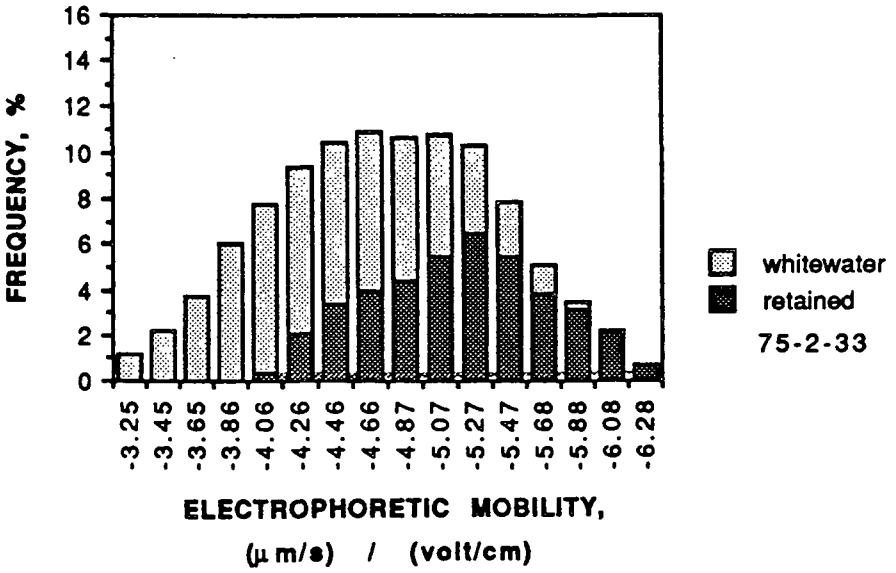

Figure A42. EM distributions for sample 75-2-33. Headbox distribution (total % frequency at each EM) is the sum of whitewater and retained distributions.

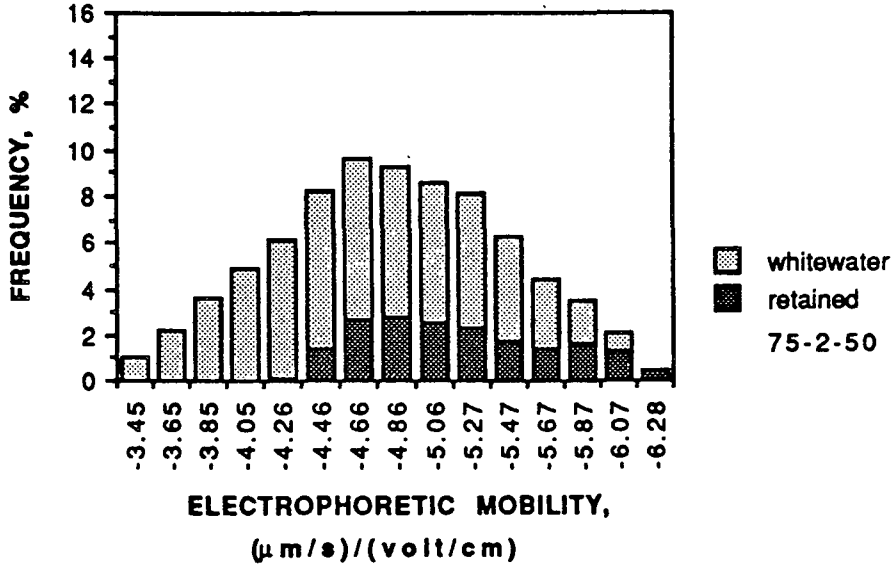

Figure A43. EM distributions for sample 75-2-50. Headbox distribution (total % frequency at each EM) is the sum of whitewater and retained distributions.

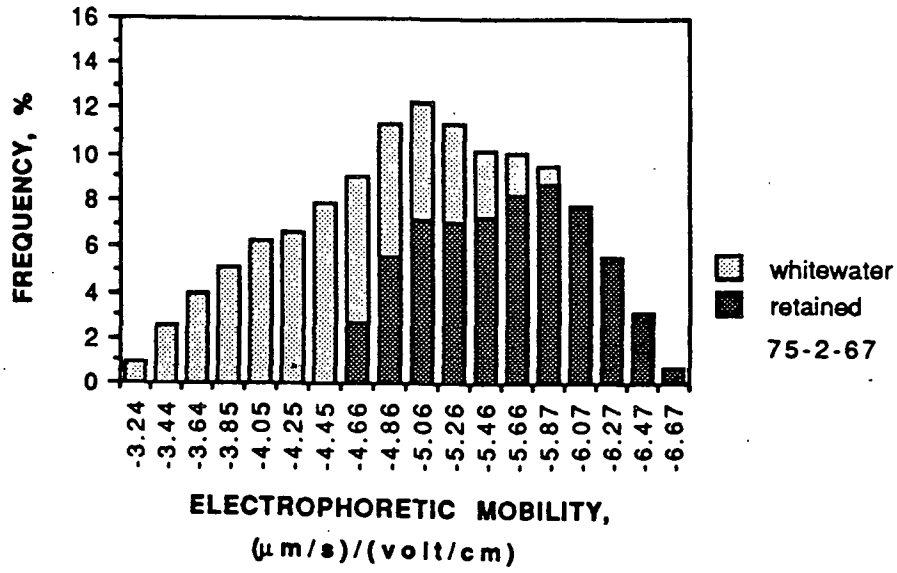

Figure A44. EM distributions for sample 75-2-67. Headbox distribution (total % frequency at each EM) is the sum of whitewater and retained distributions.

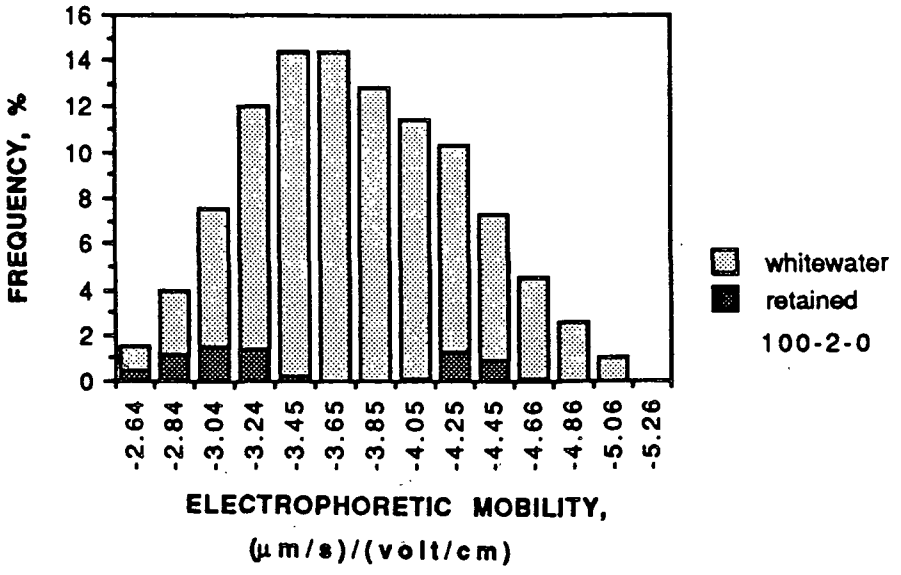

Figure A45. EM distributions for sample 100-2-0. Headbox distribution (total % frequency at each EM) is the sum of whitewater and retained distributions.

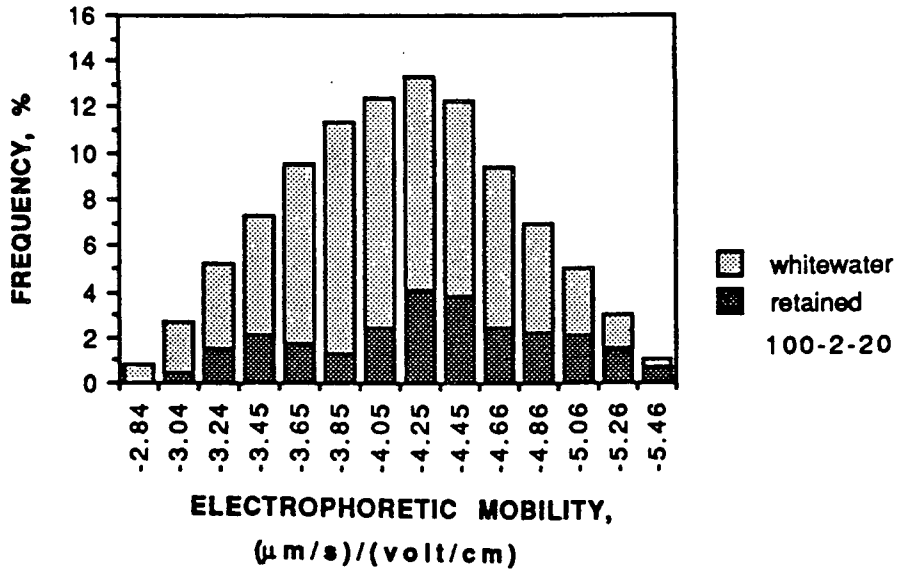

Figure A46. EM distributions for sample 100-2-20. Headbox distribution (total % frequency at each EM) is the sum of whitewater and retained distributions.

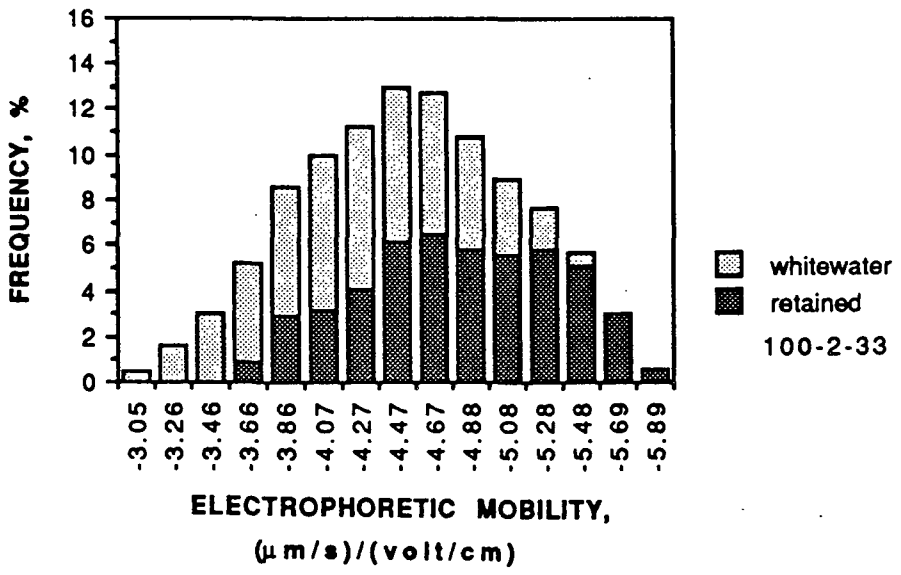

Figure A47. EM distributions for sample 100-2-33. Headbox distribution (total % frequency at each EM) is the sum of whitewater and retained distributions.

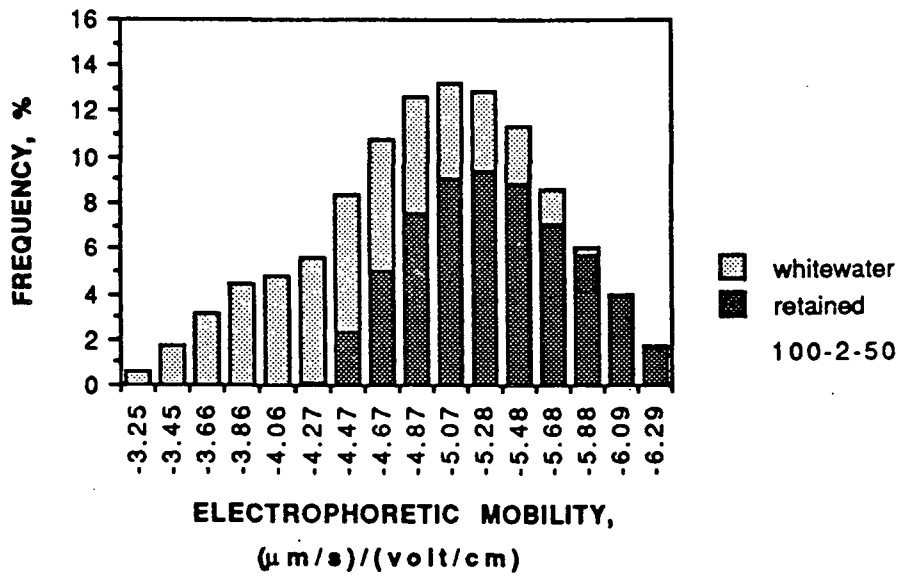

Figure A48. EM distributions for sample 100-2-50. Headbox distribution (total % frequency at each EM) is the sum of whitewater and retained distributions.

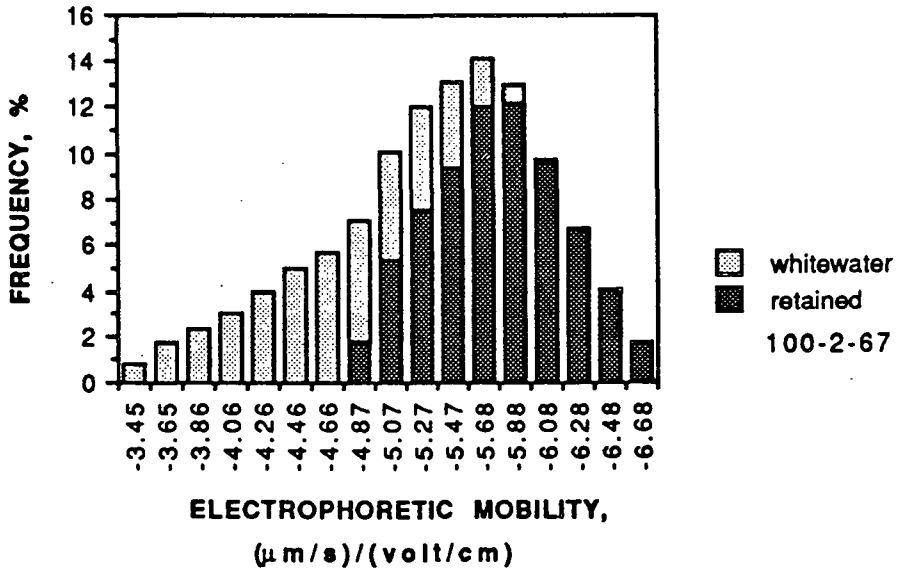

Figure A49. EM distributions for sample 100-2-67. Headbox distribution (total % frequency at each EM) is the sum of whitewater and retained distributions.

Polymer Dosage: 1.5 mg/g or 3.0 lb/ton

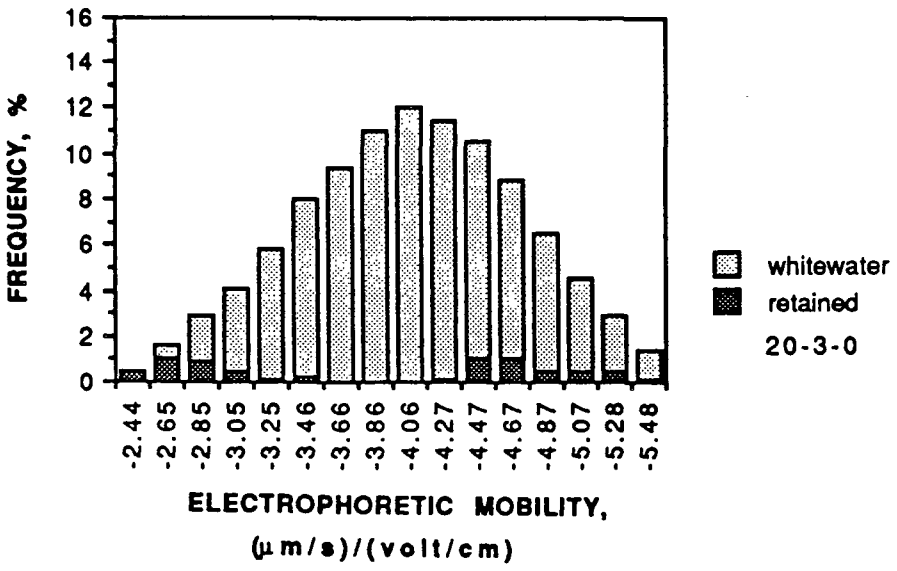

Figure A50. EM distributions for sample 20-3-0. Headbox distribution (total % frequency at each EM) is the sum of whitewater and retained distributions.

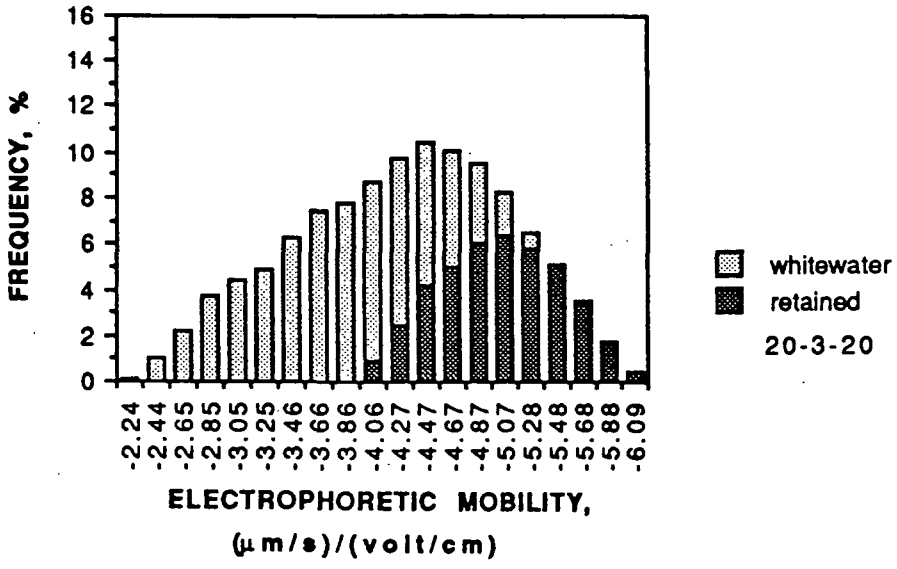

Figure A51. EM distributions for sample 20-3-20. Headbox distribution (total % frequency at each EM) is the sum of whitewater and retained distributions.

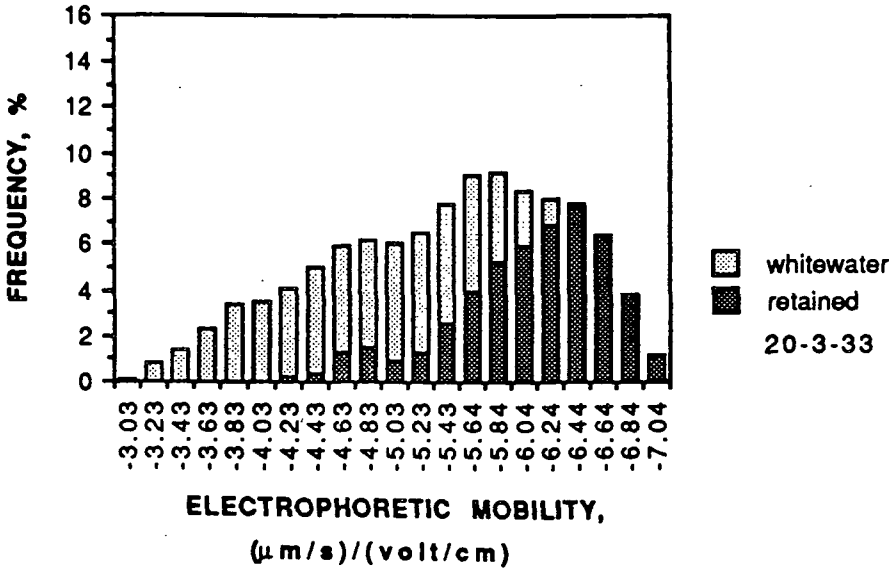

Figure A52. EM distributions for sample 20-3-33. Headbox distribution (total % frequency at each EM) is the sum of whitewater and retained distributions.

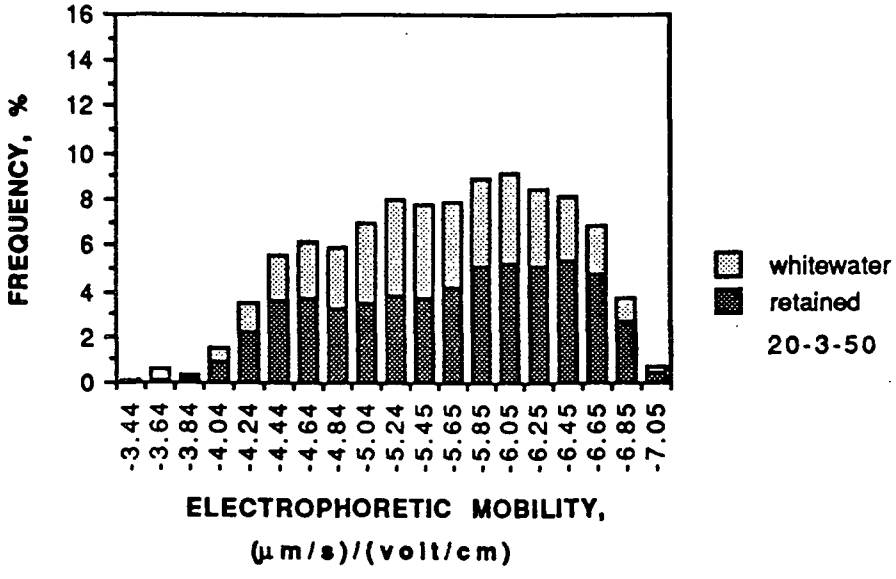

Figure A53. EM distributions for sample 20-3-50. Headbox distribution (total % frequency at each EM) is the sum of whitewater and retained distributions.

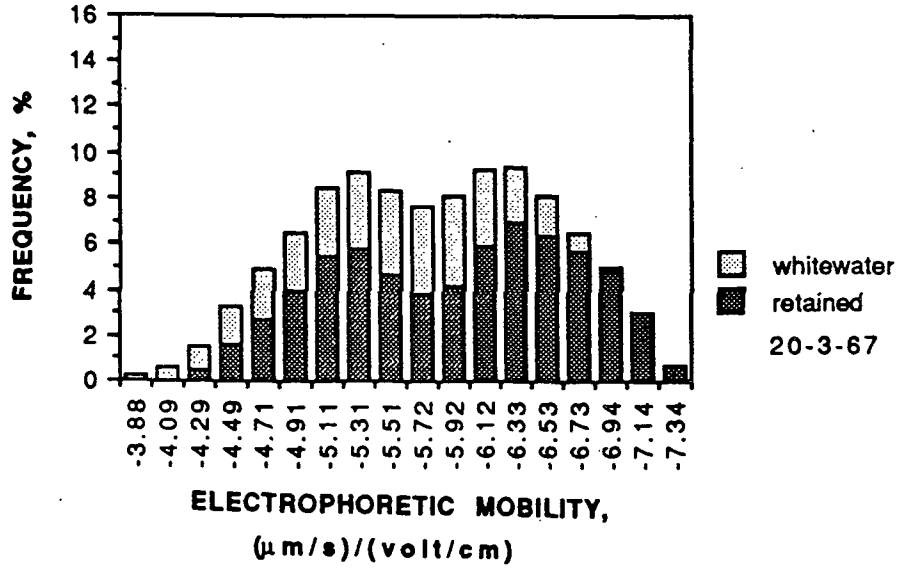

Figure A54. EM distributions for sample 20-3-67. Headbox distribution (total % frequency at each EM) is the sum of whitewater and retained distributions.

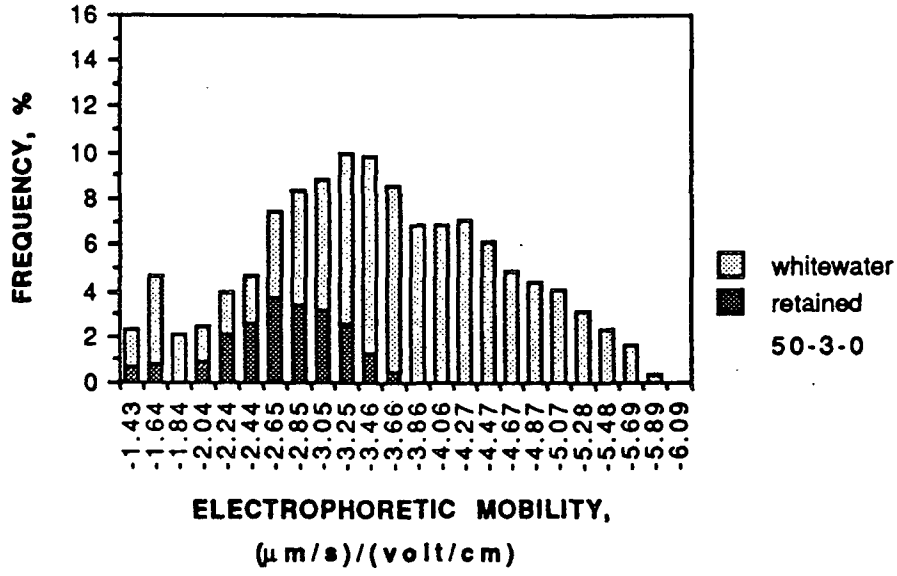

Figure A55. EM distributions for sample 50-3-0. Headbox distribution (total % frequency at each EM) is the sum of whitewater and retained distributions.

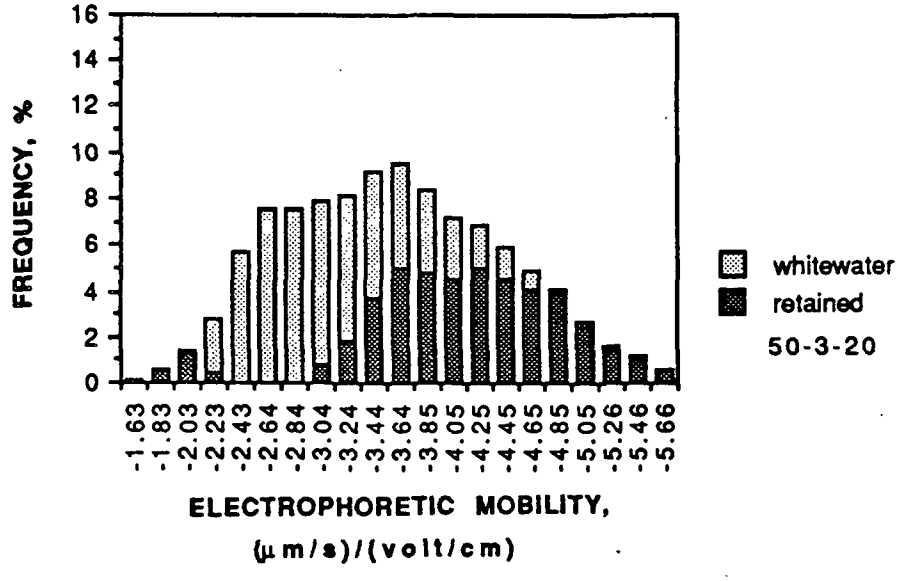

Figure A56. EM distributions for sample 50-3-20. Headbox distribution (total % frequency at each EM) is the sum of whitewater and retained distributions.

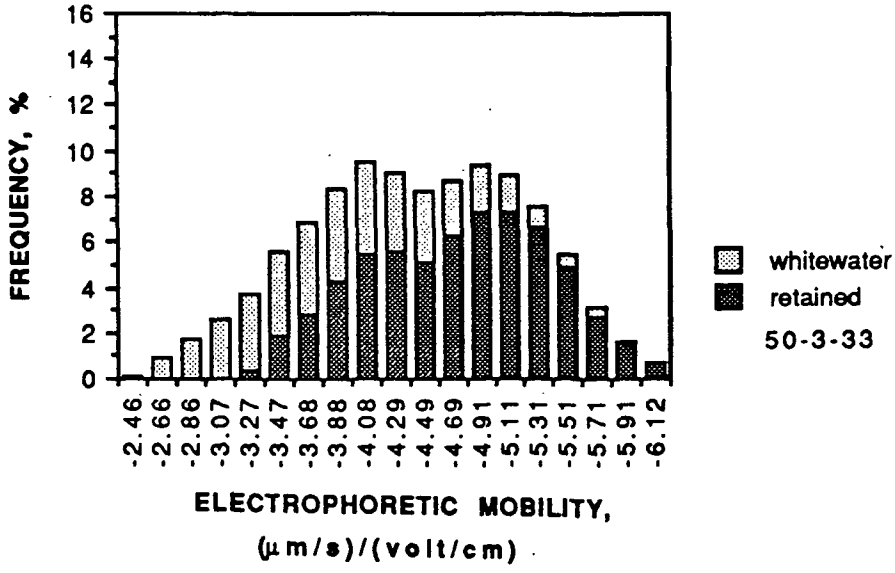

Figure A57. EM distributions for sample 50-3-33. Headbox distribution (total % frequency at each EM) is the sum of whitewater and retained distributions.

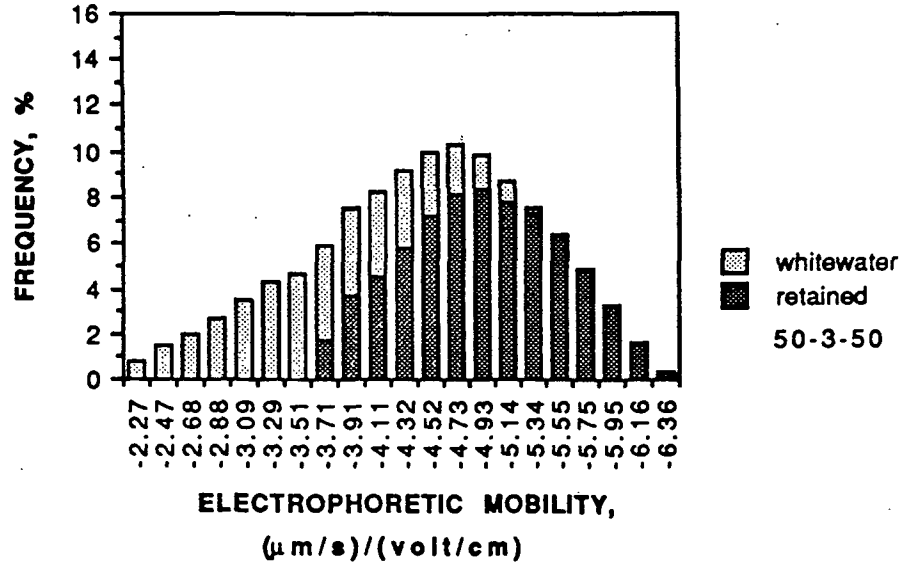

Figure A58. EM distributions for sample 50-3-50. Headbox distribution (total % frequency at each EM) is the sum of whitewater and retained distributions.

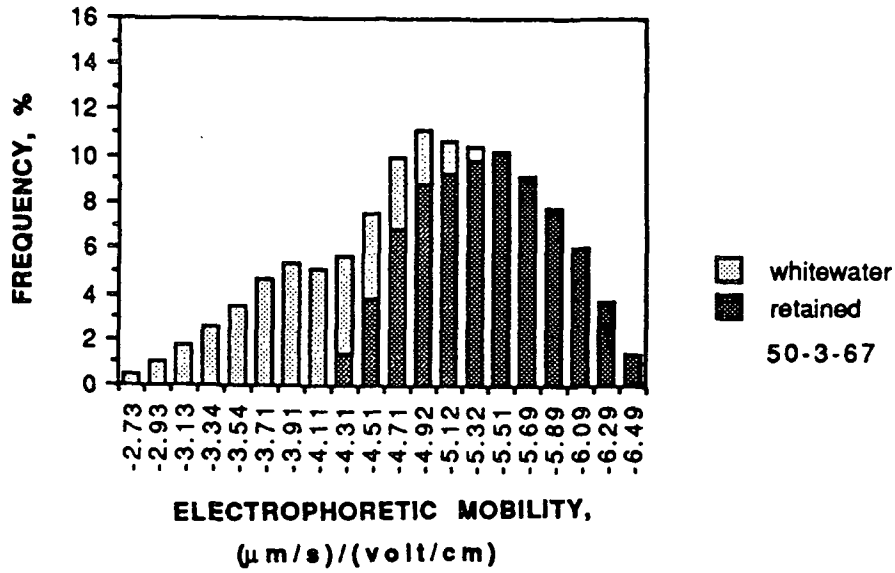

Figure A59. EM distributions for sample 50-3-67. Headbox distribution (total % frequency at each EM) is the sum of whitewater and retained distributions.

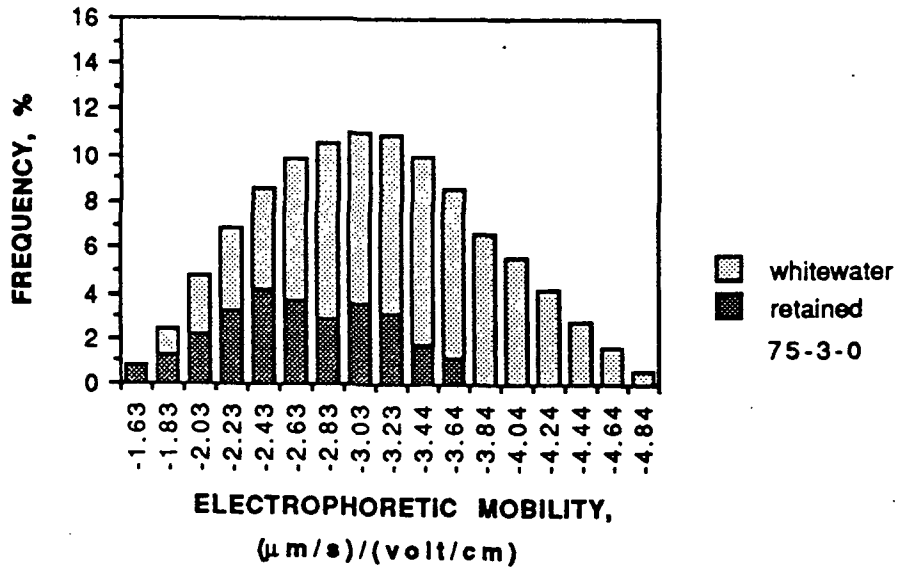

Figure A60. EM distributions for sample 75-3-0. Headbox distribution (total % frequency at each EM) is the sum of whitewater and retained distributions.

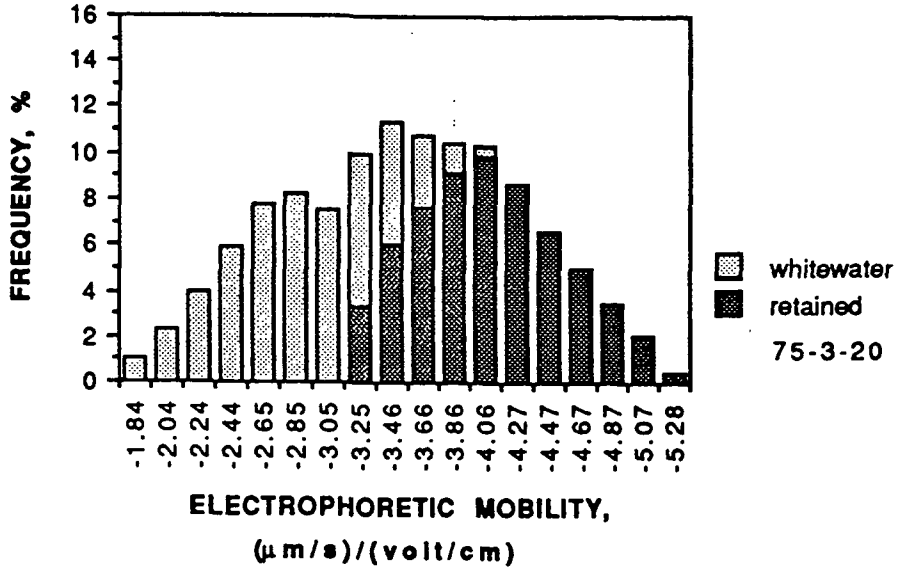

Figure A61. EM distributions for sample 75-3-20. Headbox distribution (total % frequency at each EM) is the sum of whitewater and retained distributions.

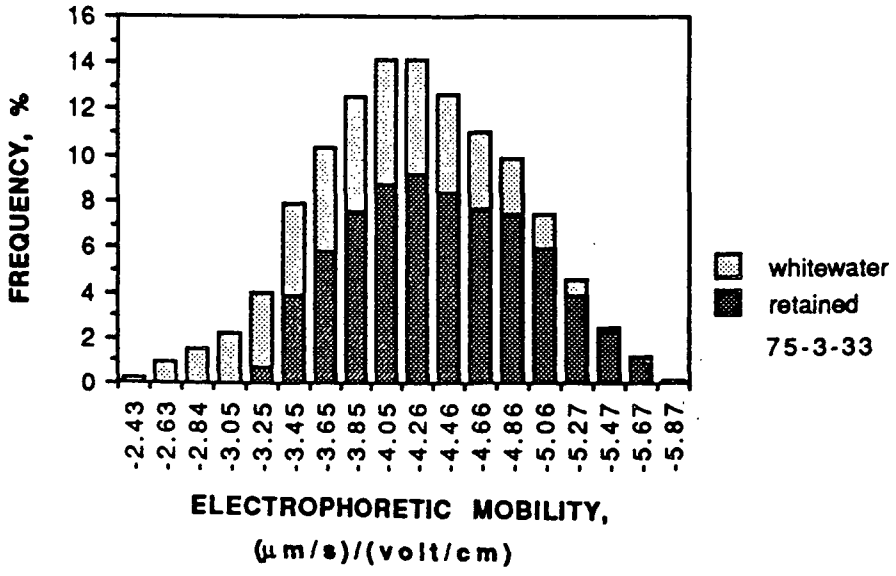

Figure A62. EM distributions for sample 75-3-33. Headbox distribution (total % frequency at each EM) is the sum of whitewater and retained distributions.

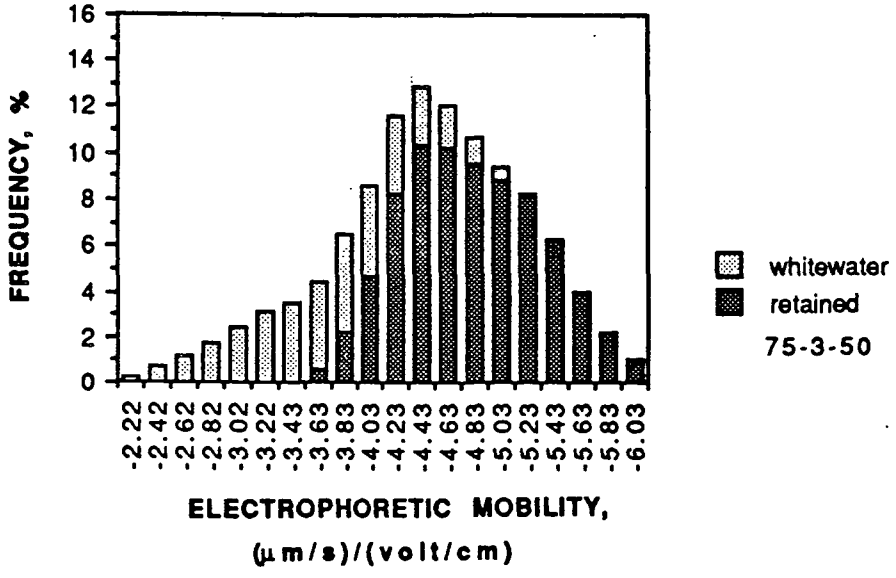

Figure A63. EM distributions for sample 75-3-50. Headbox distribution (total % frequency at each EM) is the sum of whitewater and retained distributions.

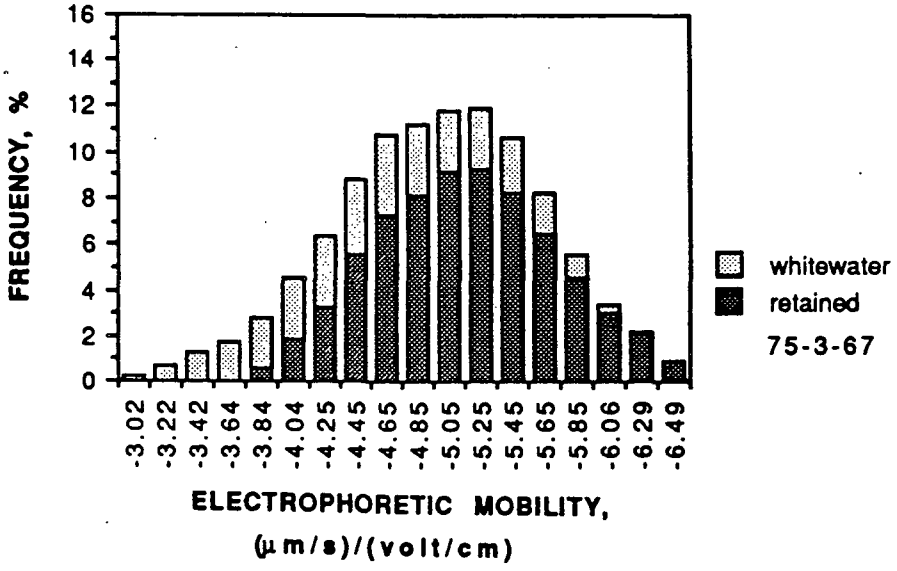

Figure A64. EM distributions for sample 75-3-67. Headbox distribution (total % frequency at each EM) is the sum of whitewater and retained distributions.

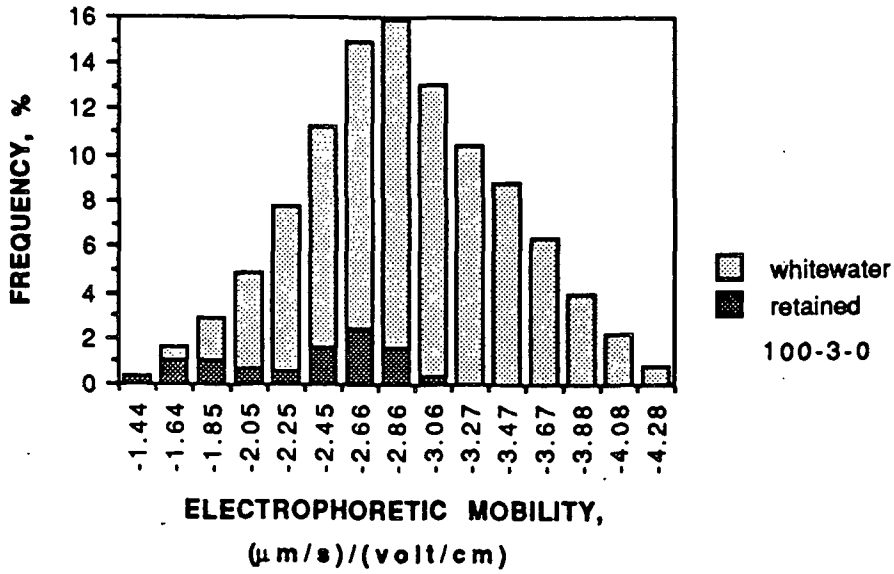

Figure A65. EM distributions for sample 100-3-0. Headbox distribution (total % frequency at each EM) is the sum of whitewater and retained distributions.

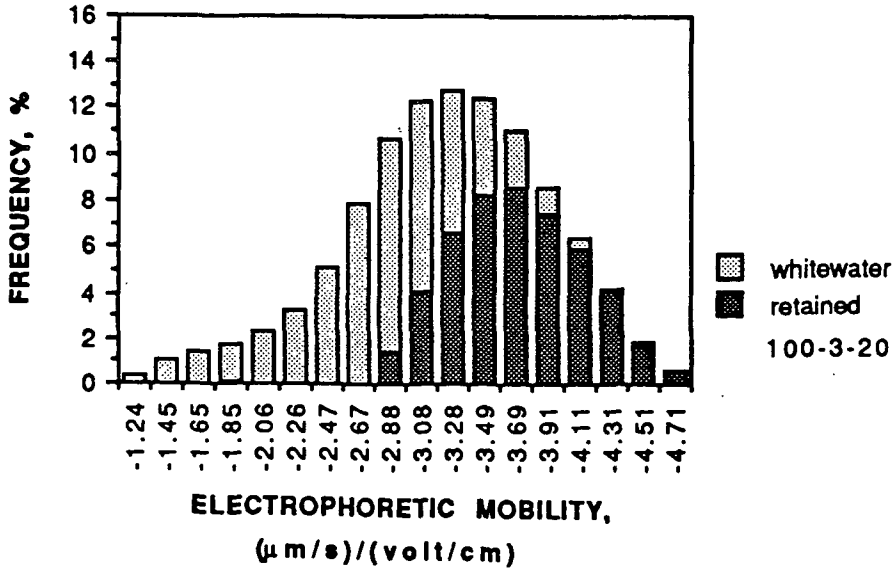

Figure A66. EM distributions for sample 100-3-20. Headbox distribution (total % frequency at each EM) is the sum of whitewater and retained distributions.

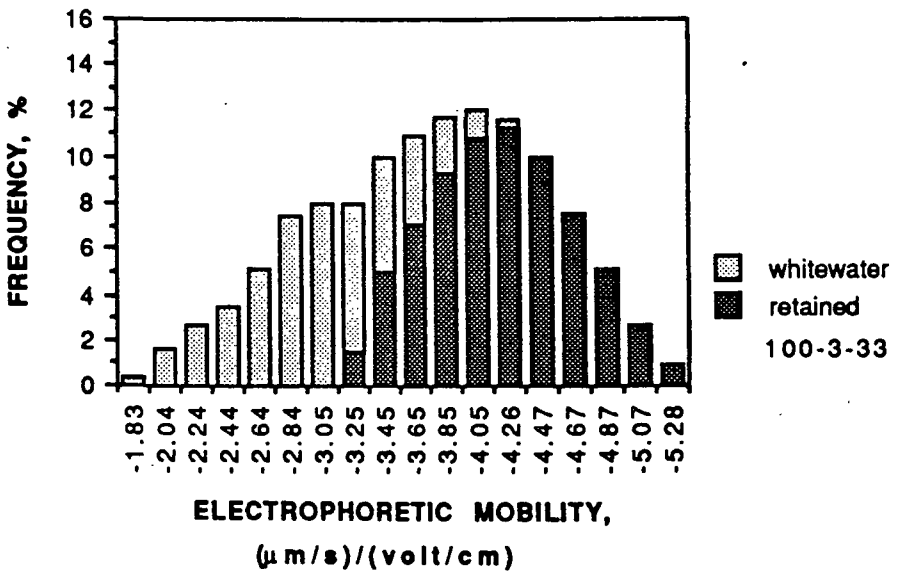

Figure A67. EM distributions for sample 100-3-33. Headbox distribution (total % frequency at each EM) is the sum of whitewater and retained distributions.

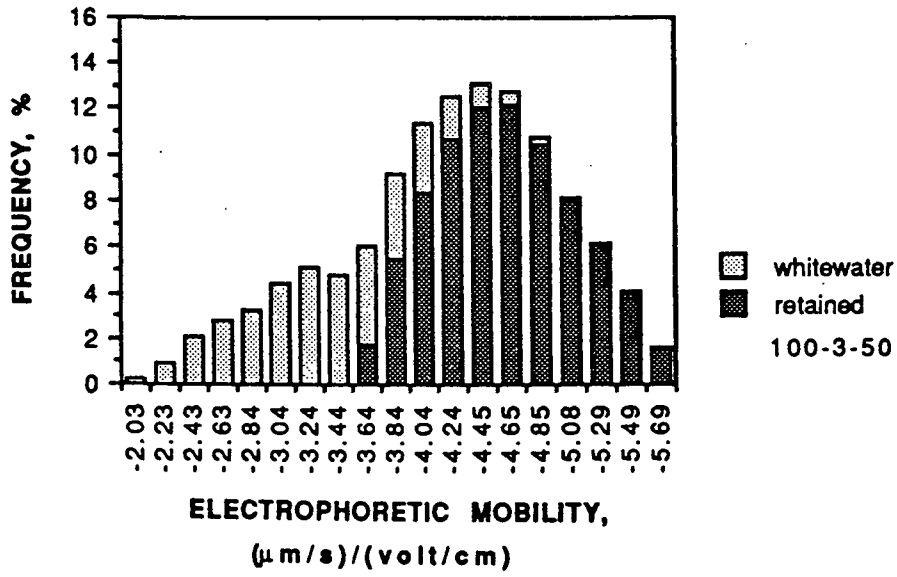

Figure A68. EM distributions for sample 100-3-50. Headbox distribution (total % frequency at each EM) is the sum of whitewater and retained distributions.

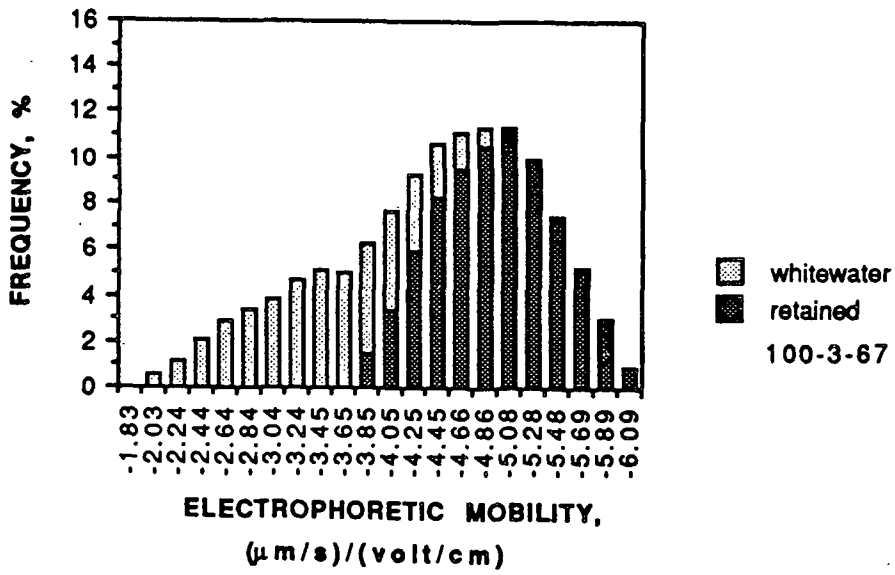

Figure A69. EM distributions for sample 100-3-67. Headbox distribution (total % frequency at each EM) is the sum of whitewater and retained distributions.

APPENDIX X

ELECTROPHORETIC MOBILITY DATA

Sample	Electrophoretic Mobility, (μm/s) / (volt/cm)			
	Treated	Headbox	Whitewater	Retained
20-1-0	-1.77	-5.65	-5.70	-4.88
20-1-20	-2.15	-5.97	-5.55	-6.55
20-1-33	-2.79	-6.00	-5.85	-6.42
20-1-50	-3.22	-5.54	-5.79	-5.22
20-1-67	-3.95	-5.82	-5.97	-5.59
0-1-100	n. a.	-6.60	n. m.	n. m.
50-1-0	-3.55	-5.01	-5.40	-4.43
50-1-20	-4.41	-5.84	-5.76	-6.05
50-1-33	-4.86	-6.02	-5.84	-6.44
50-1-50	-4.73	-5.71	-5.53	-5.99
50-1-67	-5.65	-6.14	-6.07	-6.19
0-1-100	n. a.	-6.60	n. m.	n. m.
75-1-0	-4.80	-5.23	-5.27	-5.10
75-1-20	-4.92	-5.24	-5.45	-4.84
75-1-33	-5.19	-5.58	-5.54	-5.72
75-1-50	-5.46	-5.73	-5.69	-5.74
75-1-67	-5.63	-5.96	-5.77	-6.07
0-1-100	n. a.	-6.60	n. m.	n. m.
100-1-0	-5.05	-5.12	-5.22	-4.77
100-1-20	-5.23	-5.13	-5.19	-4.91
100-1-33	-5.50	-5.41	-5.27	-5.55
100-1-50	-5.86	-5.80	-5.68	-5.91
100-1-67	-6.05	-6.14	-5.84	-6.40
0-1-100	n. a.	-6.60	n. m.	n. m.

n. a. = not applicable
n. m. = not measured

ELECTROPHORETIC MOBILITY DATA (CONT.)

Sample	Electrophoretic Mobility, (μm/s) / (volt/cm)			
	Treated	Headbox	Whitewater	Retained
20-2-0	-0.34	-5.47	-5.69	-4.05
20-2-20	-0.75	-5.50	-5.22	-6.28
20-2-33	-1.04	-4.94	-4.87	-5.15
20-2-50	-1.78	-5.67	-5.44	-5.94
20-2-67	-2.46	-5.61	-5.08	-5.92
0-2-100	n. a.	-6.60	n. m.	n. m.
50-2-0	-2.14	-4.23	-4.27	-4.02
50-2-20	-2.69	-4.68	-4.11	-5.08
50-2-33	-3.09	-5.05	-4.48	-5.27
50-2-50	-3.38	-5.19	-4.70	-5.44
50-2-67	-4.35	-5.63	-5.15	-5.78
0-2-100	n. a.	-6.60	n. m.	n. m.
75-2-0	-3.18	-3.88	-4.06	-3.20
75-2-20	-3.74	-4.36	-4.28	-4.57
75-2-33	-3.99	-4.79	-4.45	-5.19
75-2-50	-4.32	-4.89	-4.73	-5.22
75-2-67	-5.03	-5.34	-4.50	-5.60
0-2-100	n. a.	-6.60	n. m.	n. m.
100-2-0	-3.90	-3.93	-3.99	-3.47
100-2-20	-4.39	-4.15	-4.12	-4.30
100-2-33	-4.65	-4.57	-4.29	-4.81
100-2-50	-5.05	-5.09	-4.51	-5.33
100-2-67	-5.64	-5.53	-4.73	-5.76
0-2-100	n. a.	-6.60	n. m.	n. m.

n. a. = not applicable
n. m. = not measured

ELECTROPHORETIC MOBILITY DATA (CONT.)

Sample	Electrophoretic Mobility, (μm/s) / (volt/cm)			
	Treated	Headbox	Whitewater	Retained
20-3-0	0.30	-4.07	-4.10	-3.85
20-3-20	0.27	-4.42	-3.87	-5.04
20-3-33	-0.27	-5.54	-4.85	-6.08
20-3-50	-0.86	-5.44	-5.15	-5.62
20-3-67	-1.49	-5.80	-5.54	-5.94
0-3-100	n. a.	-6.60	n. m.	n. m.
50-3-0	-1.04	-3.41	-3.91	-2.71
50-3-20	-1.75	-3.62	-3.17	-4.12
50-3-33	-2.62	-4.49	-3.98	-4.73
50-3-50	-3.04	-4.68	-3.71	-4.94
50-3-67	-3.45	-5.17	-4.08	-5.39
0-3-100	n. a.	-6.60	n. m.	n. m.
75-3-0	-2.24	-3.04	-3.26	-2.68
75-3-20	-2.85	-3.70	-2.89	-4.11
75-3-33	-3.26	-4.22	-3.44	-4.40
75-3-50	-4.03	-4.61	-3.73	-4.85
75-3-67	-4.56	-5.05	-4.59	-5.14
0-3-100	n. a.	-6.60	n. m.	n. m.
100-3-0	-2.96	-2.85	-2.94	-2.37
100-3-20	-3.38	-3.29	-2.90	-3.71
100-3-33	-3.81	-3.95	-3.02	-4.20
100-3-50	-4.39	-4.48	-3.36	-4.61
100-3-67	-4.73	-4.74	-3.51	-4.95
0-3-100	n. a.	-6.60	n. m.	n. m.

n. a. = not applicable
n. m. = not measured

APPENDIX XI

STANDARD DEVIATION DATA

Sample	Standard Deviation of the Distribution, (μm/s) / (volt/cm)			
	Treated	Headbox	Whitewater	Retained
20-1-0	0.441	0.746	0.695	1.069
20-1-20	0.654	0.627	0.594	0.389
20-1-33	0.538	0.618	0.597	0.521
20-1-50	0.525	0.654	0.625	0.569
20-1-67	0.652	0.611	0.585	0.631
0-1-100	n. a.	0.448	n. m.	n. m.
50-1-0	0.724	0.636	0.648	0.442
50-1-20	0.551	0.602	0.622	0.490
50-1-33	0.588	0.650	0.597	0.568
50-1-50	0.577	0.600	0.630	0.532
50-1-67	0.588	0.559	0.534	0.604
0-1-100	n. a.	0.448	n. m.	n. m.
75-1-0	0.518	0.617	0.574	0.732
75-1-20	0.526	0.576	0.589	0.505
75-1-33	0.509	0.564	0.537	0.490
75-1-50	0.480	0.550	0.552	0.544
75-1-67	0.479	0.471	0.571	0.463
0-1-100	n. a.	0.448	n. m.	n. m.
100-1-0	0.556	0.538	0.553	0.490
100-1-20	0.539	0.605	0.509	0.791
100-1-33	0.567	0.568	0.553	0.552
100-1-50	0.533	0.545	0.551	0.534
100-1-67	0.496	0.516	0.514	0.442
0-1-100	n. a.	0.448	n. m.	n. m.

n. a. = not applicable
n. m. = not measured

STANDARD DEVIATION DATA (CONT.)

Sample	Standard Deviation of the Distribution, (μm/s) / (volt/cm)			
	Treated	Headbox	Whitewater	Retained
20-2-0	0.337	0.624	0.523	0.518
20-2-20	0.305	0.715	0.637	0.333
20-2-33	0.317	0.741	0.687	0.821
20-2-50	0.431	0.675	0.615	0.684
20-2-67	0.509	0.617	0.630	0.500
0-2-100	n. a.	0.448	n. m.	n. m.
50-2-0	0.449	0.778	0.696	1.196
50-2-20	0.452	0.697	0.670	0.555
50-2-33	0.516	0.657	0.654	0.579
50-2-50	0.548	0.623	0.597	0.552
50-2-67	0.539	0.664	0.639	0.641
0-2-100	n. a.	0.448	n. m.	n. m.
75-2-0	0.464	0.590	0.581	0.506
75-2-20	0.527	0.623	0.505	0.781
75-2-33	0.535	0.637	0.574	0.519
75-2-50	0.557	0.592	0.610	0.508
75-2-67	0.573	0.587	0.621	0.509
0-2-100	n. a.	0.448	n. m.	n. m.
100-2-0	0.573	0.523	0.491	0.644
100-2-20	0.544	0.548	0.531	0.606
100-2-33	0.563	0.571	0.536	0.437
100-2-50	0.581	0.555	0.595	0.461
100-2-67	0.570	0.503	0.577	0.432
0-2-100	n. a.	0.448	n. m.	n. m.

n. a. = not applicable
n. m. = not measured

STANDARD DEVIATION DATA (CONT.)

Sample	Standard Deviation of the Distribution, (μm/s) / (volt/cm)			
	Treated	Headbox	Whitewater	Retained
20-3-0	0.344	0.655	0.603	1.032
20-3-20	0.406	0.747	0.654	0.470
20-3-33	0.297	0.814	0.747	0.590
20-3-50	0.380	0.783	0.706	0.800
20-3-67	0.483	0.742	0.620	0.757
0-3-100	n. a.	0.448	n. m.	n. m.
50-3-0	0.457	0.876	1.024	0.502
50-3-20	0.530	0.807	0.590	0.775
50-3-33	0.508	0.700	0.704	0.645
50-3-50	0.492	.0711	0.705	0.617
50-3-67	0.593	0.631	0.588	0.517
0-3-100	n. a.	0.448	n. m.	n. m.
75-3-0	0.589	0.635	.0675	0.508
75-3-20	0.485	0.673	0.477	0.470
75-3-33	0.492	0.625	0.571	0.571
75-3-50	0.544	0.599	0.608	0.503
75-3-67	0.584	0.611	0.689	0.571
0-3-100	n. a.	0.448	n. m.	n. m.
100-3-0	0.509	0.542	0.523	0.448
100-3-20	0.537	0.622	0.418	0.424
100-3-33	0.560	0.585	0.492	0.466
100-3-50	0.619	0.551	0.571	0.493
100-3-67	0.596	0.597	0.660	0.575
0-3-100	n. a.	0.448	n. m.	n. m.

n. a. = not applicable
n. m. = not measured

APPENDIX XII

PARTICLE SIZE DATA

Sample	Volume, μm^3	Number Frequency, % Treated	Headbox	Whitewater
20-3-0	0.065	46.6	65.7	71.0
	0.131	22.1	20.3	18.1
	0.262	15.9	6.6	5.1
	0.524	8.2	3.5	2.9
	1.047	3.9	2.0	1.6
	2.094	1.7	0.9	0.7
	4.189	0.9	0.6	0.4
	8.378	0.4	0.2	0.1
50-3-0	0.065	40.1	69.2	75.7
	0.131	22.3	15.8	13.7
	0.262	18.1	7.0	4.9
	0.524	10.0	3.7	2.6
	1.047	5.0	2.1	1.5
	2.094	2.1	0.9	0.6
	4.189	1.3	0.6	0.4
	8.378	0.6	0.3	0.2
100-3-0	0.065	36.0	46.1	48.2
	0.131	21.8	22.4	22.7
	0.262	18.8	16.1	15.5
	0.524	11.7	8.4	7.5
	1.047	6.2	3.8	3.2
	2.094	2.6	1.5	1.3
	4.189	1.5	0.9	0.8
	8.378	0.7	0.4	0.4

	Volume, μm^3	Number Frequency,%
Untreated	0.065	82.2
Latex	0.131	17.8

APPENDIX XIII

DETERMINATION OF SALT CORRECTION

Since all samples were prepared in 0.01 M NaCl, the gravimetric retention samples contained salt. The weight of this salt had to be calculated and subtracted from the dry weight in each whitewater solids sample. The weight of salt water added to each headbox sample was noted. Each headbox sample had a slightly different makeup such that the final electrolyte background varied slightly (not enough to drastically change the conductance as seen in Appendix VIII). So the concentration of salt in each headbox sample was individually calculated using a personal computer. Hence, when a whitewater sample was taken, the concentration of salt was known. The only value needed was the wet weight (volume) of sample taken. This value was required for the solids determination as well and was measured immediately after the sample was placed in the weighing dish. The amount of salt could then be subtracted from the dry weight to give the weight of latex in the whitewater sample.

APPENDIX XIV

RETENTION RESULTS

Sample	Retention %	Standard Deviation	Fract. Q5 on Fibers	Polymer Loading*
20-1-0	6.4	0.4	0.00	0.0125
20-1-20	24.0	1.6	0.20	0.0100
20-1-33	29.6	1.9	0.33	0.0084
20-1-50	41.7	2.7	0.50	0.0063
20-1-67	39.1	2.6	0.67	0.0041
0-1-100	7.8	1.6	1.00	0.0000
50-1-0	8.1	1.4	0.00	0.0050
50-1-20	26.1	1.4	0.20	0.0040
50-1-33	29.7	2.8	0.33	0.0034
50-1-50	30.9	4.2	0.50	0.0025
50-1-67	33.3	1.7	0.67	0.0017
0-1-100	7.8	1.6	1.00	0.0000
75-1-0	15.2	1.5	0.00	0.0033
75-1-20	29.5	3.0	0.20	0.0027
75-1-33	35.6	0.6	0.33	0.0022
75-1-50	39.1	0.7	0.50	0.0017
75-1-67	45.3	0.5	0.67	0.0011
0-1-100	7.8	1.6	1.00	0.0000
100-1-0	16.2	1.5	0.00	0.0025
100-1-20	21.9	1.3	0.20	0.0020
100-1-33	44.2	5.8	0.33	0.0017
100-1-50	51.3	5.9	0.50	0.0013
100-1-67	46.8	1.3	0.67	0.0008
0-1-100	7.8	1.6	1.00	0.0000

* Polymer loading is defined as the grams of Q5 added per gram of latex treated. Mobilities are in (μm/s) / (volt/cm).

RETENTION RESULTS (CONT.)

Sample	Retention %	Standard Deviation	Fract. Q5 on Fibers	Polymer Loading*
20-2-0	8.9	3.4	0.00	0.0250
20-2-20	10.5	1.7	0.20	0.0200
20-2-33	27.9	3.3	0.33	0.0168
20-2-50	40.0	1.7	0.50	0.0125
20-2-67	49.7	0.6	0.67	0.0083
0-2-100	37.7	1.3	1.00	0.0000
50-2-0	11.1	2.9	0.00	0.0100
50-2-20	44.1	0.9	0.20	0.0080
50-2-33	63.5	3.6	0.33	0.0067
50-2-50	57.0	3.6	0.50	0.0050
50-2-67	65.4	9.4	0.67	0.0033
0-2-100	37.7	1.3	1.00	0.0000
75-2-0	7.6	3.2	0.00	0.0067
75-2-20	27.4	1.7	0.20	0.0053
75-2-33	38.8	1.6	0.33	0.0045
75-2-50	38.6	1.3	0.50	0.0033
75-2-67	40.7	2.9	0.67	0.0022
0-2-100	37.7	1.3	1.00	0.0000
100-2-0	3.4	1.4	0.00	0.0050
100-2-20	25.6	2.8	0.20	0.0040
100-2-33	47.4	1.5	0.33	0.0034
100-2-50	51.1	1.7	0.50	0.0025
100-2-67	55.9	2.9	0.67	0.0017
100-2-80	45.4	0.7	0.80	0.0010
0-2-100	37.7	1.3	1.00	0.0000

* Polymer loading is defined as the grams of Q5 added per gram of latex treated. Mobilities are in (μm/s) / (volt/cm).

RETENTION RESULTS (CONT.)

Sample	Retention %	Standard Deviation	Fract. Q5 on Fibers	Polymer Loading*
20-3-0	4.2	1.5	0.00	0.0375
20-3-10	7.7	2.0	0.10	0.0340
20-3-20	29.8	3.1	0.20	0.0300
20-3-33	42.7	5.5	0.33	0.0251
20-3-50	58.0	1.4	0.50	0.0188
20-3-67	65.4	3.8	0.67	0.0124
20-3-80	50.0	0.5	0.80	0.0070
0-3-100	40.7	1.9	1.00	0.0000
50-3-0	1.1	0.5	0.00	0.0150
50-3-20	43.3	3.8	0.20	0.0120
50-3-33	60.0	4.2	0.33	0.0101
50-3-50	57.8	0.6	0.50	0.0075
50-3-67	60.0	13.6	0.67	0.0050
0-3-100	40.7	1.9	1.00	0.0000
75-3-0	22.3	2.0	0.00	0.0100
75-3-20	39.4	4.3	0.20	0.0080
75-3-33	62.7	2.7	0.33	0.0067
75-3-50	55.5	2.4	0.50	0.0050
75-3-67	67.4	4.2	0.67	0.0033
0-3-100	40.7	1.9	1.00	0.0000
100-3-0	4.6	3.2	0.00	0.0075
100-3-20	45.2	4.1	0.20	0.0060
100-3-33	52.1	5.4	0.33	0.0050
100-3-50	61.2	2.7	0.50	0.0038
100-3-67	53.7	2.0	0.67	0.0025
0-3-100	40.7	1.9	1.00	0.0000

* Polymer loading is defined as the grams of Q5 added per gram of latex treated. Mobilities are in (μm/s) / (volt/cm).

APPENDIX XV

STATISTICAL DATA

Table A1. ANOVA table for statistical model using currently measurable variables.

Data File: Retention Model

Source	Sum of Squares	Deg. of Freedom	Mean Squares	F-Ratio	Prob>F
Model	2974.618	2	1487.309	4.772	0.012
Error	17767.084	57	311.703		
Total	20741.702	59			

Coefficient of Determination	0.143
Coefficient of Correlation	0.379
Standard Error of Estimate	17.655
Durbin-Watson Statistic	1.714

Table A2. Model coefficients for currently measurable variables.

Data File: Retention Model Dependent Variable: retention

Variable Name	Coefficient	Std. Err. Estimate	t Statistic	Prob > t
Constant	-30.124	28.805	-1.046	0.300
dosage	14.279	4.828	2.957	0.004
ww e. mobility	-8.216	4.331	-1.897	0.063

Table A3. ANOVA table for statistical model using whitewater mobility.

Data File: Retention Model

Source	Sum of Squares	Deg. of Freedom	Mean Squares	F-Ratio	Prob>F
Model	16823.090	5	3364.618	46.366	0.000
Error	3918.612	54	72.567		
Total	20741.702	59			

Coefficient of Determination	0.811
Coefficient of Correlation	0.901
Standard Error of Estimate	8.519
Durbin-Watson Statistic	1.487

Table A4. Model coefficients for each variable using whitewater mobility.

Data File: Retention Model Dependent Variable: retention

Variable Name	Coefficient	Std. Err. Estimate	t Statistic	Prob > t
Constant	-15.973	23.974	-0.666	0.508
fract. on fiber	137.345	16.016	8.575	0.000
fract. squared	-111.471	23.375	-4.769	0.000
% latex treated	8.508	5.356	1.589	0.118
dosage	7.683	3.363	2.285	0.026
ww e. mobility	-0.964	3.388	-0.285	0.777

Table A5. ANOVA table for model using whitewater mobility and standard deviation of the mobility distribution.

Data File: Retention Model

Source	Sum of Squares	Deg. of Freedom	Mean Squares	F-Ratio	Prob>F
Model	16823.729	6	2803.955	37.930	0.000
Error	3917.973	53	73.924		
Total	20741.702	59			

Coefficient of Determination	0.811
Coefficient of Correlation	0.901
Standard Error of Estimate	8.598
Durbin-Watson Statistic	1.478

Table A6. Model coefficients for each variable using whitewater mobility and standard deviation of the mobility distribution.

Data File: Retention Model Dependent Variable: retention

Variable Name	Coefficient	Std. Err. Estimate	t Statistic	Prob > t
Constant	-15.297	25.266	-0.605	0.547
fract. on fiber	137.111	16.360	8.381	0.000
fract. squared	-111.206	23.764	-4.680	0.000
% latex treated	8.358	5.642	1.481	0.144
dosage	7.755	3.480	2.229	0.030
ww e. mobility	-1.003	3.445	-0.291	0.772
std. deviation	-1.449	15.577	-0.093	0.926

Table A7. ANOVA table for statistical model using headbox mobility.

Data File: Retention Model

Source	Sum of Squares	Deg. of Freedom	Mean Squares	F-Ratio	Prob>F
Model	19475.351	5	3895.070	55.344	0.000
Error	4645.024	66	70.379		
Total	24120.375	71			

Coefficient of Determination	0.807
Coefficient of Correlation	0.899
Standard Error of Estimate	8.389
Durbin-Watson Statistic	1.452

Table A8. Model coefficients for each variable using headbox mobility.

Data File: Retention Model Dependent Variable: retention

Variable Name	Coefficient	Std. Err. Estimate	t Statistic	Prob > t
Constant	-55.023	16.940	-3.248	0.002
e. mobility	-7.105	2.735	-2.598	0.011
fract. on fiber	135.883	10.915	12.449	0.000
fract. squared	-130.147	9.787	-13.299	0.000
% latex treated	12.158	4.092	2.971	0.004
dosage	12.462	1.989	6.266	0.000